
# Modelling of Ringkøbing Fjord to support policy-makers for compliance with the EU Water Framework Directive

DRAFT REPORT

DECEMBER 2023

Leonard Bernard-Jannin, Joao G. Ferreira, Joao Lencart e Silva,
Alhambra M. Cubillo, Gerhardus Diedricks

# Contents

# Executive summary

Ringkøbing Fjord is a coastal lagoon system in western Jutland (Denmark), with a north-south orientation. The fjord is approximately 30 kilometres long and 10-15 kilometres wide. It has an area of almost 300 square kilometres and is on average just under 2 metres deep.

The fjord is connected to the North Sea through an artificial structure (a sluice) and receives freshwater inputs from the Skjern and smaller streams Ringkøbing Fjord drains a basin of about 3 500 km$^2$, where agriculture, which covers 65-70% of the catchment, is the dominant activity.

The Water Framework Directive (WFD – 2000/60/EC) classifies Ringkøbing Fjord as having poor ecological potential. In light of this situation, and with a view to continuing the long-standing tradition of local cooperation, the Ringkøbing-Skjern Municipality brought together relevant stakeholders through the creation of the Coastal Water Council to promote the development of an ecosystem modelling framework (EMF) for the fjord. The purpose of this framework was to (i) provide a thorough understanding of the interactions among the catchment, the fjord, and the sluice; (ii) to offer insights into how the stakeholders can work together effectively to achieve the targets set by the WFD; and (iii) to support policy makers.

The EMF framework combined a range of complementary mathematical models, aimed at (i) simulating water inputs and nutrient loading from the catchment; (ii) reproducing water circulation inside the fjord and water exchange at the ocean boundary by means of the sluice, essential to understand the role of physical processes in the distribution of nutrients and phytoplankton; and (iii) deploying ecosystem models for decadal periods to simulate key biogeochemical and ecological processes in the water column and sediments of Ringkøbing Fjord.

In order to examine management options for Ringkøbing Fjord, it was essential to capture the complexity of the processes that occur within it (Fig. 1).

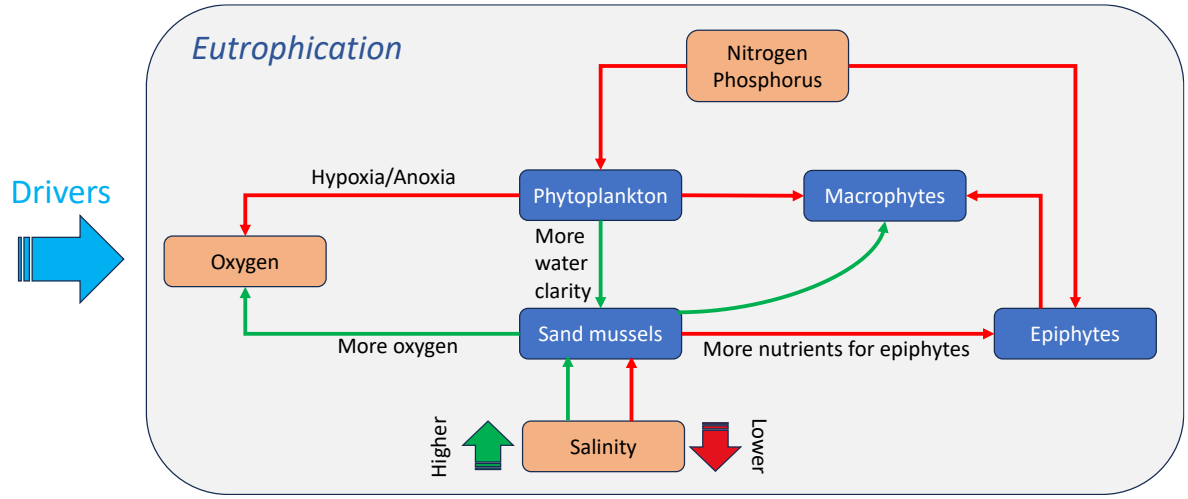


*Fig. 1. Conceptual diagram illustrating interactions of key ecosystem components in Ringkøbing Fjord*

The catchment model was used to simulate the impacts of land use change and wetland restoration scenarios on nitrogen loading. The results show that above a certain threshold, restoring wetlands is more effective than eliminating all agricultural activities. The model indicates that restoring 23 000 ha of wetlands (7% of the Ringkøbing Fjord catchment) could reduce the nitrogen loading by around 38% (Table 1). The model also indicates that urban inputs are a negligible source of nitrogen.

*Table 1. Main nitrogen inputs and exports simulated by the catchment model under several scenarios.*

| Scenario | Fertiliser inputs (tons/kg.ha-1) | Exports to Ringkøbing Fjord (tons/kg.ha-1) | Export reduction compared to baseline | Wetland area (ha) |
|---|---|---|---|---|
| 0 – Baseline | 45 485/135 | 4 518/13.4 | | 4 031 |
| 1 – No farming | 0/0 | 2 248/6.7 | 50% | 4 031 |
| 2 – Full wetland | 37 836/112 | 1 191/3.5 | 74% | 53 937 |
| 3 – 60% wetlands | 41 005/122 | 2 425/7.2 | 46% | 32 029 |
| 4 – 50% wetlands | 41 781/124 | 2 797/8.3 | 38% | 26 966 |
| 5 – 40% wetlands | 42 557/126 | 3 158/9.4 | 30% | 21 903 |
| 6 – No wastewater | 45 485/135 | 4 507/13.3 | 0% | 4 031 |

The integration of benthic primary (macrophytes) and secondary producers (bivalves – the softshell clam *Mya arenaria*) in this framework is a major asset since it allows policy makers to evaluate trade-offs.

The model results indicate that chlorophyll concentrations are below the threshold for good ecological potential, set to 8.4 $\mu g.L^{-1}$ by the current River Basin Management Plan (RBMP), in 48 out of the 50 model boxes. In the examples provided in this report, a 35% reduction in land-based loading from all sources—corresponding to the reduction in nitrogen targeted by the RBMP - shows reductions of 0.2 to 4.2 $\mu g.L^{-1}$ in summer chlorophyll concentrations (Table 2). This 35% reduction also results in a decrease of epiphyte risk and is a potentially important measure to mitigate eutrophication in the fjord, although epiphytes are not part of the WFD Biological Quality Elements (BQE). The reduction in epiphyte risk is greater for boxes located at the edge of the fjord, where the risk is presently highest. Reducing the load by half of the 35% target shows a reduction in summer chlorophyll concentrations of between 0.1 and 1.7 $\mu g.L^{-1}$ and halves the decrease in epiphyte risk compared to the 35% reduction.

*Table 2. Ranges of simulated indicator values under different top-down and bottom-up scenarios.*

| Indicator | Scenario | Lower boxes (min-max) | Upper boxes (min-max) |
|---|---|---|---|
| May-September chlorophyll a ($ug.L^{-1}$) | Baseline | 0.4-3.0 | 3.1-9.0 |
| | No *Mya arenaria* | 12.7-17.1 | 10.0-19.7 |
| | Loading reduced by 17.5% | 0.3-2.3 | 2.6-7.7 |
| | Loading reduced by 35% | 0.1-1.4 | 1.7-5.2 |
| Winter Dissolved Inorganic Nitrogen (DIN, $mg.L^{-1}$) | Baseline | 1.5-1.9 | 1.6-2.1 |
| | No *Mya arenaria* | 1.5-2.0 | 1.6-2.1 |
| | Loading reduced by 17.5% | 1.2-1.6 | 1.3-1.7 |
| | Loading reduced by 35% | 0.9-1.2 | 0.9-1.3 |
| Epiphyte risk score (range 1-5) | Baseline | 1.1-3.9 | not applicable |
| | No *Mya arenaria* | 1.1-3.8 | not applicable |
| | Loading reduced by 17.5% | 1.1-3.7 | not applicable |
| | Loading reduced by 35% | 1.1-3.5 | not applicable |

The presence of shellfish (*Mya arenaria*) within the fjord is a key factor in the top-down control of eutrophication, as summer concentrations of chlorophyll can increase by an order of magnitude in bottom boxes in the absence of filter feeders and exceed the threshold for good ecological potential in the entire fjord (Table 2). This therefore corresponds to an important regulatory ecosystem service supplied by bivalves.

The ecosystem modelling framework will be a valuable resource for the Coastal Water Council as they work to understand the local dynamics and identify the most effective solutions to improve the water quality of Ringkøbing Fjord.

# Introduction and objectives

## General objectives

The Ringkøbing Fjord water body has been rated as having a poor ecological potential according to the Water Framework Directive (WFD). In light of this situation and with a view to continuing the long-standing tradition of local cooperation, the Ringkøbing-Skjern municipality has come together with the relevant stakeholders through the creation of the Coastal Water Council and requested the development of an ecosystem modelling framework for Ringkøbing Fjord. The purpose of this framework is to provide a thorough understanding of the complex interactions between the catchment, the fjord, and the sluice that control eutrophication in the fjord (Fig. 1), and to offer insights into how the stakeholders can work together effectively to achieve the targets set by the WFD. The ecosystem modelling framework will be a valuable resource for the Coastal Water Council as they work to understand the local dynamics and identify the most effective solutions to improve the water quality of the Ringkøbing Fjord.

The objective of this work was to develop an ecosystem modelling framework for Ringkøbing Fjord to support policy-makers for compliance with the EU Water Framework Directive. The main aims were: of:

1. To analyse and interpret the WFD classification of this Heavily Modified Water Body (HMWB);
2. To apply the ecosystem modelling framework to examine various scenarios, with an emphasis on catchment loading scenarios, and top-down control of primary production;
3. To provide the Coastal Water Council with a set of tools enabling the simulation of key processes within Ringkøbing Fjord as a legacy output of this work;
4. To support policy decisions with respect to the sustainable management of Ringkøbing Fjord.

The ecosystem modelling framework is made up of the following components:

1. A catchment model for the Ringkøbing Fjord watershed. The catchment model was developed using the SWAT+ model to simulate the nutrient discharge through the Ringkøbing Fjord watershed, taking into account agricultural management practices based on the best available data;
2. A hydrodynamic model using the Delft3D platform to simulate water circulation in Ringkøbing Fjord, using discharge inputs provided by SWAT+ and accounting for the Ringkøbing Fjord sluice operation;
3. A model simulating the physiology of the softshell clam *Mya arenaria* using a net energy balance approach, providing outputs for individual growth and environmental effects;
4. A model simulating benthic macrophyte biomass and including a risk-based approach to colonisation of benthic vegetation by epiphytes;
5. An ecological model integrating the various components above to simulate key physical and biogeochemical processes within Ringkøbing Fjord.

## Overview of Ringkøbing Fjord

### General features

Ringkøbing Fjord is a shallow lagoon in the western part of Denmark. The fjord is approximately 30 kilometres long and 10-15 kilometres wide. It has an area of almost 300 square kilometres and is on average just under 2 metres deep. The maximum depth of the fjord is 6 metres. Ringkøbing Fjord drains approximately 9 percent of Denmark's area, including the Skjern Å catchment.

The physical regime of the fjord may be described as artificial since it is governed by a sluice where the water level in the fjord and the water exchange with the North Sea are actively regulated via a lock at Hvide Sande based on an adopted lock practice. Compared to the North Sea, the water in the

fjord is relatively fresh, as a result of a large influx of fresh water from Skjern Å, which drains a large part of West Jutland.

In the past, Ringkøbing Fjord has experienced eutrophication due to elevated nutrient loads from the land and the regulated exchange with the North Sea. A modification of the operational practices of the sluice occurred in 1995 with the aim of increasing salinity in the estuary. This adjustment aimed to reduce phytoplankton biomass and enhance the spatial coverage of benthic flora. One notable consequence was the significant recruitment of soft shell clams (*Mya arenaria*), whose filtering capacity led to a remarkable reduction in phytoplankton biomass in the years following the change in sluice practices (Nielsen et al. 2005).

Today, the fjord has a wide range of uses, including recreational activities such as kite surfing, and commercial and leisure fishing. It is also a biodiversity reserve, as it is a RAMSAR site and includes the Tipperne bird reserve. These uses were put at risk in 2019 with the appearance of a major algal bloom in the fjord.

## Catchment and loading

The Ringkøbing Fjord catchment covers an area of approximately 3 500 $km^2$. It is a flat landscape, with a maximum altitude of 147 m and an average altitude of 40 m, consisting mainly of sandy soils developed on till and outwash deposits.

It includes the Skjern Å, which flows for 94 km and is Denmark's largest river in terms of volume. This river covers an area of 2 100 $km^2$ and has an average flow rate of 37 $m^3.s^{-1}$. It was the subject of a major restoration plan in the early 2000s, following initial drainage and straightening in the 1960s. Today, its waters are of fairly good quality, as evidenced by the presence of salmon.

The main land use in the catchment is agriculture, which covers 65-70% of the catchment and is dominated by pig farms. The remainder is taken up by woodland (15-20%) and other natural areas such as wetlands and heathland.

The catchment is a relatively sparsely populated area with a few urban areas, the largest being the towns of Ringkøbing, Brande, Skjern, and part of the town of Ikast.

Annual rainfall in the region averages 1 026 mm, with the wettest months being September and October and the driest April and May.

## Legislative context and environmental classification

The EU primarily regulates the water environment through the Water Framework Directive (WFD, 2000/60/EC). The purpose of the WFD is to establish a framework for the protection and sustainable management of water resources across the European Union.

Under the WFD, Ringkøbing Fjord is a coastal water body classified as a Heavily Modified Water Body (HMWB). Its current ecological potential is poor and the objective is to reach at least good ecological potential by the end of 2027. The good ecological potential of the fjord is not currently being achieved because of two indicators:

1. The concentration of chlorophyll a for the May-September period, which must be less than 8.4 $\mu g.L^{-1}$ to achieve good ecological potential;
2. The depth limit for macrophyte expansion, which must be greater than 3.1 m to achieve the good ecological potential.

# Methods

## General modelling framework

The key elements of the ecological modelling framework (EMF) applied to Ringkøbing Fjord are shown in Fig. 2.

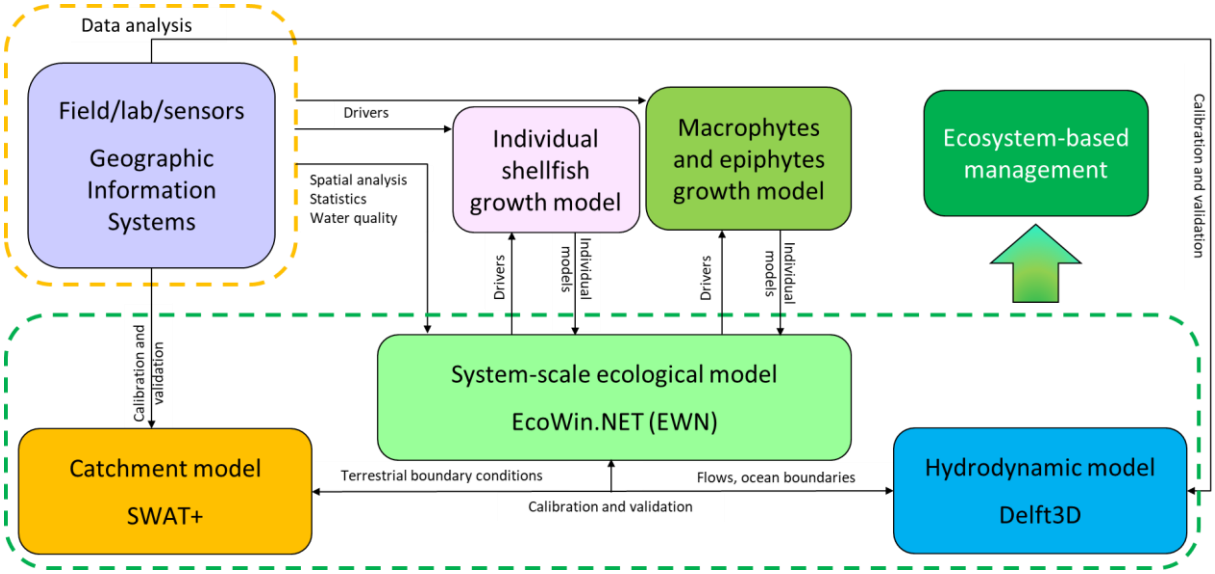


*Fig. 2. Key components of the ecological modelling framework applied to Ringkøbing Fjord.*

This EMF addresses (i) the nutrient loading from land; (ii) the circulation of water and water properties within Ringkøbing Fjord and the exchange with the North Sea through the operated sluice; (iii) the growth of shellfish inside the Fjord; (iv) the growth of macrophytes and associate epiphytes, (v) the biogeochemistry of Ringkøbing Fjord, including the role of shellfish and vegetation on ecosystem status.

*Table 3. Models, scope of application.*

| Name | Scope |
|---|---|
| Soil and Water Assessment Tool + – SWAT+ | Catchment loading of water, nutrients, organic matter, and solids |
| 3D hydrodynamic model - Delft3D | 3D detailed circulation within the bay |
| Shellfish individual growth model – AquaShell | Individual growth and environmental effects of *Mya arenaria* (sand mussel) |
| Vegetation growth model – AquaFrond | Growth of macrophytes and associated epiphytes. Risk classification for epiphytes. |
| Ecosystem carrying capacity model – EcoWin.NET | Ecosystem-scale model for the fjord, including relevant biogeochemistry |

Each model has a number of uses *per se* and addresses different management challenges, and the linkages among models allow the whole set to be leveraged for improved decision-support (Table 3).

# Data

## Catchment data

### *Land use data*

The land use map used is a Danish national map used in the 3rd River Basin Management Plan downloaded from MiljøGIS.dk. The land use map has been reclassified to match the SWAT+ land use classes (Fig. 3).

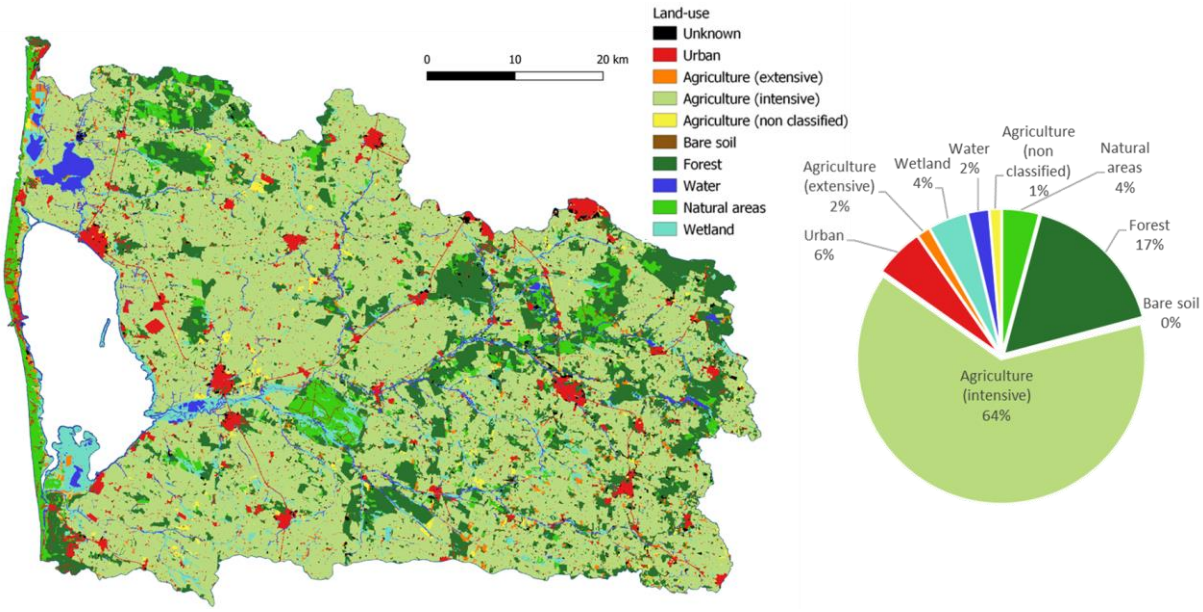


*Fig. 3. Land use of the Ringkøbing Fjord catchment.*

The agricultural area was subdivided according to data collected by the Ministry of Agriculture and compiled by SEGES Innovation for the Ringkøbing Fjord catchment area. In total 19 different crop rotations representing 10 farm types have been defined and implemented in the model (Table 4). The various crop rotations include conventional and organic farming practices. The agricultural practices including sowing date, fertilizer application, harvest date and catch crop are known for each rotation (see Annex 1). Permanent crops are also included in the model and are defined as permanent grassland.

*Table 4. List of farm types implemented in the SWAT+ model for the Ringkøbing Fjord catchment.*

| Farm type | Number of crop rotations | Area (ha) | % of agricultural area |
|---|---|---|---|
| Seed production/Frøavl | 1 | 20 959 | 0.08% |
| Potato farm/Kartofler | 1 | 1 516 026 | 5.62% |
| Cattle farm with more than 20% whole crop for fodder | 2 | 4 352 462 | 16.15% |
| Cattle farm with less than 20% whole crop for fodder | 2 | 4 341 982 | 16.11% |
| Plant farm | 4 | 4 740 201 | 17.59% |
| Pig farm with more than 80 kg N pr ha fertilizer | 4 | 4 492 188 | 16.67% |
| Pig farm with less than 80 kg N pr ha fertilizer | 1 | 6 986 | 0.03% |
| Cattle > 170 kg N | 1 | 3 196 230 | 11.86% |
| Other plants/Anden planteavl | 1 | 3 730 682 | 13.84% |
| Cattle farm with less than 80 kg N pr ha fertilizer | 2 | 179 897 | 0.67% |
| Permanent crop | n/a | 377 260 | 1.40% |

In addition, information on drained areas has been provided by the different municipalities of the Ringkøbing Fjord catchment and was included in the model setup.

### *Soil data*

The soil input data were based on the national topsoil texture map with a 250 m grid resolution (Fig. 4) derived from approximately 45 000 soil samples, interpolated using ordinary kriging (Greve et al., 2007).

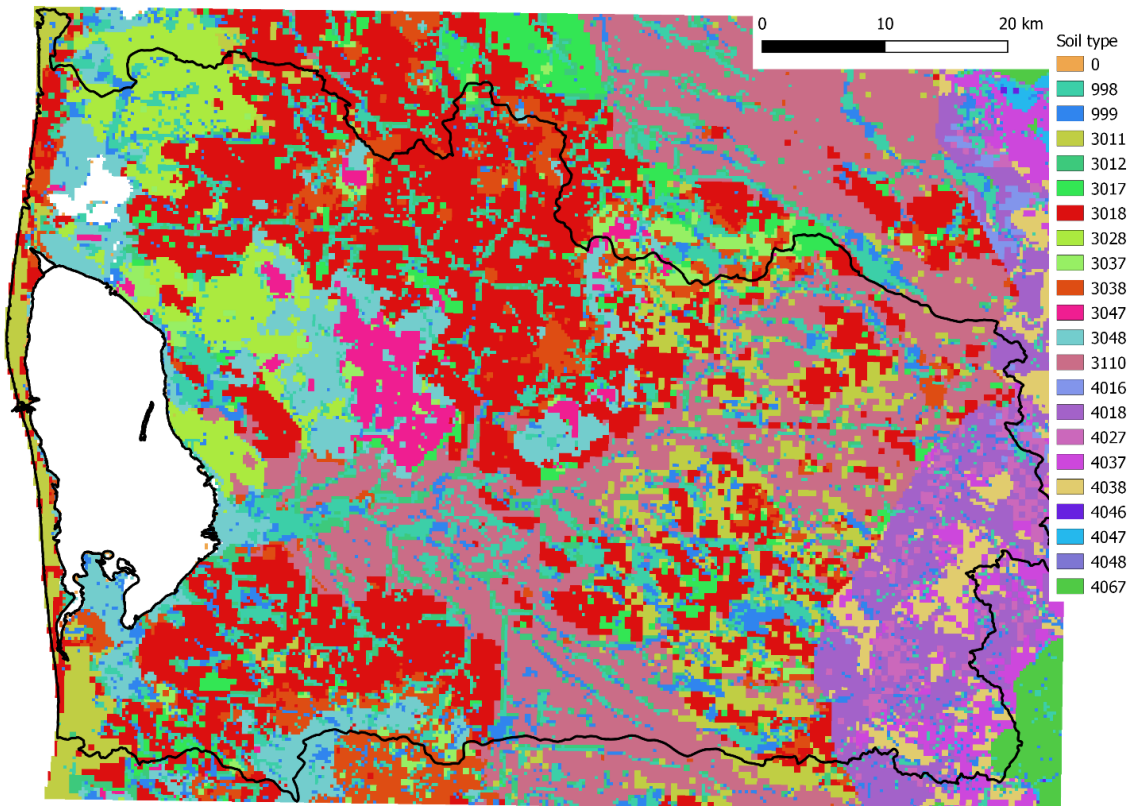


*Fig. 4. Soil map for the Ringkøbing Fjord catchment. Soil types are defined according to (Greve et al., 2007).*

### *Wastewater data*

Data on nutrient content (Tot-N and Tot-P) as well as discharge flow have been collected from utility companies and major businesses with outlets to Ringkøbing Fjord for a 5-year period from 2017 to 2022. These data have been incorporated into the catchment model SWAT+.

### *Climate data*

Daily precipitation data were obtained from the national 10 km grid (Scharling, 2001) and corrected with the Danish Meteorological Institute (DMI) precipitation correction model with the help from the Geological Survey of Denmark and Greenland GEUS. Data on daily minimum and maximum air temperatures, relative humidity, wind speed, and solar radiation were obtained for the Ringkøbing Fjord catchment area from the 10 km DMI dataset.

### *Streamflow and water quality data*

The simulation of the streamflow is calibrated against data collected in a selection of hydrometric stations. Stations for which more than 5 years of daily data are available for the period 2012-2020 were selected. Two stations for which the quality of the data is least good according to the Danish Environmental Protection Agency (Miljøstyrelsen) have been withdrawn from this selection.

Twelve to 18 measurements per year are available for the same station used for flow calibration and validation. Measured parameters include nitrate + nitrite load ($NO_3$+$NO_2$), total nitrogen load (TN), phosphate load ($PO_4$) total phosphorus load (TP) and suspended sediment load (SS).

### Hydrodynamic data

Water level data were used to calibrate and validate the hydrodynamic model. Three stations record the water level in the fjord: Hvide Sande, next to the sluice, Ringkøbing in the northern part, and Bork in the southern part of the fjord (Fig. 5).

Conductivity, temperature, and depth (CTD) profiles were also used to calibrate and validate the hydrodynamic model. Fortnightly profiles are available for three stations in the fjord (Fig. 5).

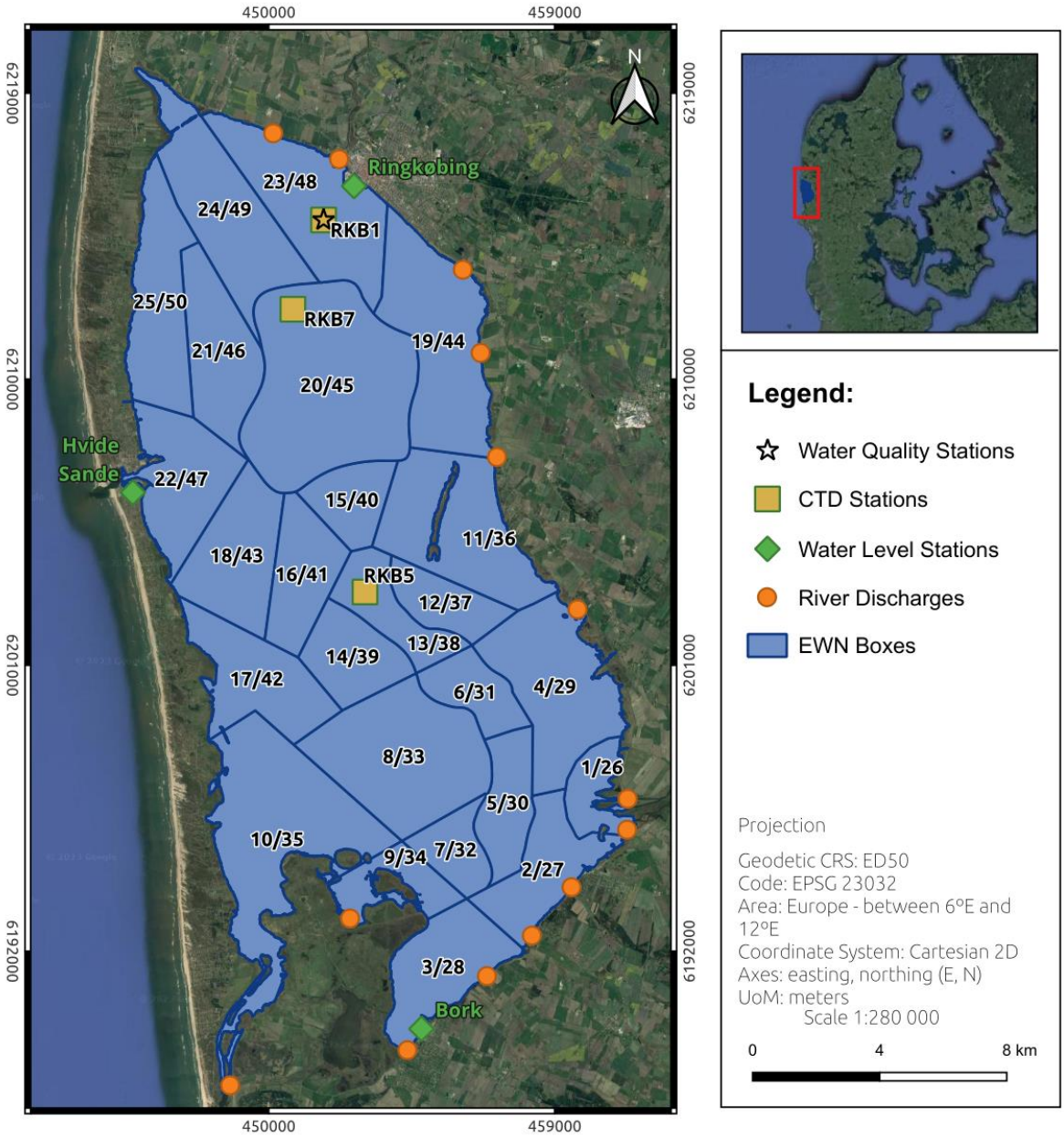


*Fig. 5. Ringkøbing Fjord, showing monitoring stations, river discharges, and EcoWin.NET boxes (labelled 1-25 for boxes in the upper layer of the water column and 26-50 for the lower layer).*

## Water quality and benthic data

Water quality data from 2010 are only available at one site, RKB1 (Fig. 5), at monthly or fortnightly intervals. They include measurements of concentration for nitrate + nitrite ($NO_3$+$NO_2$), total nitrogen (TN), phosphate ($PO_4$), total phosphorus (TP), total suspended matter (TPM), and particulate organic matter (POM). TPM and SPM are only available until 2015.

Data on *Mya arenaria* biomass and densities are available for 15 to 20 sampling locations and for 1 to 3 occurrences per year. These data are highly variable and, in order not to include errors due to the spatial interpolation method, the median value was considered to be an appropriate representation of *Mya arenaria* density in Ringkøbing Fjord.

Several vegetation transects have been sampled in Ringkøbing Fjord, but they provide qualitative rather than quantitative information and cannot be used to parameterise the macrophyte and epiphyte model.

## Model box definition

For ecological modelling with EcoWin, Ringkøbing Fjord Lough was divided into simulation areas or model boxes (Fig. 5). Ideally, the system should be subdivided into enough boxes to take into account spatial heterogeneity, but without making the model excessively complex, which might limit its subsequent utility.

In practice, achieving a balance between these goals requires a detailed analysis of the spatial variability of the system. The methodology used to achieve this relied on assessing several spatial heterogeneity criteria. For Ringkøbing Fjord, the following criteria were applied:

- bathymetry;
- salinity gradients;
- river discharge locations;
- benthic sampling locations

A first approach for defining homogenous regions using these criteria was then submitted to the Coastal Water Council for approval.

The boxes were also subdivided into a lower and an upper layer, due to the observed vertical stratification of salinity and currents depending on exchanges with the North Sea and streamflow. The subdivision was achieved using a sigma layer approach, where the boundary between upper and lower boxes was set in the upper one-third of the total depth. This resulted in 50 boxes, 25 for surface waters and 25 for bottom waters.

## Hydrological modelling

SWAT+, which stands for "Soil and Water Assessment Tool Plus," is an advanced hydrological model used for assessing and simulating the complex interactions between land use, climate, and water resources within a specific watershed or river basin. SWAT+ is an enhanced version of the well-known SWAT model (Soil and Water Assessment Tool), developed to provide more robust and flexible capabilities for addressing contemporary water resource management challenges.

SWAT+ is a powerful tool that helps water managers understand and predict various aspects of the hydrological cycle, including rainfall, runoff, erosion, sediment transport, and nutrient loading (Bieger et al., 2017). It takes into account factors such as land cover, soil types, land management practices, and climate data to model how these elements impact water quality and quantity. This information is crucial for making informed decisions related to land use planning, water resource management, and environmental conservation. SWAT+ was chosen for its advanced features to simulate nutrient loadings from the Ringkøbing Fjord catchment.

### SWAT+ model setup

The catchment delineation of the Ringkøbing Fjord catchment area was performed using the national Digital Elevation Model (DEM) with a 25x25 m resolution.

The simulated catchment of Ringkøbing fjord has an area of 3 372 $km^2$. The outlets of each subbasin have been placed according to the location of the existing gauging stations. The catchment delineation results in the creation of 109 subbasins with an average area of 31 $km^2$. Those 109 subbasins have been subdivided into smaller drained areas and separated between upslope and floodplain area, leading to the creation of 433 landscape units in total. There are 14 outlets discharging into the fjord that are input into the fjord ecosystem model, the largest of which corresponding to the Skjern river. There are 9 lakes integrated in the model delineation, including the Stadil Fjord.

*Table 5. Characteristics of the catchment delineation for the Ringkøbing Fjord watershed.*

| Characteristic | Value |
|---|---|
| Simulated area ($km^2$) | 3 372 |
| Number of subbasins | 109 |
| Number of landscape units | 433 |
| Contact points with the coastal model | 14 |
| Number of lakes | 9 |

The main characteristics of the catchment delineation are shown in Table 5 and the delineation is shown in Fig. 6.

In order to better simulate the hydrological processes, the shallow aquifer, usually simulated as a single unit, was divided into a slow and a fast aquifer in this application of the SWAT+ model to Ringkøbing Fjord catchment. This division has already been used to improve hydrological processes simulation in rural lowland areas (Wagner et al., 2022) such as the Ringkøbing Fjord catchment.

A good representation of wetlands role is a key feature for the outcomes of this study. In SWAT+, wetlands are simulated as individual units for which water and nutrients retention are calculated.

However, in the default SWAT+ settings, the water enters the wetland units through surface runoff and rainfall only. This was considered to not accurately reproduce the reality of the Ringkøbing Fjord catchment where wetlands can also be supplied with groundwater flow. For this reason, a dedicated connectivity structure was specifically developed for the application of SWAT+ to the Ringkøbing Fjord catchment. A fraction of the upland fast shallow aquifer outflow is now connected to the wetland

units located in the floodplain area. This fraction corresponds to the percentage of cover of the wetland area units in the floodplain area. This modification allows to better represent the reality and to better assess the impact of wetlands on the nutrient exports in Ringkøbing Fjord catchment.

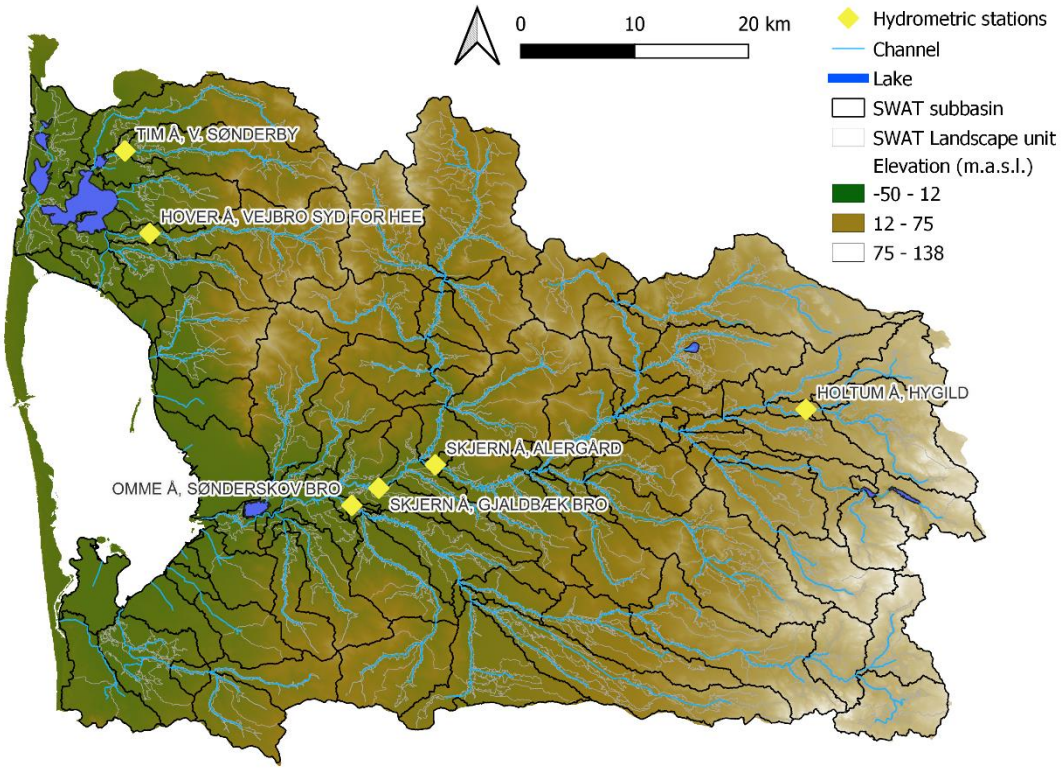


*Fig. 6. SWAT+ Catchment delineation of the Ringkøbing Fjord catchment.*

The model is run for the 2008-2019 period with a 4-year spin-up period. The model outputs were analysed from 2012 onward so as not to be affected by the shift in the rainfall data collection reported to have occurred in 2011.

## Model calibration and validation

Hydrological models such as the SWAT+ model require calibration. This means that the parameters controlling different processes (evaporation, runoff, nutrient cycling, etc.) must be tuned to correctly represent reality. The calibration of the model can be separated in two main steps: (i) calibration of the streamflow (water quantity) and (ii) calibration of the water quality (suspended and dissolved mass loads and concentrations). The results of the model are compared with the observations and the different parameters are adjusted until they converge. The model is then validated by comparing simulation results with independent observations.

### *Streamflow*

The streamflow was calibrated and validated for 5 selected hydrometric stations located over the Ringkøbing Fjord catchment The station with the largest recorded streamflow is “Skjern Å, Gjaldbæk Bro”, located on the Skjern river, the main river of the Ringkøbing Fjord catchment. The five stations selected cover 70% of the simulated area of the Ringkøbing Fjord catchment, which ensures good coverage of the simulated area and increases confidence in the model results.

The simulation of the streamflow was calibrated against data collected in a selection of hydrometric stations. Stations for which more than 5 years of daily data were available for the period 2012-2020 were selected. Two stations for which the quality of the data is the least good according to the Danish Environmental Protection Agency (Miljøstyrelsen) have been withdrawn from this selection. Finally, the streamflow is calibrated and validated for 5 selected hydrometric stations located over the Ringkøbing Fjord catchment (Fig. 6). The station with the largest recorded streamflow is "Skjern Å, Gjaldbæk Bro", located on the Skjern river, the main river of the Ringkøbing Fjord catchment. The five stations selected cover 70% of the simulated area of the Ringkøbing Fjord catchment, which ensures good coverage of the simulated area and increases confidence in the model results.

The performance of the model was assessed using the Nash-Sutcliffe efficiency criteria (NS) and the percent bias (PBIAS) which are commonly used in hydrology. The model performance was evaluated based on Moriasi *et al*. (2015) classification that ranges from *Non-Satisfactory* to *Very Good*. The dataset is split between a calibration (2012-2015) and a validation period (2016-2019). Model performances are summarised in Table 6. Of the 20 measurements calculated, 4 indicate *Very Good* model performance, 9 *Good* model performance, 4 *Satisfactory* model performance and only 3 *Non-Satisfactory* model performance. Model performance was never rated *Non-Satisfactory* for all 4 measurements calculated at each station. Model performance is the lowest for the "Hover Å Vejbro Syd For Hee" station, which covers the smallest drainage area of the 5 stations. Model performance for the largest station is rated from *Good* to *Very Good*. Fig. 7 and Fig. 8 show the time series of observed and simulated water discharge. Overall, the model results are satisfactory. The good flow reproduction for all stations and in particular for the station covering the largest catchment area gives good confidence in the model results and subsequent conclusions regarding the project objectives.

*Table 6. SWAT+ model performance for the calibration and validation period. The model performance according to Moriasi et al. (2015) classification is indicated in parenthesis.*

| Station | NS calibration | NS validation | PBIAS calibration | PBIAS validation |
|---|---|---|---|---|
| Hover Å Vejbro Syd For Hee | 0.52 (*Satisfactory*) | 0.48 (*Non-Satisfactory*) | 3.6 (*Very Good*) | 17.0 (*Non-Satisfactory*) |
| Omme Å Sønderskov Bro | 0.75 (*Good*) | 0.76 (*Good*) | 14.8 (*Satisfactory*) | 16.9 (*Non-Satisfactory*) |
| Skjern Å Alergård | 0.72 (*Good*) | 0.72 (*Good*) | 8.7 (*Good*) | 9.6 (*Good*) |
| Skjern Å Gjaldbæk Bro | 0.78 (*Good*) | 0.78 (*Good*) | 2.6(*Very Good*) | 4.9(*Very Good*) |
| Tim Å V Sønderby | 0.51 (*Satisfactory*) | 0.63 (*Satisfactory*) | -4.8(*Very Good*) | 2.4(*Very Good*) |

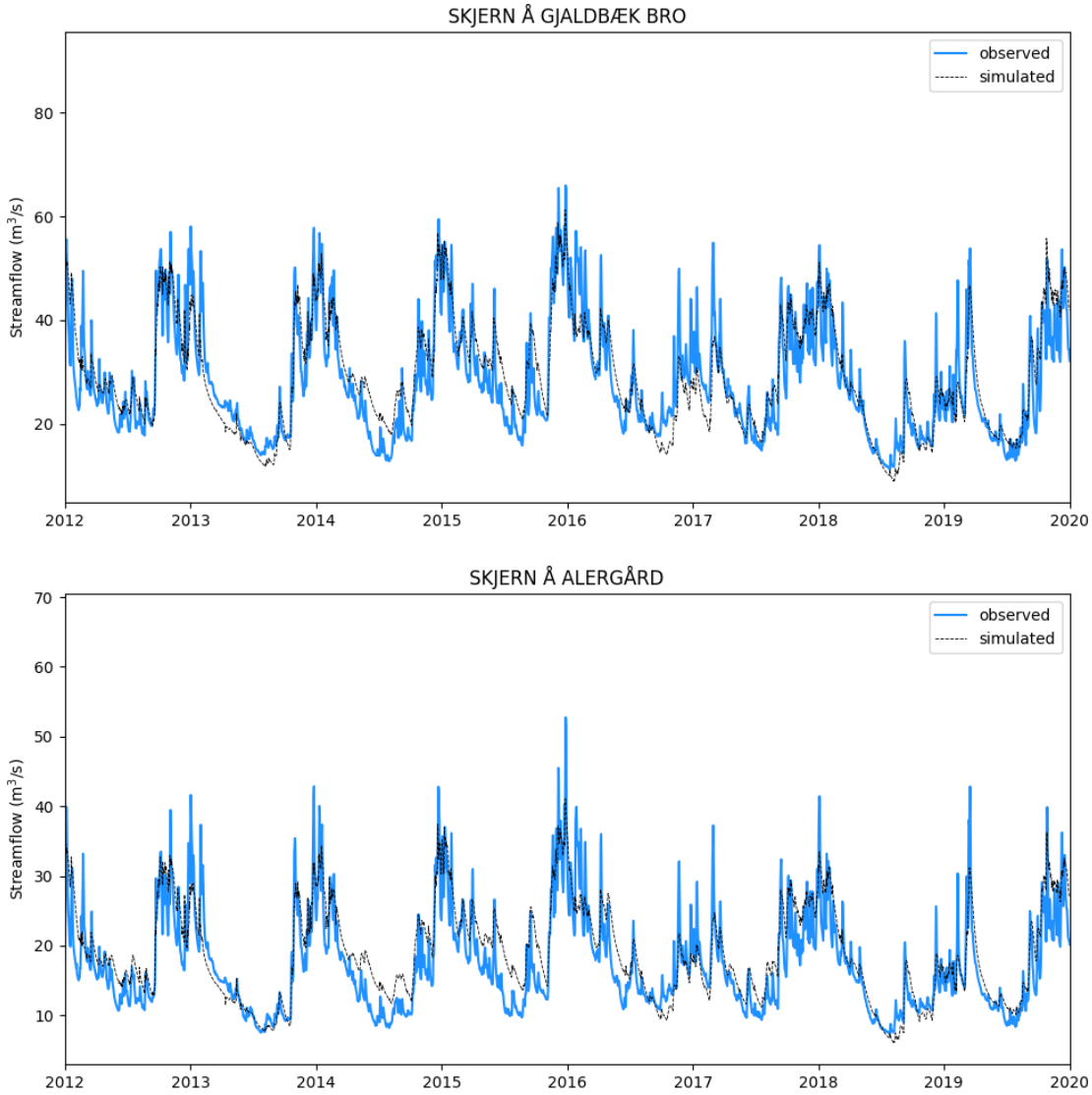


*Fig. 7. Time series of the observed and SWAT+ simulated streamflow for the 01/01/2012 to the 31/12/2019 period at Skjern Å Gjaldbæk Bro and Skjern Å Alergård.*

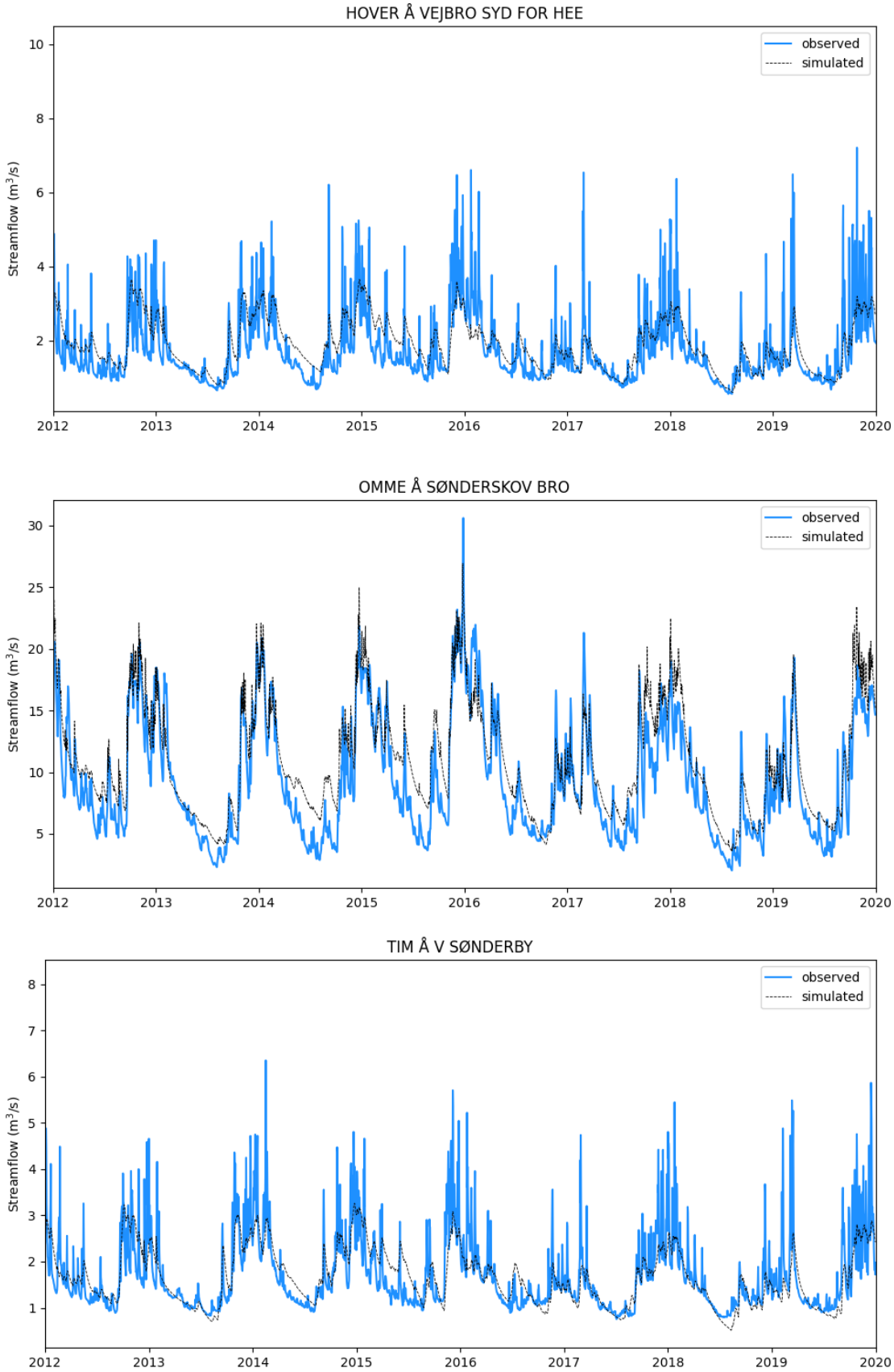


*Fig. 8. Time series of the observed and SWAT+ simulated streamflow for the 01/01/2012 to the 31/12/2019 period at Hover Å Vejbro Syd For Hee, Omme Å Sønderskov Bro and Tim Å V Sønderby.*

### *Water quality*

The model was calibrated and validated for nitrate + nitrite load (NO3+NO2), total nitrogen load (TN), phosphate load (PO4) total phosphorus load (TP) and suspended sediment load (SS). Twelve to 18 measurements per year are available for the same station used for flow calibration and validation and these data were used to calibrate and validate the model. Since the frequency of measurements is much lower than that of streamflow, the performance of the model cannot be reliably assessed by calculating the performance parameters that are used for larger data sets. Instead, model performance is in this case assessed by expert visual analysis of time series of simulated and observed nutrient and sediment loads.

The results are presented for the main station "Skjern Å Gjaldbæk Bro" in Fig. 9 to Fig. 11.

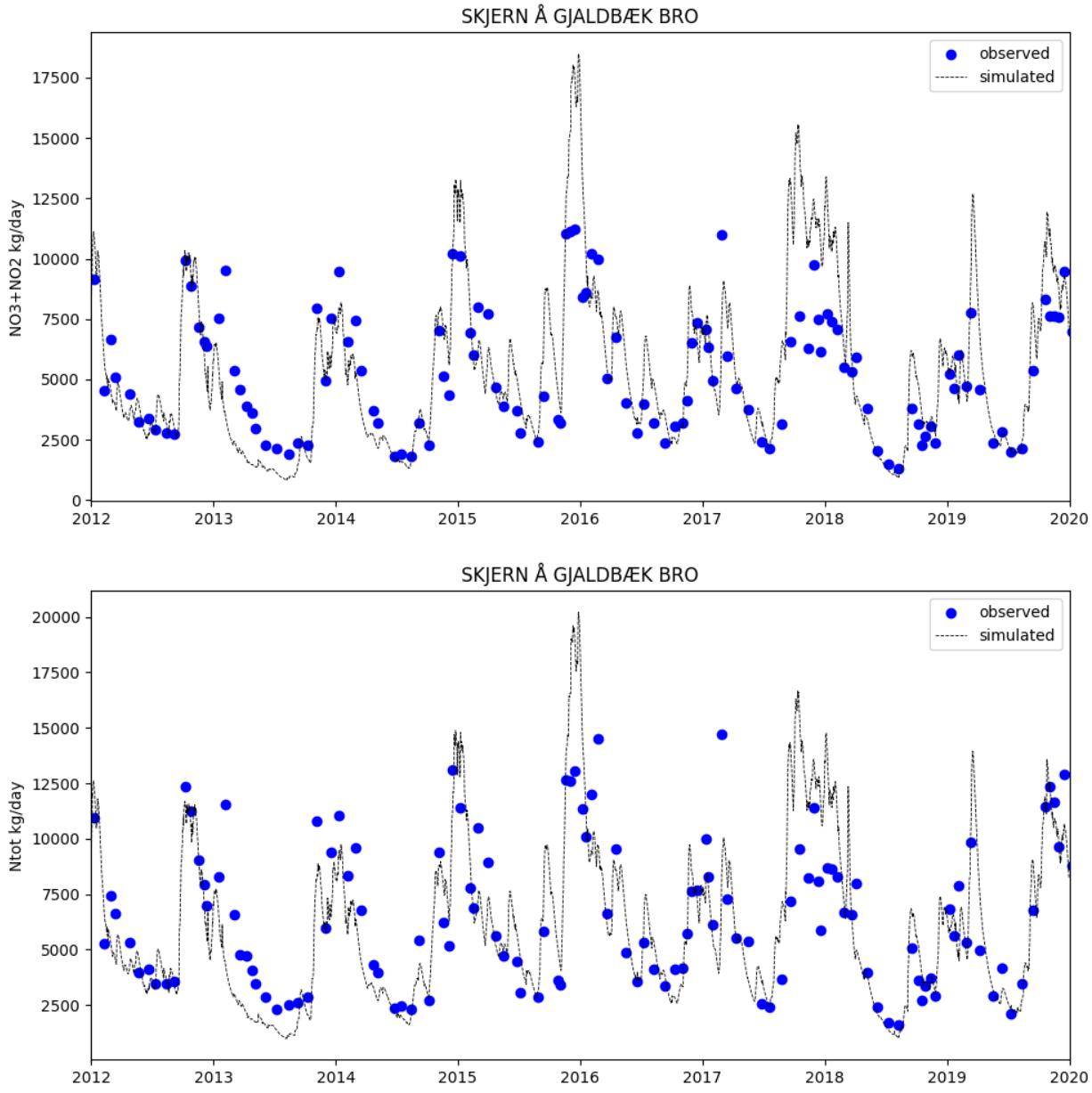


*Fig. 9. Simulated and observed loads for nitrate and nitrite (top) and total nitrogen (bottom) for the Skjern Å Gjaldbæk Bro station.*

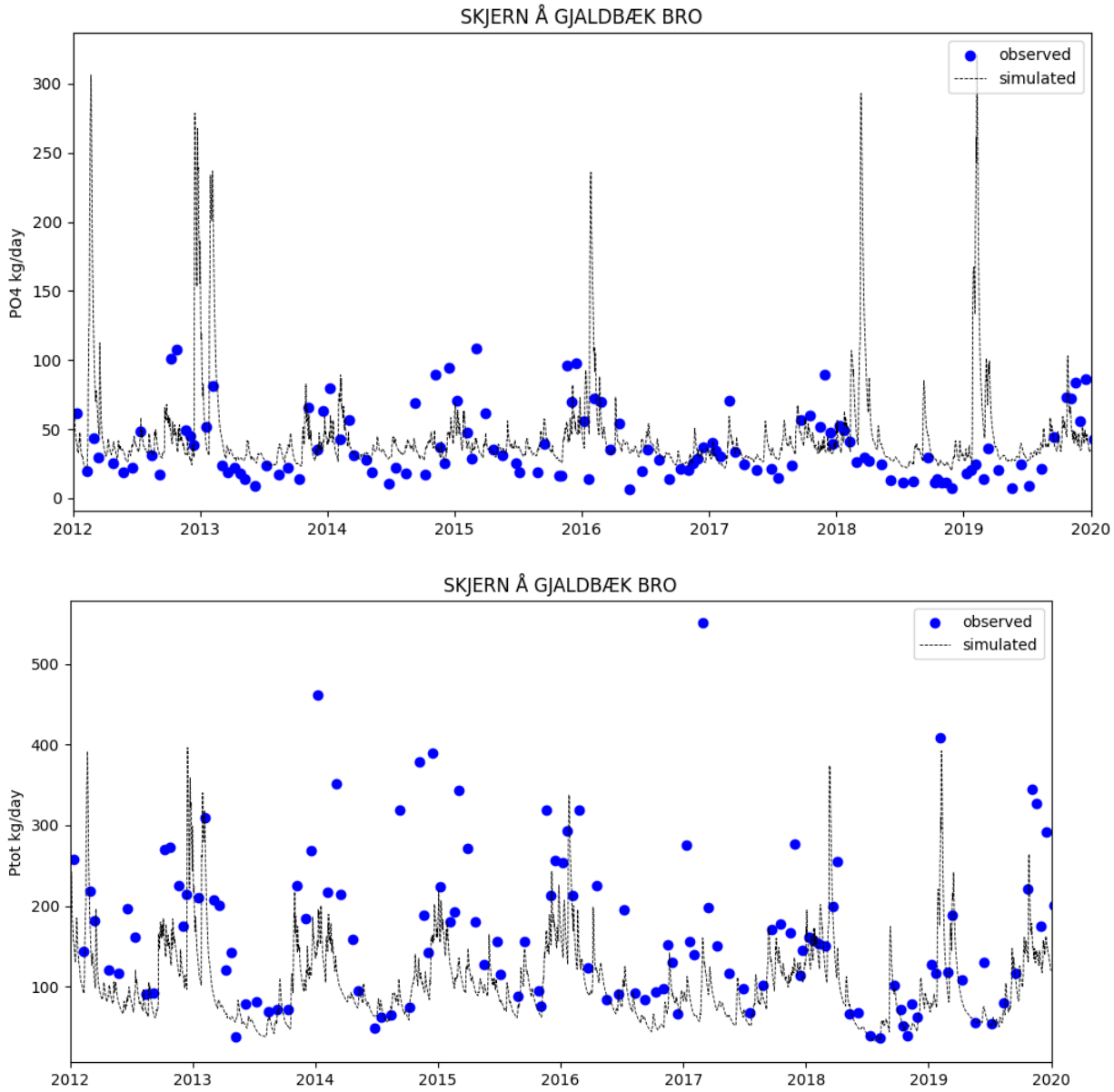


*Fig. 10. Simulated and observed loads for phosphate (top) and total phosphorus (bottom) for the Skjern Å Gjaldbæk Bro station.*

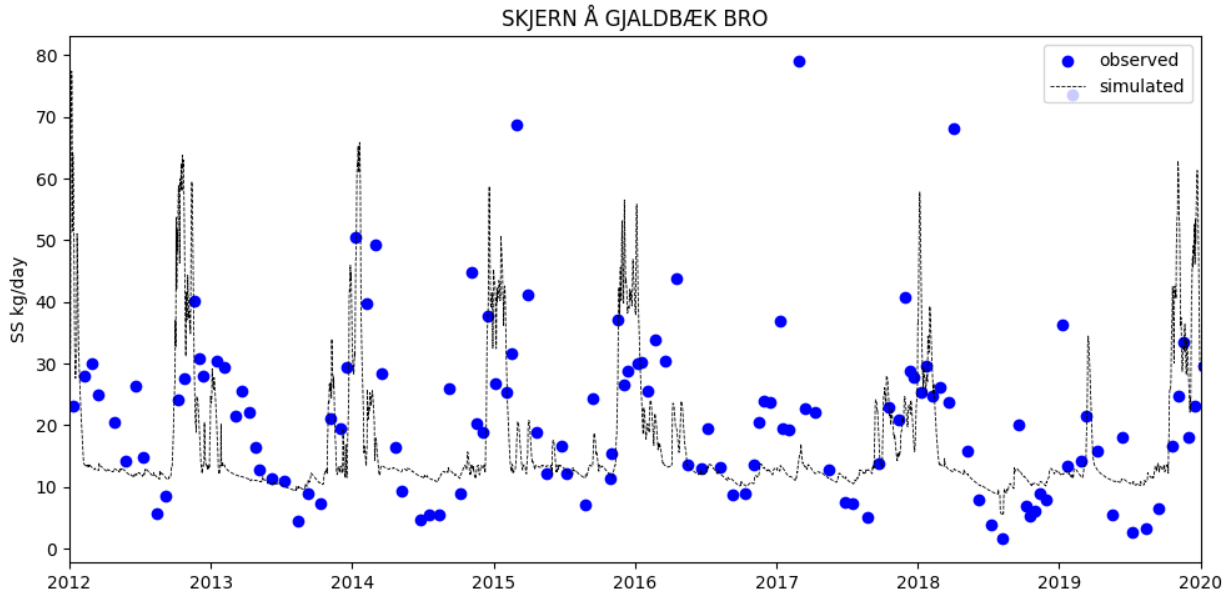


*Fig. 11. Simulated and observed suspended sediment loads for the Skjern Å Gjaldbæk Bro station.*

The simulation of nutrients is reasonably good for all the parameters but is especially satisfactory for NO3+NO2 and TN loads for which seasonal patterns are well simulated. This good model performance is due in particular to the good knowledge of land-use management practices in the catchment area.

The simulation of PO4 loads is generally underestimated and that of TP overestimated, although the seasonal pattern is partially reproduced for both parameters. Results for phosphorus loads are expected to be less accurate than those for nitrogen, given that phosphorus behaves in a more complex way in the environment than nitrogen.

The suspended sediment simulation reproduces well the range of loads observed and the timing of peaks. Suspended sediment transport is influenced by the hydrodynamic conditions of rivers and streams. Modelling the interactions between water flow, sediment transport and river morphology requires a detailed understanding of the hydraulic properties of the system, which can be difficult to capture accurately.

Although data on agricultural practices are relatively detailed for the Ringkøbing Fjord catchment, it is difficult to know exactly when and how much fertiliser is applied to the agricultural plot. Since it is able to reproduce overall seasonal patterns, the nutrient simulation can be considered satisfactory in terms of the project's objective of simulating the loads reaching the fjord.

### *Nutrient retention in wetlands*

Ensuring the accurate simulation of wetland effects on nutrient loads is crucial for the outcomes of the project, as wetland restoration constitute a key measure under consideration for nutrient mitigation in the Ringkøbing Fjord catchment. The primary challenge lies in the absence of data for wetland parameterization and the calibration/validation of the wetland-related processes. Furthermore, the diverse nature of wetlands in terms of area, morphology, and connectivity to the river network adds complexity to this endeavour.

To address the data gap, model results have been cross-referenced with findings from recent studies on nutrient retention in wetlands. Specifically, a study conducted by Audet et al. (2020) investigated nitrogen and phosphorus retention in restored Danish wetlands, including a wetland within the Ringkøbing Fjord catchment (Tim Enge). The study identified a relationship between total nitrogen (TN) removal and TN load. By comparing our model results for the entire Ringkøbing catchment with this established relationship, we found our values aligning within the expected range (Fig. 12). This comparative analysis significantly increases our confidence in the model's ability to accurately reproduce the impact of wetlands on nutrient loads.

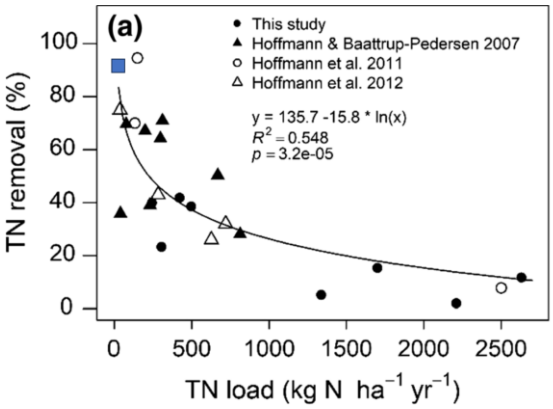


*Fig. 12. Total nitrogen removal (%) versus TN load per surface area of restored wetland from Audet et al. (2020). The blue square represents the average of the values obtained for the wetlands simulated with the SWAT+ model applied to the Ringkøbing Fjord catchment.*

Moreover, the satisfactory representation of TN loads and the development of a specialized methodology for assessing wetland connectivity with groundwater further contribute to the overall reliability of the model. These factors collectively support the reliability of the model's predictions and its capacity to effectively capture the influence of wetlands on nutrient dynamics in the Ringkøbing Fjord catchment.

However, while the model provides a good estimation of the role of wetlands in nutrient retention at the catchment scale, it is not advisable for assessing site-scale impacts. The intricacies of wetland characteristics, which vary widely in terms of size, morphology, and connectivity within the catchment, suggest that a more detailed, case-by-case study is necessary to comprehensively understand and assess the site-specific impacts of wetlands on nutrient dynamics. Therefore, caution should be exercised when extrapolating these catchment-scale results to specific individual sites, as the model's generalization may not capture the nuanced variations present at smaller spatial scales.

## Conclusion

The calibration and validation procedure on the SWAT+ model developed for the Ringkøbing Fjord catchment allows us to conclude the following:

- Streamflow simulations exhibits a *Satisfactory* to *Very Good* fit for 9 out of the 12 calculated metrics, with the streamflow simulation at the largest station being rated from *Good* to *Very Good*;
- The model accurately represents the seasonal variation of nitrogen loads indicating that processes related to nitrogen are well taken into account in the model;
- The model reasonably represents the phosphorus and suspended sediment loads, considering the inherent complexity of the processes governing the transport of these parameters. This suggests that the model correctly reproduces the annual loads of phosphorus and suspended sediment from the catchment;
- The model simulates nitrogen retention rates in wetlands in agreement with published results and is expected to accurately estimate the impact of wetlands on nitrogen loads at the catchment scale.

Given all the above, we consider that (i) the model is well-suited to provide land-based nutrient and suspended sediment loads for ecosystem modelling of Ringkøbing Fjord with EcoWin, and (ii) the model is capable of predicting changes in nutrient loads under scenarios affecting land use change, including wetland restoration.

## Hydrodynamic modelling

The main objectives of the Delft3D-Flow model are to simulate the lagoon dynamics inside Ringkøbing Fjord and the lagoon's connection with the neighbouring North Sea. The products of this work can either be used together with other Deltares tools, such as DELWAQ or be included in the ecosystem modelling framework for Ringkøbing Fjord, bridging between the SWAT+ (Soil and Water Assess Tool) catchment model and the EcoWin.NET ecological model.

This section describes the development of the Delft3D-FLOW model for the Ringkøbing Fjord which includes the model setup, calibration and validation of water levels and salinity.

The simulation software that is used is Delft3D-Flow developed by Deltares in the Netherlands over the last three decades (Deltares, 2010; Lesser et al., 2004). The version used in this study allows for the modelling by means of curvilinear grids. The terrain-following vertical coordinates it uses together with advanced turbulence close methods, improves the simulation of stratification and mixing processes at shallow depths.

### Calibration and validation procedure

The assessment of the model performance was made along three vectors, namely statistical point-to-point assessment and qualitative assessment. The strategy of implementing a model representing the response to atmospheric, catchment inputs and artificial operation of the exchange with the North Sea serves the purpose of allowing for a calibration strictly done at the hydrodynamic level. Thus, transport is only validated by comparing salinity at a stage that the model is independent from the initial condition. For that, the model was spun-up between the 1$^{st\ of}$ September and the 31$^{st}$ of December of the year before the simulation, from uniform water level and velocity, and with uniform salinity. A calibration run was performed for 2017 and validation was made for 2019. Due to the limited variables observed routinely in the lagoon, water level was the only parameter available to allow a quantitative analysis. Salinity was used qualitatively to ascertain the exchange with the North Sea and to determine the capability of the model to express stratification observed in CTD profiles.

Three statistical estimators were used to assess the model's water level fitness: Root Mean Square Error (RMSE), skill and bias. RMSE is expressed in meters and bias as percentage of the total water level range at a given station.

Skill is defined by Willmott (1981):

$$1 - \frac{\sum |model - obs|^2}{\sum \left( |model - \overline{obs}| + |obs - \overline{obs}| \right)^2}$$

where the horizontal bar represents a temporal mean. Perfect agreement between model results and observations will yield a skill of one and complete disagreement yields a skill of zero. This fitness estimator is akin to $r^2$ correlations but has the advantage of correcting the inflation of correlation coefficients due to the autocorrelation of the variable. Skill values higher than 0.95 should be considered representative of an excellent agreement between model results and observations.

### Physical conditions

Ringkøbing Fjord is a shallow estuary in the western part of Denmark. The fjord is approximately 30 kilometres long and 10-15 kilometres wide. It has an area of almost 300 square kilometres and is on average just under 2 metres deep. The deepest place in the fjord is approximately 6 metres. Ringkøbing Fjord drains approximately 9 percent of Denmark's area, including the Skjern Å catchment.

The fjord can be described as artificial since it is a sluice fjord where the water level in the fjord and the water exchange with the North Sea are actively regulated via a lock at Hvide Sande based on an adopted lock practice. Compared to the North Sea, the water in the fjord is relatively fresh, as a result of a large influx of fresh water from Skjern Å, which drains a large part of West Jutland.

The flow through the sluice enters at a significantly higher salinity, with values higher than 30 PSU when the water inside is often lower than 10 PSU. This causes a marked stratification that generates a saline bottom gravity plume that spreads through the lagoon until it is eroded by vertical wind mixing.

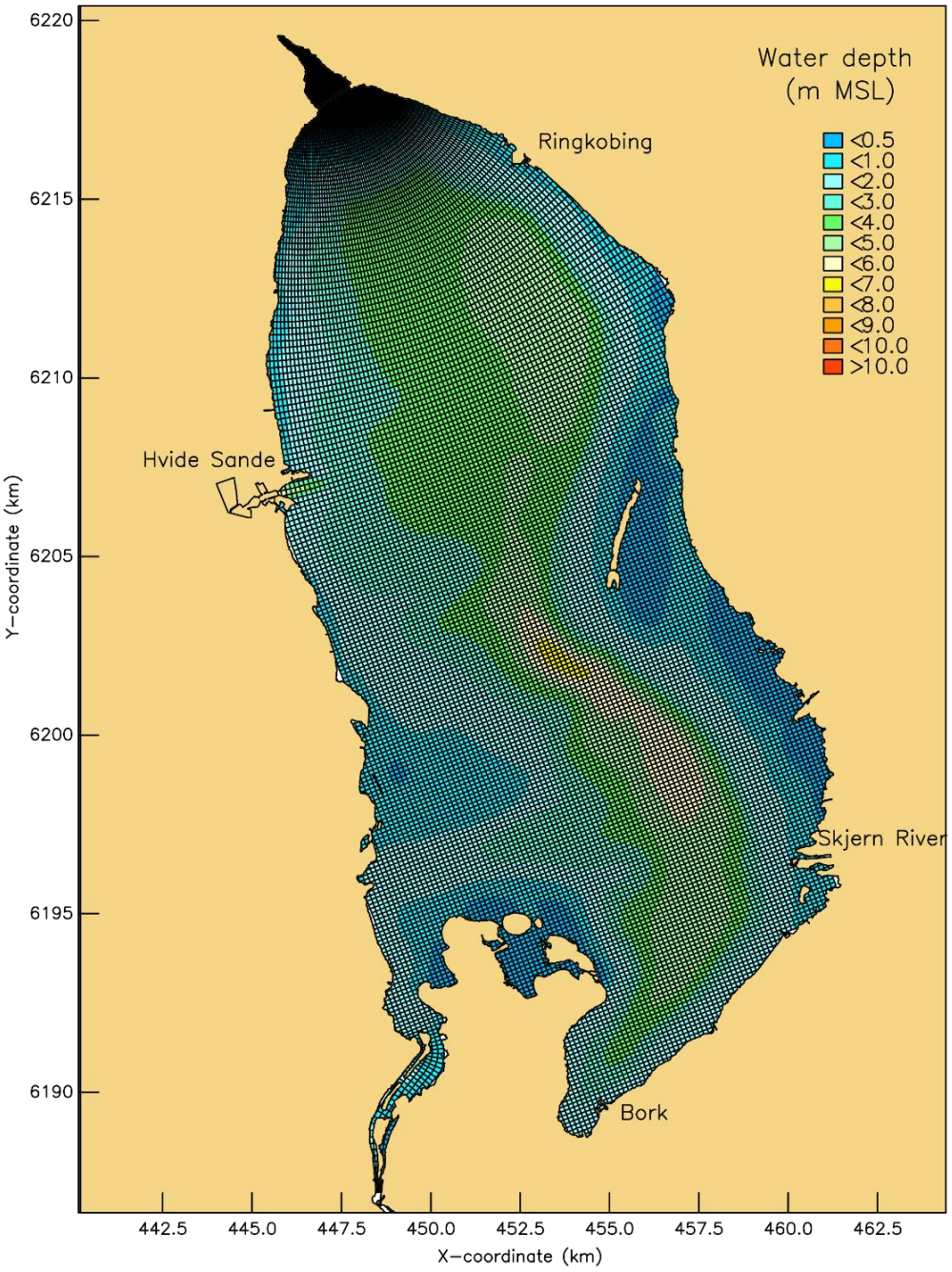


*Fig. 13. A view of the bathymetry and grid for Ringkøbing Fjord.*

## Computational grids and bathymetry

The computational grid has 114 by 278 grid cells in the horizontal and 12 layers in the vertical. The vertical grid has a refined resolution at the bottom to allow for the correct development and erosion of heavy salinity plumes. For the horizontal grid sizes in the southern part are 132 m by 116 m. Opposite the sluice, the grid sizes are 140 m by 140 m which is slightly larger than the total width of the sluice area. Further north, the grid cells are 40 m by 100 m. The overall grid with bathymetry is shown on Fig. 13. The model is set up in WGS84 UTM 32 N coordinates and depths are relative to mean sea level. Bathymetry supplied by DHI is dated from 1990, gridded with 10 m resolution and with the unique identifier f163d21f-dd92-40a5-805c-e6ecbc08ef39.

## Model parametrization

The hydrodynamics in the estuary are driven by freshwater inflow from rivers, inflow and outflow through the sluice at Hvide Sande and winds. The discharge of water through the sluice has been calculated using the zero-dimensional model described in Nielsen et al. (2005). This model uses the water level differences in the North Sea and fjord to determine the discharge through the sluice. These discharges are then used in Delft3D-Flow as sources and sinks. Examples of these discharges for the first four months of 2017 and 2019 are shown in the top panels of Fig. 14 and Fig. 15.

River flow is included for the Skjern River draining into the estuary and a total of 13 other smaller rivers and inflows using the SWAT+ model quantity. The total freshwater inflows for the first four months of 2017 and 2019 are also shown in the top panels of Fig. 14 and Fig. 15.

Hourly wind speed and wind direction were also provided to the model and are also shown in Fig. 14 and Fig. 15. These were obtained from DMI's met station at Hvide Sande.

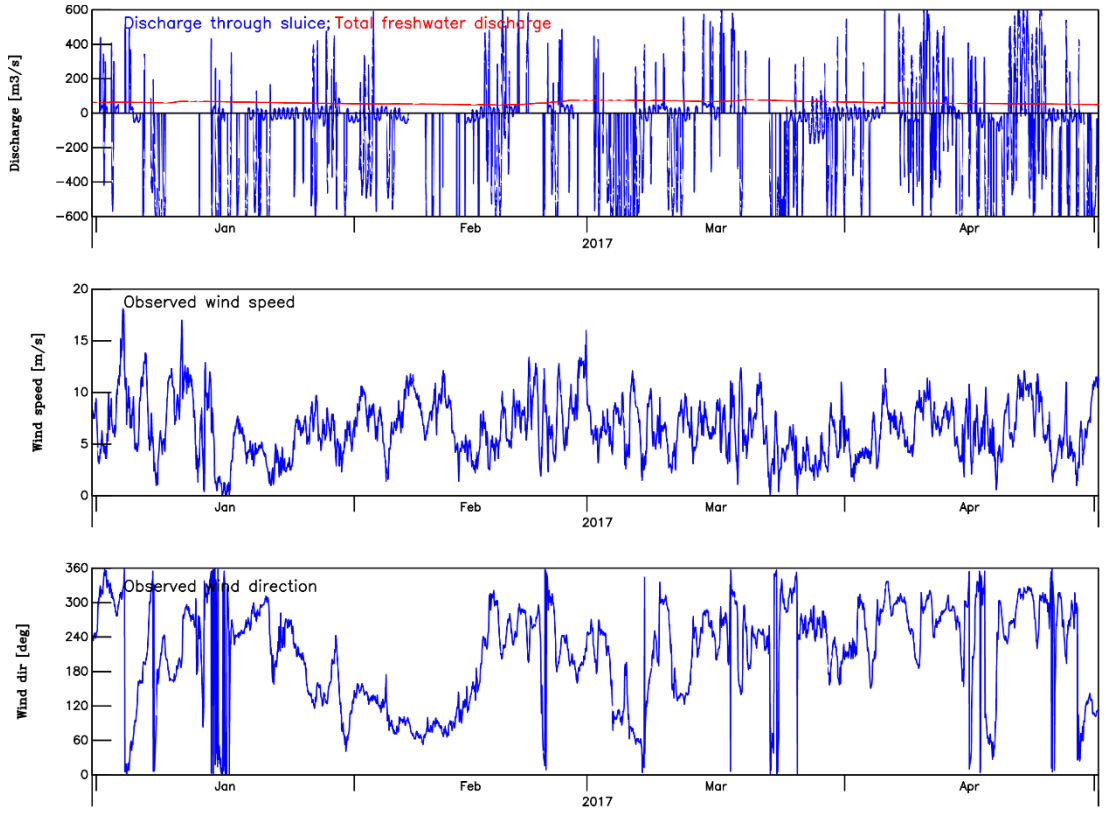


*Fig. 14 Discharge through the sluice and total freshwater inflow (top panel) and wind speed (centre panel) and wind direction (bottom panel) for part of 2017.*

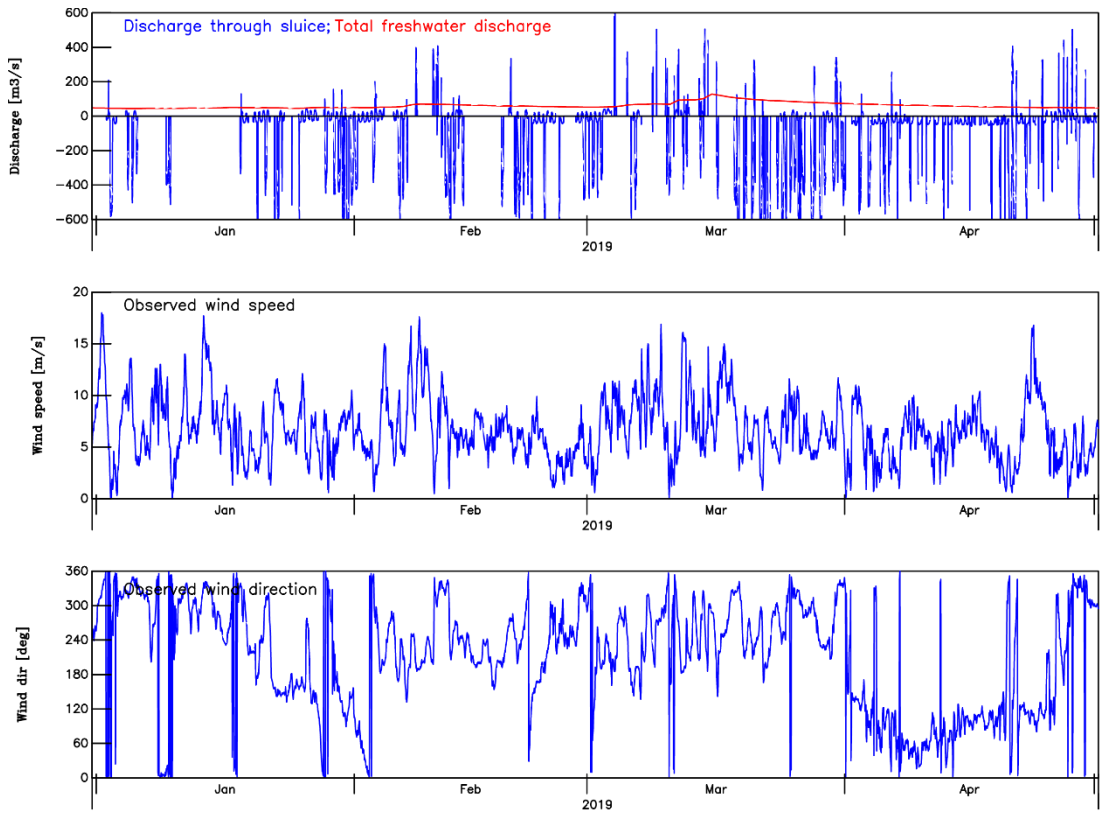


*Fig. 15. Discharge through the sluice and total freshwater inflow (top panel) and wind speed (centre panel) and wind direction (bottom panel) for part of 2019.*

Bottom friction is modelled with a Chézy coefficient obtained from the White-Colebrook formulation defined by the Nikuradse roughness length which is set to $k_s$=0.1 m. Some of the modelling parameters are provided in Table 7.

*Table 7. Hydrodynamic model parameters.*

| Parameter | Value / Setting |
|---|---|
| Horizontal eddy viscosity | 1 $m^2s^{-1}$ |
| Bottom roughness formulation | White-Colebrook |
| Roughness length | 0.1 m |
| Threshold depth | 0.1 m |
| Time step | 1 minute |

## Calibration and validation

The comparison between the simulated water levels from Delft3D-Flow and measurements at three locations within the estuary are shown in Fig. 16 for 2017 and in Fig. 17 for 2019. The measurements are from water level stations at Hvide Sande, Ringkøbing in the northern part and Bork in the south. For both years the modelled water levels compare very well to the measurements with 2019 being the better comparison of the two years.

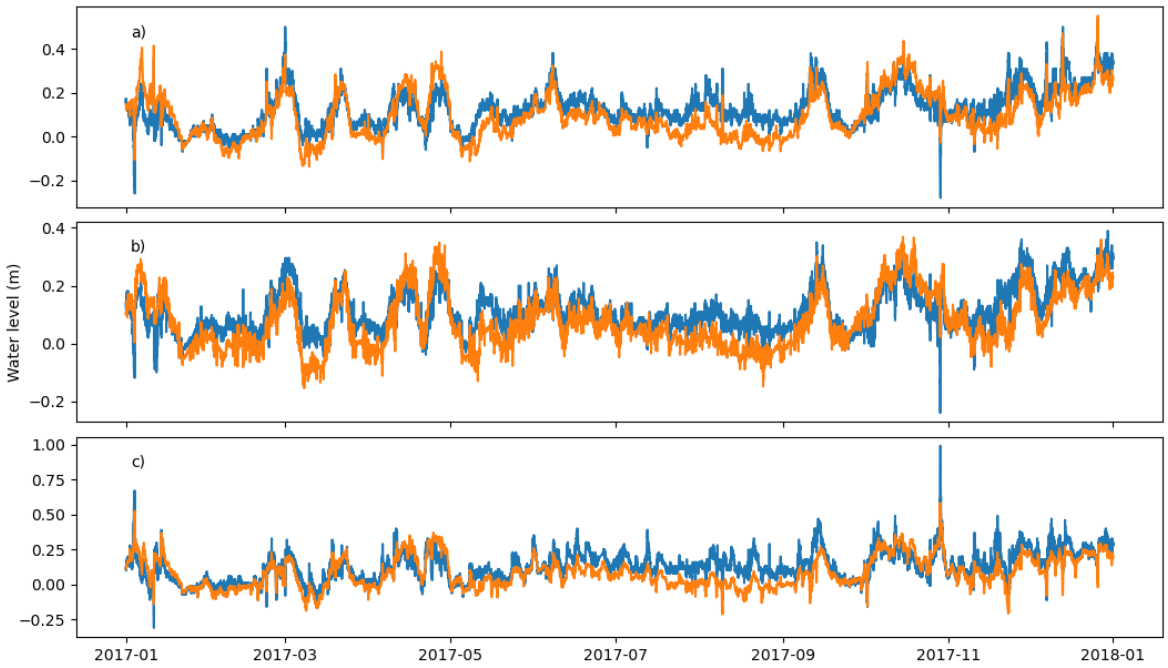


*Fig. 16. Comparison between simulated (orange) and measured (blue) water levels at Ringkøbing (a), Hvide Sande (b) and Bork (c) for 2017.*

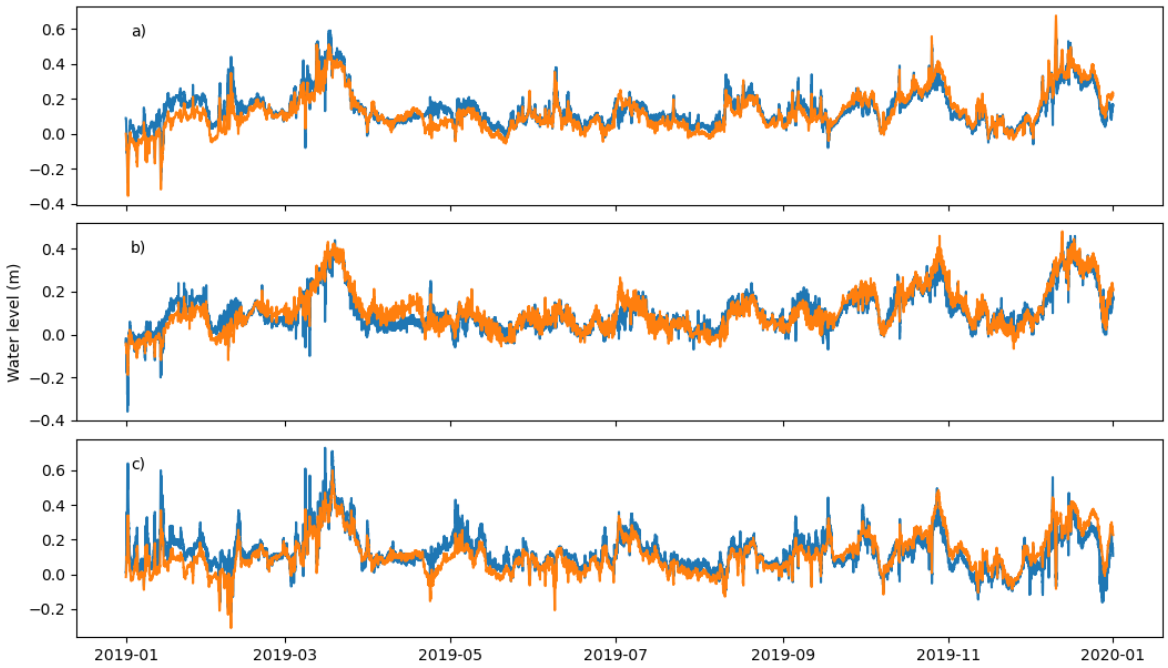


*Fig. 17. Comparison between simulated (orange) and measured (blue) water levels at Ringkøbing (a), Hvide Sande (b) and Bork (c) for 2019.*

Water level skill indicates that the model has an *Excellent* fit with exception of the Bork station in the calibration year, where the fitness can be classified as *Very Good* (Table 8). RMSE is always below 10 cm and 10% of the total range. The percent bias is negligible. Validation confirms the assumptions of the calibration run.

*Table 8. Water level performance indicators for calibration (2017) and validation (2019).*

| | RMSE | Skill | Bias |
|---|---|---|---|
| Ringkøbing 2017 | 0.07 m (8%) | 0.96 | -3.7% |
| Ringkøbing 2019 | 0.05 m (5%) | 0.98 | -1.8% |
| Hvide Sande 2017 | 0.06 m (10%) | 0.96 | -5.6% |
| Hvide Sande 2019 | 0.04 m (4%) | 0.99 | 0.3% |
| Bork 2017 | 0.08 m (6%) | 0.94 | -3.3% |
| Bork 2019 | 0.06 m (6%) | 0.96 | -1.5% |

Year-long periodic CTD surveys were used to assess the fitness of the exchange with the North Sea and the ability of the model to represent stratification episodes. Quantification of the fitness was not possible, but a visual comparison can be made to determine the representation of the horizontal gradient in the lagoon, the local salinity range and trend. Only 3 stations in the database were found for the calibration (Fig. 18) and validation years (Fig. 19). For both years the salinity's seasonal cycle is well represented at the 3 stations with some underestimation of salinity (less than 2 PSU). Stratification is achieved with the correct intensity and range but not always in the correct places. Extreme stratification episodes in 2019 measured at RBK5 are not reproduced, with the salinity plume typically veering to the north towards RKB1 and RKB7, placing its southern-most limit at about 4 km to the north of RBK5.

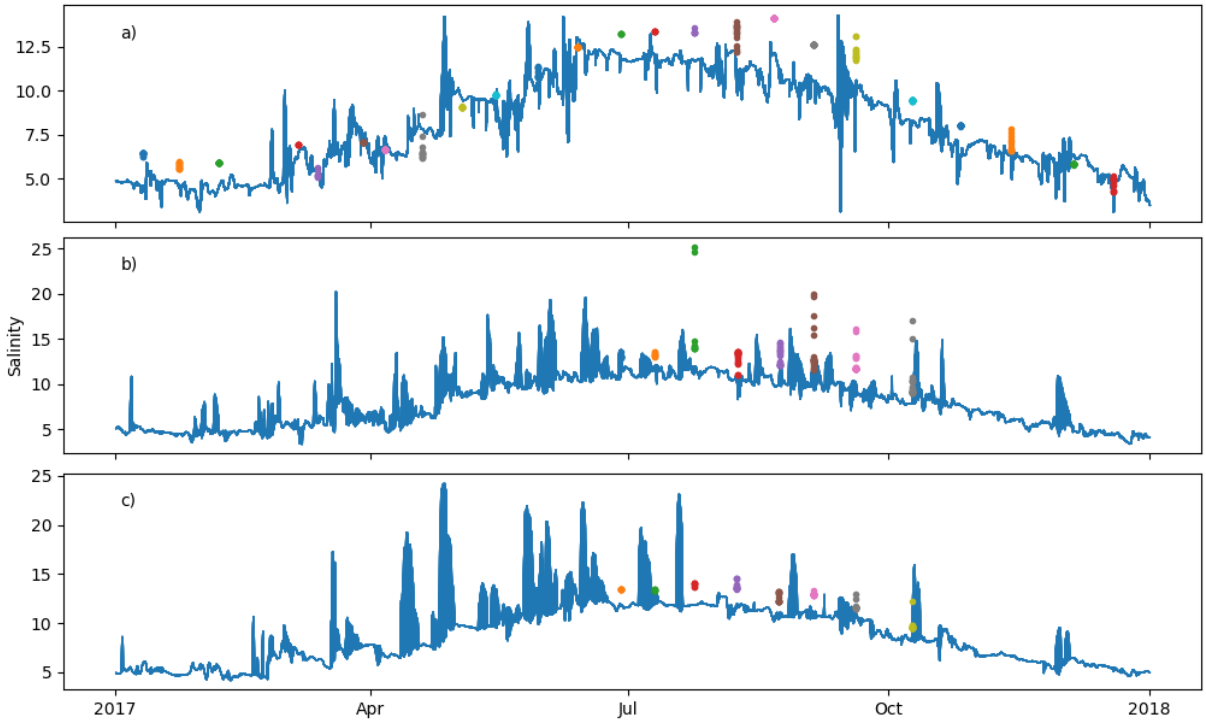


*Fig. 18. Comparison between simulated salinity envelope (blue area) and salinity from CTD observations (dots) at stations RKB1 (a), RKB5 (b) and RKB7 (c) for 2017.*

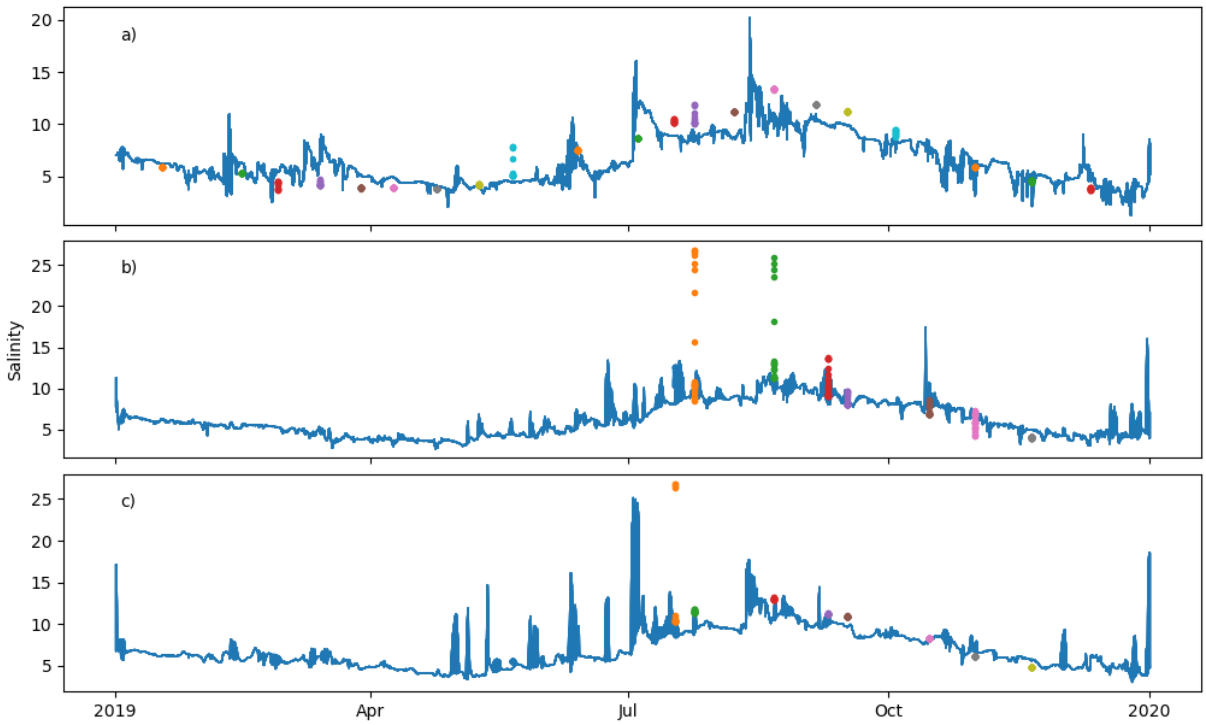


*Fig. 19. Comparison between simulated salinity envelope (blue area) and salinity from CTD observations (dots) at stations RKB1 (a), RKB5 (b) and RKB7 (c) for 2019.*

These model's shortcomings can be due to a number of factors altering the 3-dimensional pressure field and the stratification-mixing imbalance, such as bathymetric uncertainty and the representation of the transfer of momentum from the wind to the water body. In order to improve on these results, a year-long fortnightly CTD survey should be carried out at regularly spaced stations to cover the entire lagoon and constant salinity and water level monitoring should be carried out at 3 to 4 long-term moorings. With that, the source of the uncertainty can be identified and corrected.

## Conclusions

The calibration and validation procedure on the Delft3d-Flow of Ringkøbing Fjord allows us to conclude the following:

- Sea surface elevation forcing has an *excellent* fit to the available datasets with the exception to the calibration run at Bork that can be classified as *Very Good*;
- The model represents accurately the seasonal variation of salinity, implying a good representation of the exchanges between the lagoon and the North Sea;
- The salinity range is adequately represented but not always in the correct location. This implies that the model can represent stratification to the correct degree but uncertainties in the data prevent the improvement of the spatial distribution of the bottom salinity plume.

Given all the above we consider that the model is fit for the purpose of calculating the dispersion of land-based dissolved and suspended pollutants in Ringkøbing Fjord. In the context of the present work, this model is fit to provide hydrodynamic forcing for nutrient modelling by EcoWin Ringkøbing Fjord.

Possible recalibration could be achieved by implementing a year-long fortnightly CTD survey at regularly spaced stations to cover the entire lagoon and placing long-term instrumentation of salinity and water level at 3 to 4 long-term moorings.

## Shellfish modelling

An individual growth model for the *Mya arenaria* sand mussel was developed and integrated into the EcoWin.NET ecological model, with the aim of simulating distribution of sand mussel biomass across the fjord, sustainable carrying capacity, and environmental externalities (eutrophication abatement and biodeposition) of the sand mussel population at the Fjord scale.

### Model development for simulation of *Mya arenaria* growth

The individual growth model for *Mya arenaria* was developed based on the AquaShell™ framework, which has been successfully used to simulate shellfish feeding, metabolic expenditure, growth, reproductive effort, and overall mass balance of many bivalve species (oysters, mussels, and clams; see e.g. Ferreira and Bricker 2016 and Cubillo et al., 2023).

The key features of the individual growth model are:

- Simulation of key physiological functions that determine the change in individual weight and shell length;
- Integration of relevant physical and biogeochemical components such as temperature, salinity, and chlorophyll, and partitioning of phytoplankton and detrital food resources;
- Provision of environmental feedbacks of shellfish growth, such as the removal of phytoplankton and detritus, production of particulate organic waste, excretion of dissolved nitrogen, and oxygen consumption.

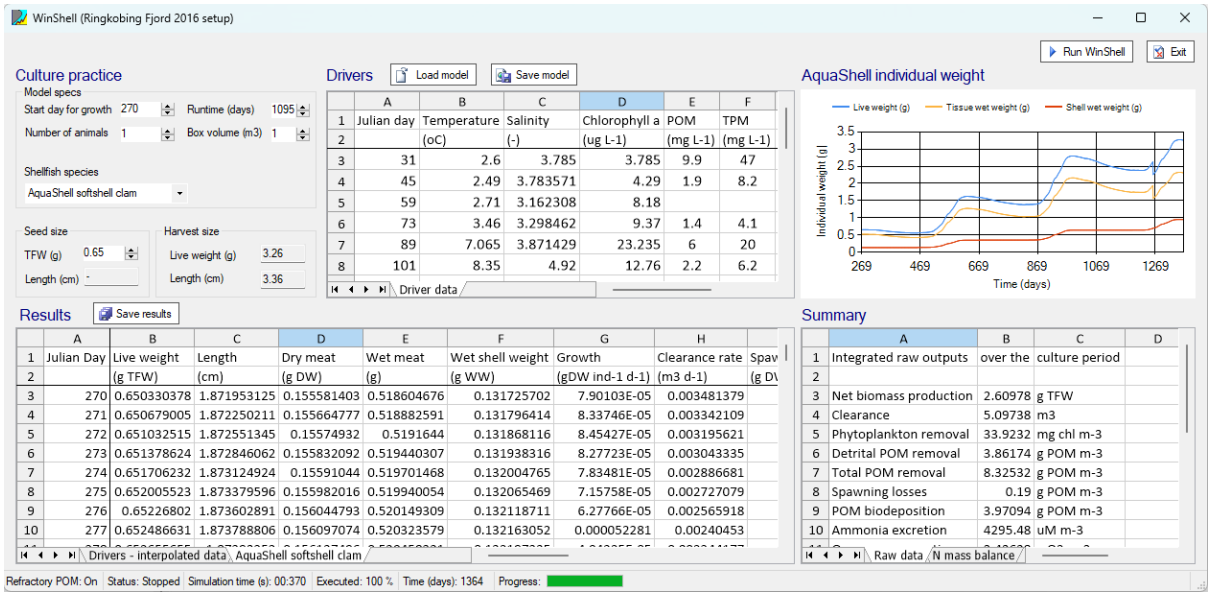


*Fig. 20. Screenshot of WinShell software showing an example 3-year model run for a sand mussel (Mya arenaria) using 2016 environmental conditions in Ringkøbing Fjord.*

WinShell (Fig. 20) is a workbench application that handles pre- and post-processing for AquaShell. It is designed to analyse growth of one single animal, provides a user-friendly interface to handle input and output from AquaShell and allows looking at the environmental and growth performance of an animal for a particular set of environmental drivers.

The AquaShell *Mya arenaria* growth model was then used at the ecosystem-scale in EcoWin.NET, to determine biomass production and environmental effects of sand mussels, using the same code that

is used for individual growth—this means that any improvement to the individual model is automatically transmitted to the higher-level EcoWin model.

### *Simulation of feeding and energy intake*

Sand mussels feed by filtering water through their inhalant siphon and retaining particles in their gills. This filtration rate depends on body size following an allometric relationship and is modulated by environmental factors, including temperature, salinity, and the concentration of suspended particles in the water (Fig. 21). While the effect of temperature on feeding rate is well-known to follow a bell-shaped curve, the effect of salinity was obtained from field and experimental observations.

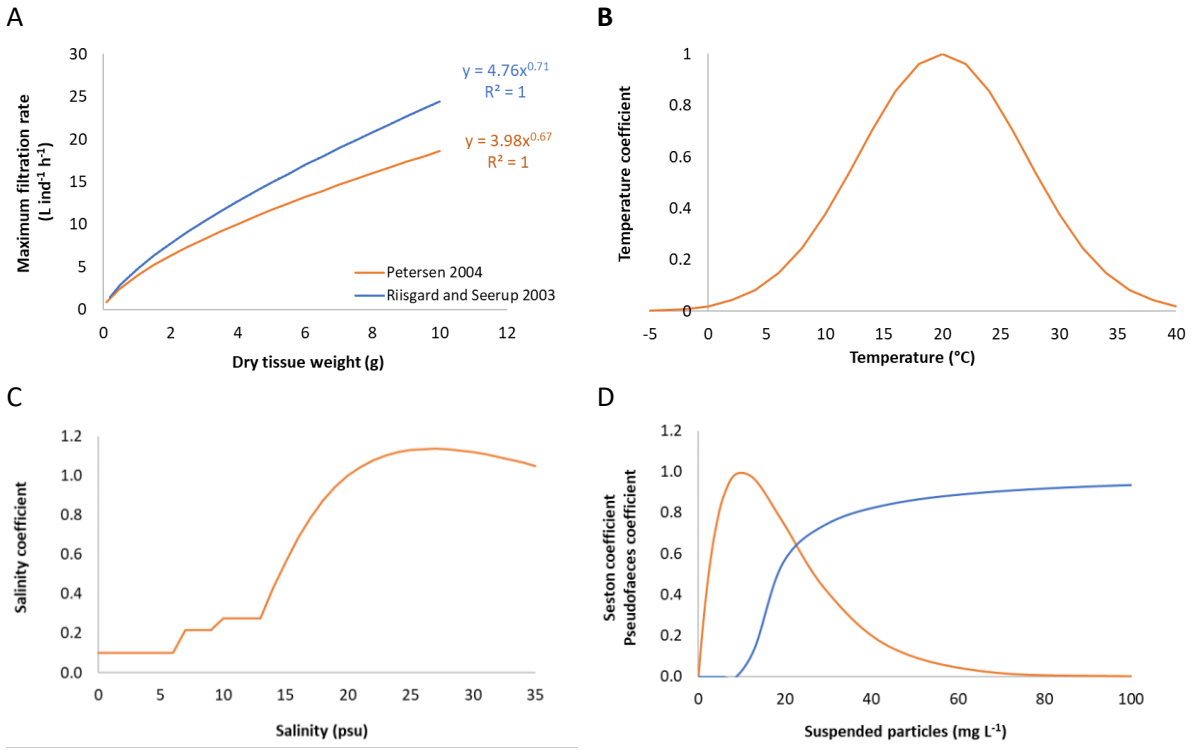


*Fig. 21. A) Allometric relationship between maximum filtration rate and sand mussel weight, obtained from Petersen (2004) and Riisgard and Seerup (2003). B) Effect of seawater temperature on the filtration rate, simulated through a temperature coefficient. C) Effect of salinity on filtration rate was simulated by means of a salinity coefficient. Minimum salinity = 6 psu; minimum reproductive salinity = 10 psu; salinity threshold above which there is less limitation = 14 psu. D) Dependence of filtration rate on the concentration of suspended particles in the water is mediated through a seston coefficient (orange line). Dependence of the pseudofaeces production rate on the concentration of suspended particles in the water is mediated through a pseudofaeces coefficient (blue line).*

In terms of available food, the range of conditions under which the filtration process is conducted at maximum capacity is limited by a lower and an upper threshold. Exposure to low food environments is considered to cause the cessation of filtration activity due to a reduction in the valve gape and retraction of mantle edges (Jorgensen et al., 1986), while above the upper threshold a reduction in filtration, termed “saturation reduction”, is interpreted as an overloading of the filtration and/or digestive system (Riisgård 2001).

The ingestion rate or food intake is limited in high seston environments by a pre-ingestive selection process that results in the production of pseudofeces (Bayne et al., 1993). The production of pseudofeces is a function of the concentration of suspended particles in the water following a Michaelis-Menten formulation.

The assimilation of food (and thus the energy assimilated by sand mussels), and the production of faeces (or discharge of waste), are both determined by the food intake and the absorption efficiency of the feeding process. The assimilation efficiency depends on food quality, measured as the organic content in seston, based on information from feeding experiments in the literature.

### *Simulation of metabolic expenditure and ammonia excretion rate*

Part of the energy assimilated by mussels is expended on metabolic processes. In the same line as Scholten and Smaal (1998), we quantify metabolic expenditure as the energy investment on respiration.

These metabolic processes include energy lost in standard metabolism, the processes necessary to survive, which are a function of body weight and sea water temperature (Fig. 22). These include maintenance of concentration gradients across membranes, osmoregulation, the turnover of structural body proteins and other macromolecules, a level of muscle tension and movement for shell closure, production of mucus, and repair of shell (Pouvreau et al., 2006). The energy lost in feeding processes is also included, and encompasses costs of capturing food, processing food (digestion, absorption), and utilization/incorporation of food materials.

Net production is defined as the difference between assimilated energy and metabolic expenditure.

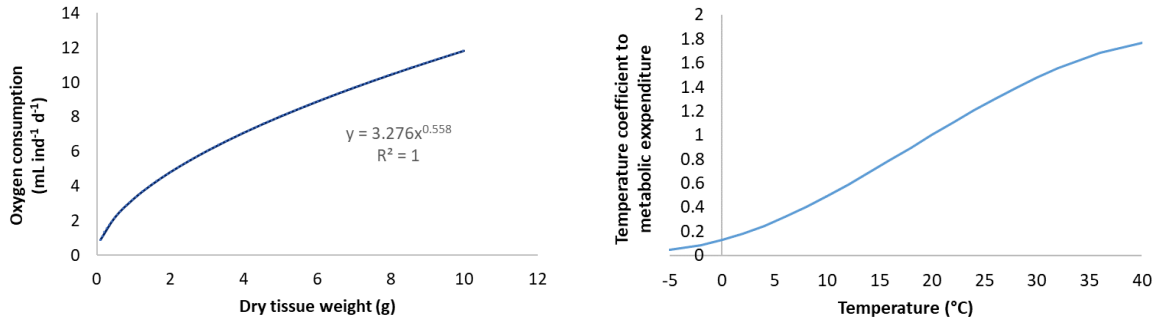


*Fig. 22. Left: The allometric relationship of oxygen consumption rate was obtained from Emerson et al,. (1988). Right: Coefficient relating temperature to the metabolic expenditure of sand mussels.*

The determination of the nitrogen excretion (as ammonia-N) is important for closing the nitrogen mass balance and assessing the environmental effects of shellfish. The ammonia excretion rate is estimated from the dissipated heat lost in aerobic metabolism based upon the energy consumed by the respiration of oxygen, the oxycaloric content of food, and the O:N atomic ratio.

### *Simulation of reproductive behaviour*

Sand mussels undergo one spawning period within its European distribution range (Ledoux et al., 2023), which typically occurs from mid-May to mid-September (Brousseau 1978). Temperature and salinity are the most important factors governing spawning. Ripening and spawning begin at temperatures >8°C (Stickney 1979, cited by Strasser 1999) which is the threshold temperature used by the model. Sexual maturity occurs at sizes ranging 2.5-3.5 cm, which are typically reached after 2-3 years, according to (Cross et al., 2012). The fraction of energy allocated for gonadal growth was set to 30% of the absorbed energy, which results in a weight loss of about 15% at each spawning event, coinciding with Ledoux et al. (2023).

## Model calibration and validation

### *Growth curves and seasonal growth pattern*

The sand mussel individual model was run against Ringkøbing Fjord environmental conditions for 15 years (2005-2019), running each year 10 times to avoid the effect of aging on the growth rate.

Average growth rates for the 10-year growth cycle ranged from 1.8 to 8.4 mm year$^{-1}$ and from 0.3 to 10.2 gLW year$^{-1}$ (Fig. 23).

Literature values range widely depending on the environmental conditions and sand mussel size, but modelled growth rates were similar to literature ranges:

- from 2 to 11 mm year$^{-1}$ (Schäffer and Zettler 2007);
- from 0.4 to 11.4 mm year$^{-1}$ (Gerasimova et al., 2015);
- from 3 to 14.5 mm year$^{-1}$ (Brousseau 1979).

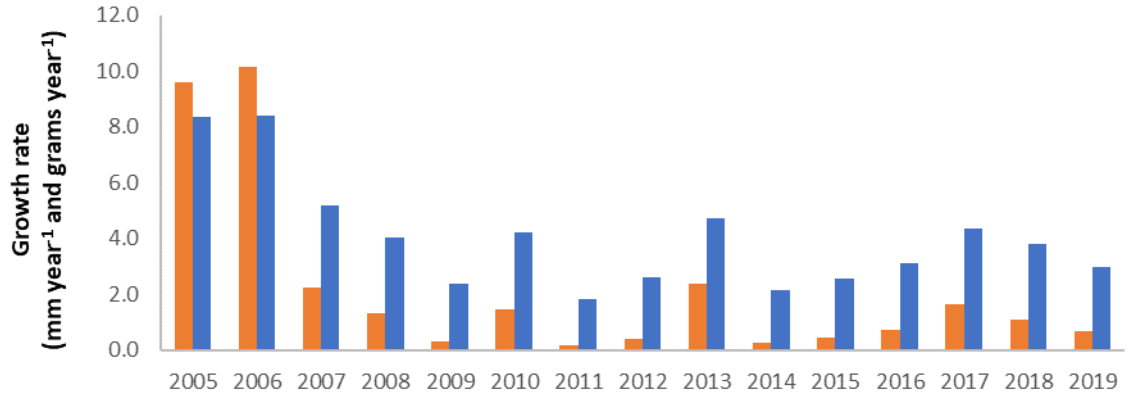


*Fig. 23. Average growth rates for shell length (mm per year, in blue) and live weight (grams of fresh weight per year, in orange) obtained when running ten times each of the years of the 2005-2019 period.*

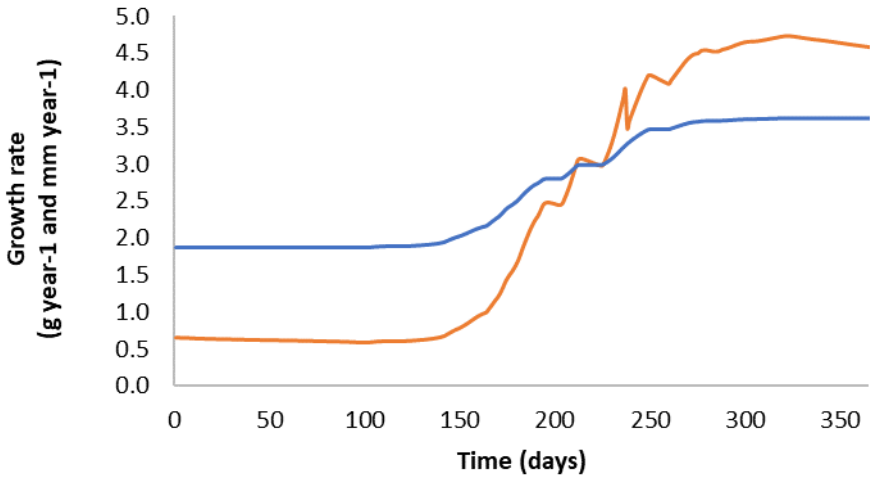


*Fig. 24. Sand mussel seasonal growth pattern for shell length (blue line, in mm) and live weight (orange line, in grams of fresh weight).*

The sand mussel model was able to reproduce seasonal growth patterns observed in field studies (e.g. Zwarts 1991) which consist of four (warmer) months of sand mussel growth and eight (cold) months of growth stagnation (Fig. 24).

### *Morphometric relationships and physiological rates*

The *Mya arenaria* individual growth model was calibrated to match experimental morphometric relationships found in the literature. Measured and simulated length-weight morphometric relationships were very similar and the shell to soft tissue ratio matched these for sand mussels from other field studies (e.g. Schäffer and Zettler 2007; Gerasimova et al., 2015).

The model is able to reproduce filtration rates, metabolic rates, and ammonia excretion rates from the literature. An example is illustrated in Fig. 25 that shows the evolution of filtration rate and sand mussel weight over time. Modelled filtration rates lie within observed values reviewed in Du Clos et al. (2017) which range from 0.2 to 7.4 L ind $^{-1}$ h$^{-1}$. It is interesting to see how the periods of sand mussel growth coincide with the peaks of filtration activity, which occur in warmer (summer) months.

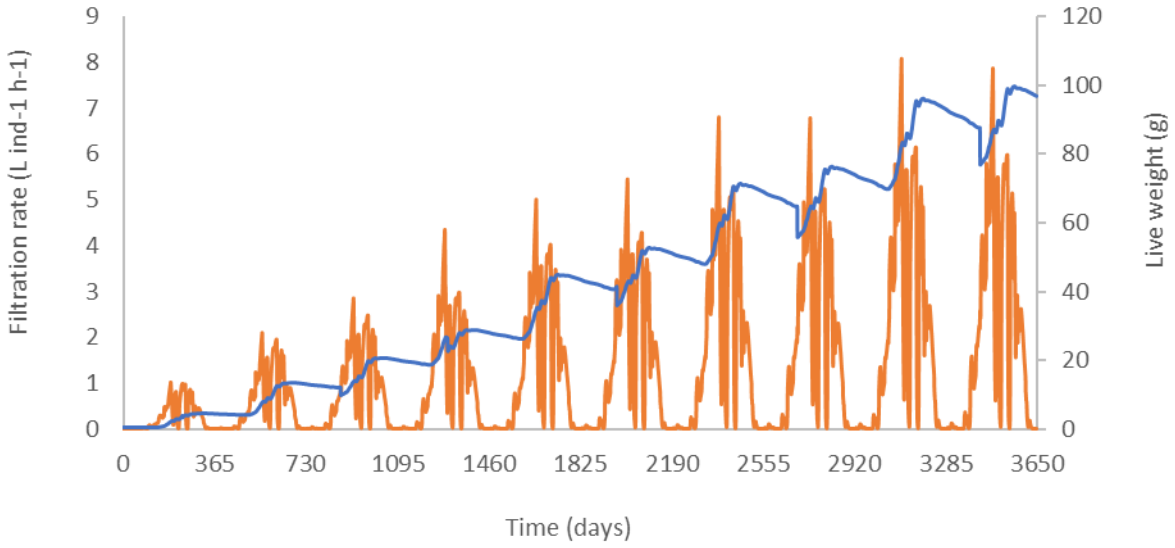


*Fig. 25. Temporal evolution of filtration rate and live weight of sand mussels in Ringkøbing Fjord over a 10-year model run.*

### *Mass balance*

Simulation of sand mussel growth using the environmental conditions at Ringkøbing Fjord provides outputs on biomass production and environmental effects, such as the suspended particles (phytoplankton and detritus) removed from the water via filtration, the organic biodeposits produced (feces and pseudofeces), and the dissolved ammonia excreted. The model also provides an integrated nitrogen mass balance over the growth cycle. During a one-year growth cycle, the model estimates that a single 2-cm sand mussel can clear on average 3.3 m$^3$ of seawater removing 12.5 g of organic particles and producing 7.8 g of organic biodeposits. During this time each sand mussel will consume 3.2 g of oxygen and remove 0.13 g of nitrogen from the environment, i.e., 2.58% of the clam biomass produced (Fig. 26).

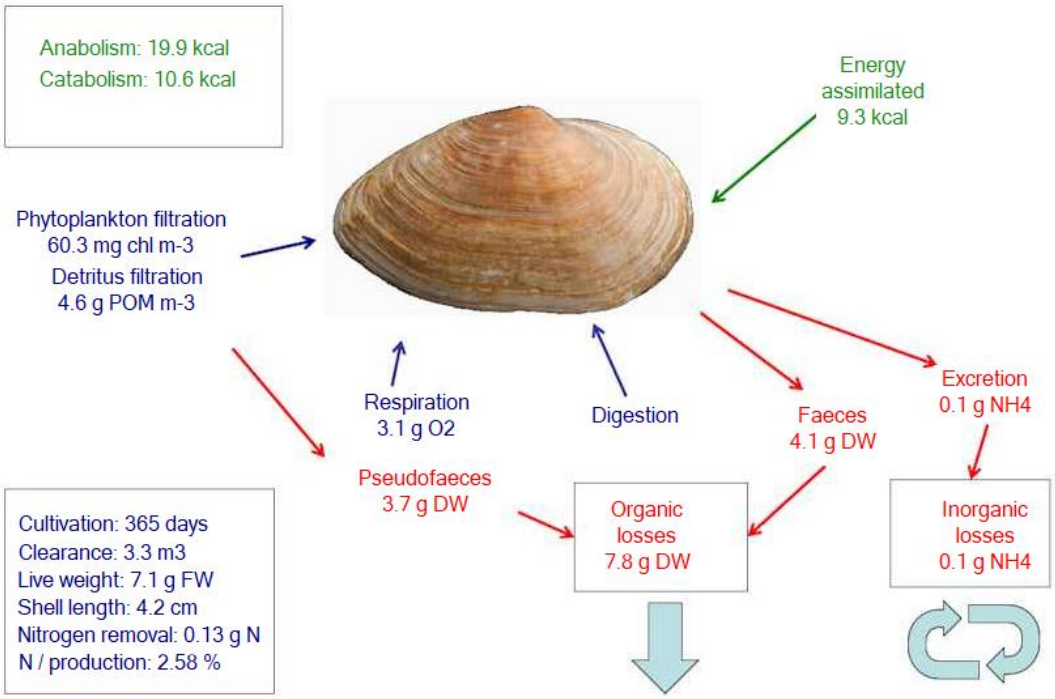


*Fig. 26. AquaShell mass balance results for an individual sand mussel over a growth cycle of one year using 2006 environmental conditions at Ringkøbing Fjord. DW (FW): dry (fresh) weight; POM: particulate organic matter. Removal processes are marked as arrows in dark blue, organic and inorganic losses to the environment are marked as red arrows, energy fluxes are shown in green. Details on the length of the growth cycle, water cleared out of suspended particles, final growth values, and nitrogen removal are indicated in the blue box.*

## Conclusions

- The *Mya arenaria* individual growth model performs well when run against measured drivers for tested years of the 2005-2019 period.
- The model matches literature growth rates from areas with similar environmental conditions.
- The model reproduces seasonal growth patterns.
- The model mimics the relationship between shell length and live weight, and the proportion between soft tissue weight and shell weight found in the literature.
- Physiological rates (clearance rate, oxygen consumption rate or ammonia excretion) match reasonably well observed ranges from field and laboratory studies.

## Macrophytes and epiphytes modelling

### Background and rationale

A range of benthic macrophytes are present in Ringkøbing Fjord, including *Zostera marina*, *Ruppia sp*., and *Potamogeton sp*. In a shallow coastal lagoon such as this one, the relative distribution of these species will be a function of physical factors such as salinity and underwater light climate. The former is mainly governed by the sluice dynamics, with respect to seawater supply, and river discharge, in terms of freshwater inputs. The latter is a function of bathymetry, but also of light attenuation in the water column, which is mainly a function of suspended particulate matter (SPM).

SPM is the sum of Particulate Organic Matter (POM), which includes both living (phytoplankton) and detrital material, and Particulate Inorganic Matter (PIM). Since the fjord connection to the ocean is artificial, there is no tidal dynamics driving resuspension of sediment, which occurs mainly through wind-induced currents. The other main factor that conditions light attenuation is phytoplankton biomass, which is the result of the balance between primary production and grazing by consumers such as the softshell clam *Mya arenaria*.

Distribution and abundance of macrophytes is one of the Biological Quality Elements (BQE) of the Water Framework Directive (WFD: 2000/60/EC) and therefore a component that must be included in an ecosystem model of Ringkøbing Fjord, where benthic vegetation is a key feature. Furthermore, nutrient loading is a driving force of both pelagic and benthic primary production, and the inclusion in EcoWin of a benthic primary production model helps to understand the partitioning of this load between the two components (Fig. 1).

The final consideration is the addition of epiphytic vegetation in the benthic macrophyte model. Epiphytes are considered a symptom of eutrophication (e.g. Bricker et al, 2003) and therefore an undesirable feature of coastal ecosystems.

The implementation of a macrophyte model in EcoWin aimed to:

1. Simulate above- and below-ground biomass of macrophytes based on the key physiological processes;
2. Simulate nitrogen removal due to benthic primary production;
3. Develop a risk-based approach to colonisation of macrophytes by epiphytes;
4. Introduce two key indicators (macrophytes and epiphytes) for eutrophication assessment into the modelling framework.

### Macrophyte model

A review of existing models for the macrophyte species relevant to Ringkøbing Fjord revealed a paucity of work in this area. The most promising model was developed by Bocci et al (1997) for *Zostera marina* and later adapted by Plus et al (2003) for *Zostera noltii*. Other work in this field has been reported by Wetzel & Neckles (1986) and Bulthuis (1987).

No adequate models were found for other macrophyte species, so the Bocci et al (1997) model was chosen for this work since (i) it is specific to *Zostera marina*, the eelgrass species found in Ringkøbing Fjord; and (ii) it includes parameterisation for Danish waters.

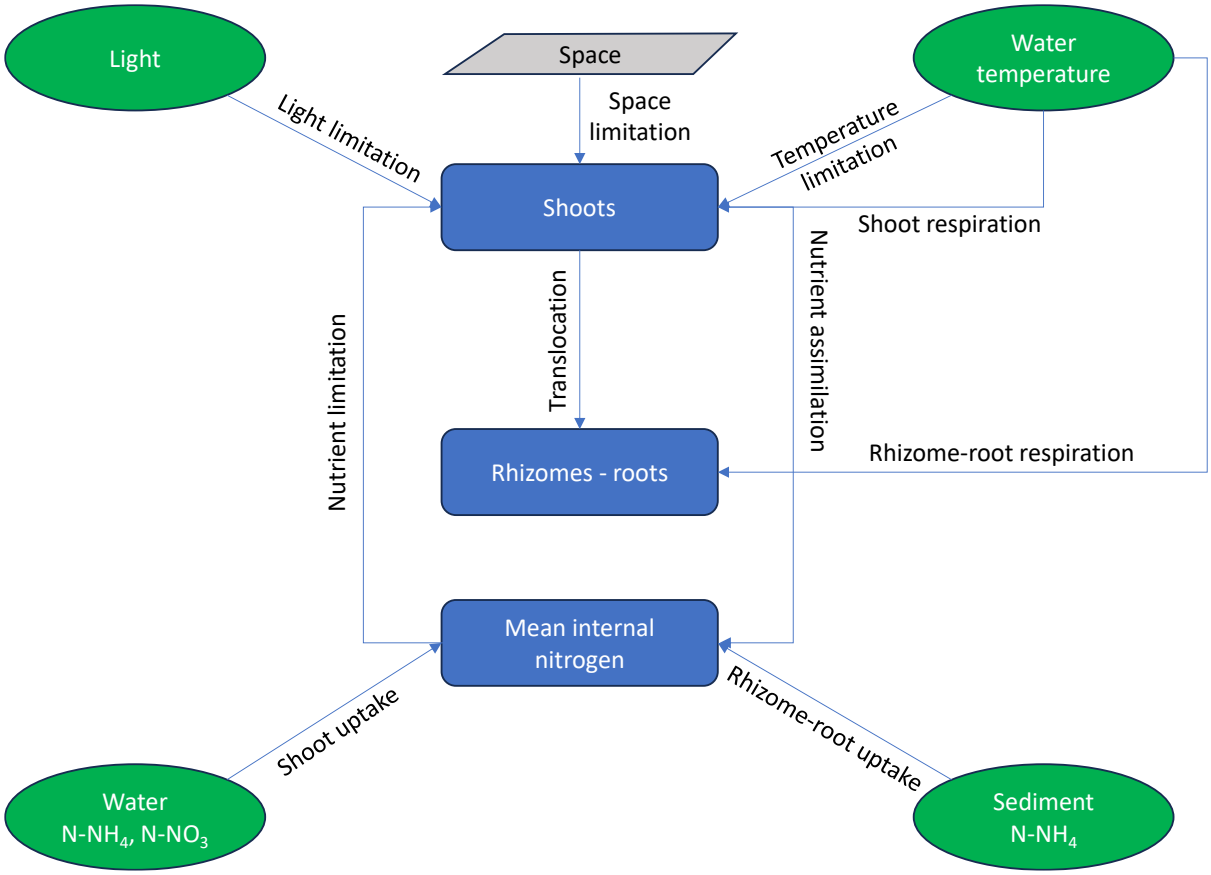


*Fig. 27. Conceptual diagram of macrophyte model (adapted from Bocci et al, 1997).*

The conceptual model is shown in Fig. 27 and contains three state variables: shoot biomass, root biomass, and internal nitrogen quota. The sum of shoot and root biomass is the stand biomass, and the model output is in dry weight per unit area (g DW $m^{-2}$).

Gross primary production is limited by four drivers: nitrogen, temperature, light, and available space. In the Ringkøbing Fjord EcoWin model, the first three drivers are derived from the biogeochemical model and available space is a calibration parameter based on the typical maximum biomass per unit area.

The model was developed in four stages. The first stage used the InsightMaker$^{tm}$ platform to develop a standalone model (Fig. 28) to test the outputs against those obtained by Bocci et al (1997).

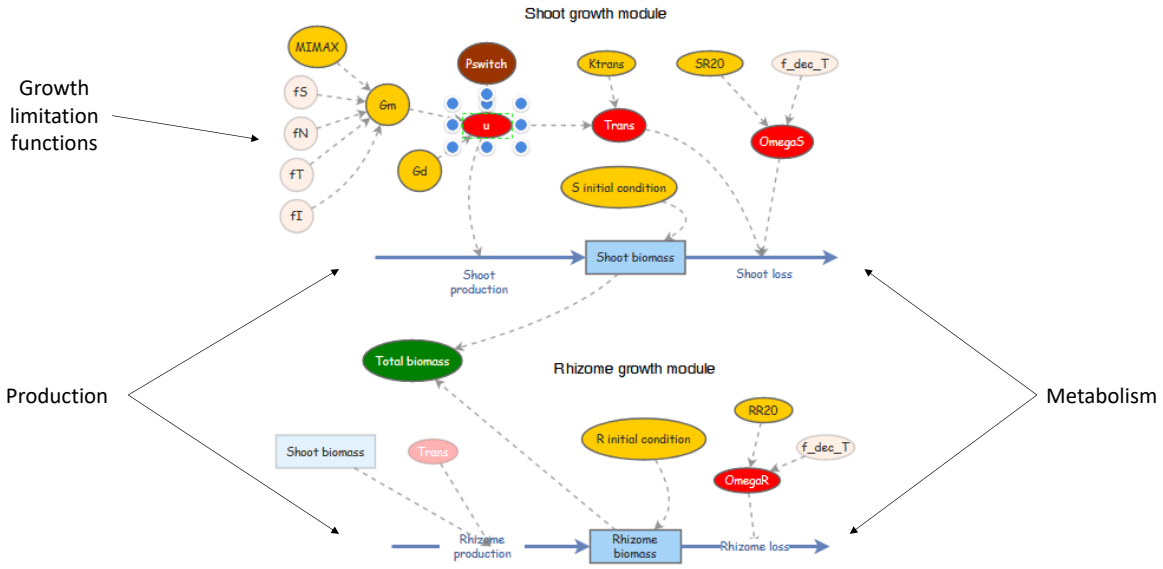


*Fig. 28. Macrophyte model implemented in InsightMaker (http://www.insightmaker.com). The production function μ is highlighted. Only the biomass modules are shown for brevity.*

The model includes a cell-quota module which regulates tissue nitrogen as a function of nitrogen available in the water and sediment. The internal tissue nitrogen is used to determine nitrogen limitation of growth (*fN* in Fig. 28).

After testing, the second stage of development extended the model to couple it with a simple model for phytoplankton production, where underwater light climate was determined by pelagic primary production and top-down control of phytoplankton by the softshell clam *Mya arenaria*. The InsightMaker visual platform was also used for this development.

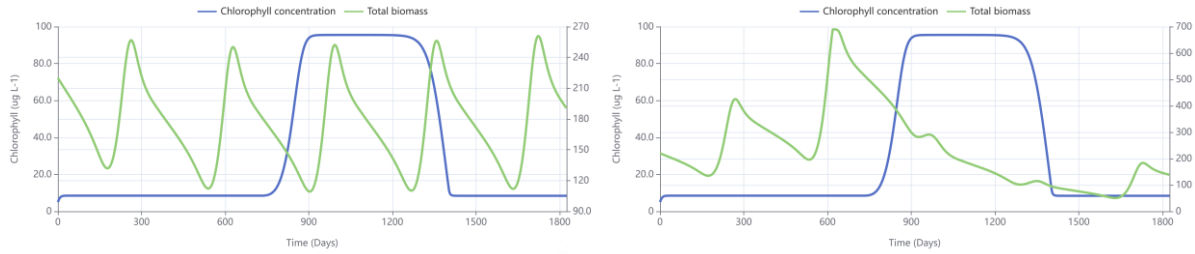


*Fig. 29. Results for macrophyte production, decoupled (left) and coupled (right) to chlorophyll concentration.*

Fig. 29 provides some example results from the second stage model: the left pane shows the macrophyte model is stable over a five-year period under decoupled conditions (i.e. light, temperature, and nitrogen follow a repeated annual cycle and phytoplankton (chlorophyll *a*) concentration does not affect the light energy available to the macrophytes; the right pane couples phytoplankton, softshell clams, and macrophytes. Stand biomass increases over the first two years because there is an appropriate underwater light climate—algal biomass remains low due to top-down control by bivalves. In the third year of the model run, high rainfall is simulated, resulting in a low salinity; clam mortality increases, and since nitrogen is abundant, the chlorophyll concentration increases rapidly. The resulting effect on light attenuation leads to a rapid die-off of macrophytes, which only begin to recover after phytoplankton biomass decreases. The reduction in chlorophyll at the end of the model run is partly due to mortality resulting from self-shading and partly due to the recovery of the clam population as salinity increases.

After verification that the visual modelling stages were functionally correct, the third stage was to code the model in C++ into the AquaFrond library. This library is used by a workbench application where the final model verification is carried out. The final stage was to incorporate the fully tested AquaFrond code into the EcoWin ecosystem model.

At this stage, the drivers for growth are calculated from the full hydrodynamics and biogeochemistry, taking into account nutrient loading from land obtained from the SWAT+ model. Several enhancements to the macrophyte model were implemented in EcoWin, in particular the spatial discretisation of model boxes and the resulting calculation of spatially distinct net primary production.

A limitation in model application at the present time is a lack of data on distribution and abundance of macrophytes in different areas of Ringkøbing Fjord. Nevertheless, the model is able to reproduce spatial differences in stand biomass due to bathymetry, seasonal changes to the light extinction coefficient due to pelagic primary production and is sensitive to different nutrient loading scenarios.

### Epiphyte risk model

Epiphytes are considered to be a symptom of eutrophication, although they are not part of the Assessment of Estuarine Trophic Status (ASSETS) model (see e.g. Ferreira et al, 2007), and are not included in the WFD. In both cases, the main reason for not including this symptom was the difficulty in performing a quantitative assessment; allied to this, the definition of a classification scheme is non-trivial. The National Estuarine Eutrophication Assessment (NEEA) developed by NOAA for US coastal systems (a precursor to ASSETS) did include epiphytes but the evaluation of this component was found to be problematic, Nevertheless, some criteria were formulated, although evaluation was at best heuristic (Bricker et al, 2003).

There are not enough data on spatial and temporal variation of epiphyte biomass in Ringkøbing Fjord and its correlation with nutrient availability, but it is recognised that three drivers are important in conditioning epiphyte biomass.

1. Substrate. By definition, epiphytes can only exist if they have a plant substrate to attach to (i.e. benthic macrophytes). Therefore, a low or residual stand biomass leads to low or negligible epiphyte biomass;
2. For macrophyte biomass to be sufficient for epiphyte colonisation, the underwater light climate must be appropriate for macrophyte growth. In Ringkøbing Fjord, this means that phytoplankton biomass (and thus chlorophyll concentration) must not be too high. This can occur either through bottom-up control (low nutrient concentration) and/or top-down control (phytoplankton filtration) by bivalves. As algal biomass increases, if there is still sufficient light at the bottom to allow for primary production, opportunistic epiphytes tend to outcompete perennial vegetation such as *Zostera*;
3. The final factor is nutrient concentration. If there is sufficient light, low nutrient concentrations allow macrophytes to outcompete epiphytes; however, in a situation where the light climate is appropriate *an*d chlorophyll is low due to top-down control, elevated concentrations of nutrients will create appropriate conditions for opportunistic epiphytes to outcompete macrophytes (Fig. 1).

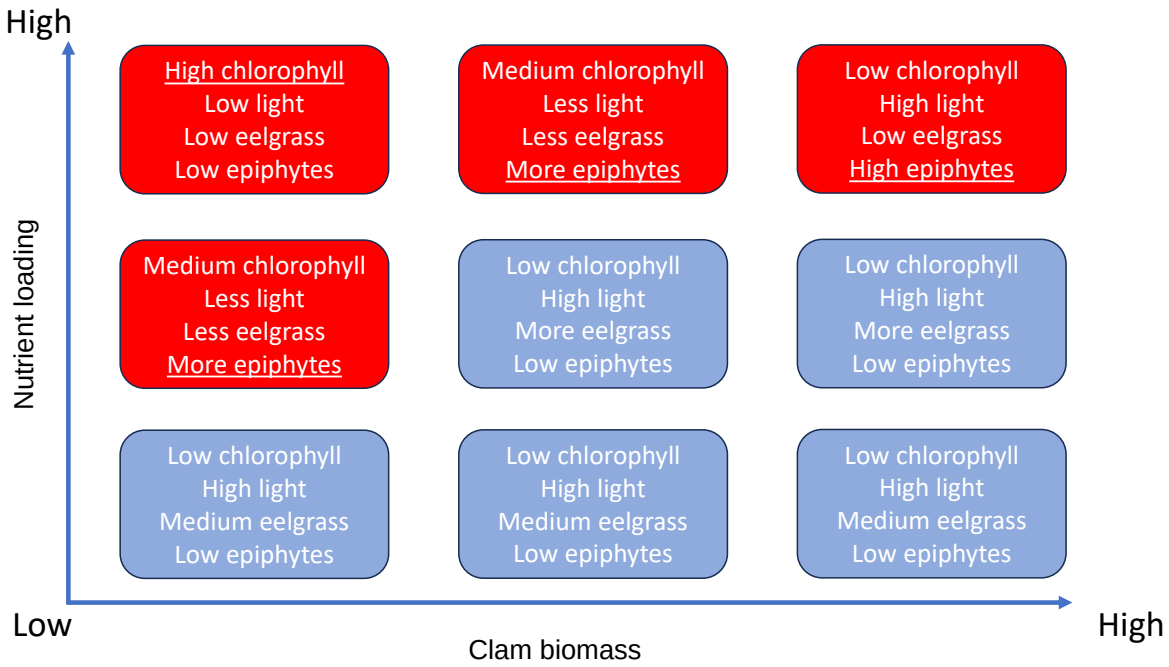


*Fig. 30. Matrix approach implemented for risk assessment in EcoWin based on nutrient loading and clam biomass.*

A risk assessment approach was implemented in EcoWin based on these factors (Fig. 30), using nutrient concentration (a proxy for loading) and stand biomass as indicators.

*Table 9. Epiphyte risk assessment indicators and thresholds.*

| Indicator | Thresholds |
|---|---|
| Stand biomass SB (g DW m-2) | 0-50, 50-100, 100-400, >400 |
| Dissolved inorganic nitrogen concentration NC (mmol.$L^{-1}$) | 0-10, 10-50, 50-100, >100 |
| **Epiphyte risk score** | **Combination matrix** |
| 1 | SB < 50<br>50<SB<100 AND NC<10<br>100<SB<400 AND NC<10<br>SB>400 AND NC<10 |
| 2 | 50<SB<100 AND 10<NC<50<br>100<SB<400 AND 10<NC<50 |
| 3 | 50<SB<100 AND 50<NC<100<br>SB>400 AND 10<NC<50 |
| 4 | 50<SB<100 AND NC>100<br>100<SB<400 AND 50<NC<100 |
| 5 | 100<SB<400 AND NC>100<br>SB>400 AND 50<NC<100<br>SB>400 AND NC>100 |

The indicators, thresholds, and combinations used are shown in Table 9. In practice, this approach can be considered as a way to associate a certain mass of epiphytes to the total stand biomass.

This epiphyte risk assessment system will be further developed in the future, in particular through local tuning of thresholds and potential incorporation of other indicators, but in the present form it already allows for some interesting scenario analyses with respect to changes in nutrient loading to Ringkøbing Fjord.

## Ecological modelling

### Model development

The ecological model for Ringkøbing Fjord was developed using the well-tested EcoWin.NET (EWN) application. EcoWin.NET is an ecosystem-scale model developed to address water quality, carrying capacity for aquaculture, and interactions between pressures and state with respect e.g. to nutrient loading from land. EWN has been extensively used over the past 25 years in many parts of the world, including the UK, Portugal, China, Indonesia and South Africa.

EWN simulates ecological processes in aquatic systems, including eutrophication in both the water column and tidal flats, saltmarsh dynamics, and production and environmental effects of aquaculture. The model has mainly been used for analysis of carrying capacity for shellfish aquaculture, but other components include finfish and macroalgae. Over the last twenty years, EWN has been used as part of a modelling framework, integrating detailed hydrodynamic models such as Delft3D, the Princeton Ocean Model, and ROMS.

EWN is built using an object-oriented programming (OOP) approach and contains an extensive library of objects that can be tailored to particular ecosystems. EWN incorporates the relevant physics to simulate water circulation, a full representation of catchment loading, including both point and diffuse sources of water and nutrients, and simulates a comprehensive set of biogeochemical processes, dealing with nutrient cycling, primary and secondary production, and addressing both the pelagic and benthic compartments of the system.

The EWN model domain is divided into functionally uniform boxes according to a multicriteria approach based on physics and water quality yielding areas that span 10-100's Delft3D-Flow calculation cells. The Delft3D-Flow subdomain was divided into 25 horizontal boxes and 2 vertical layers totalling 50 individual computation units.

The flow across the Delft3D-Flow cells at the boundary between EWN boxes was aggregated to provide water exchanges at the box boundaries with a 15 min timestep. A year simulated in Delft3D year is repeatedly cycled for a decadal simulation in EWN.

Fig. 31 shows the objects tab of the EWN application and illustrates the components of Ringkøbing Fjord model. Objects are adapted as appropriate, either through parameterisation in the EWN setup files for a particular system, which deal with water fluxes supplied by Delft3D, and with nutrient and other loads supplied by SWAT+ simulations, or outside EWN, as the shellfish and benthic vegetation growth models.

Six new objects were written specifically for the Ringkøbing Fjord model, dealing with the shellfish, the benthic vegetation, the suspended solids, the nutrients and the phytoplankton components of the model.

In total, the Ringkøbing Fjord ecosystem model contains 9 objects, 61 state variables, and 20 forcing functions and runs for a period of ten years, with a timestep of 15 minutes. Decadal periods are important to simulate multiple aquaculture cycles for the relevant species. The physical framework considers 50 boxes divided into two vertical layers, where the boundary between upper and lower boxes with the division set in the upper one-third of the total depth, resulting in 25 boxes for surface waters and 25 for bottom waters (Fig. 5). The model includes 16 boundaries, of which 2 are ocean boundaries (1 upper and 1 lower), and 14 are land boundaries (rivers discharging into the fjord).

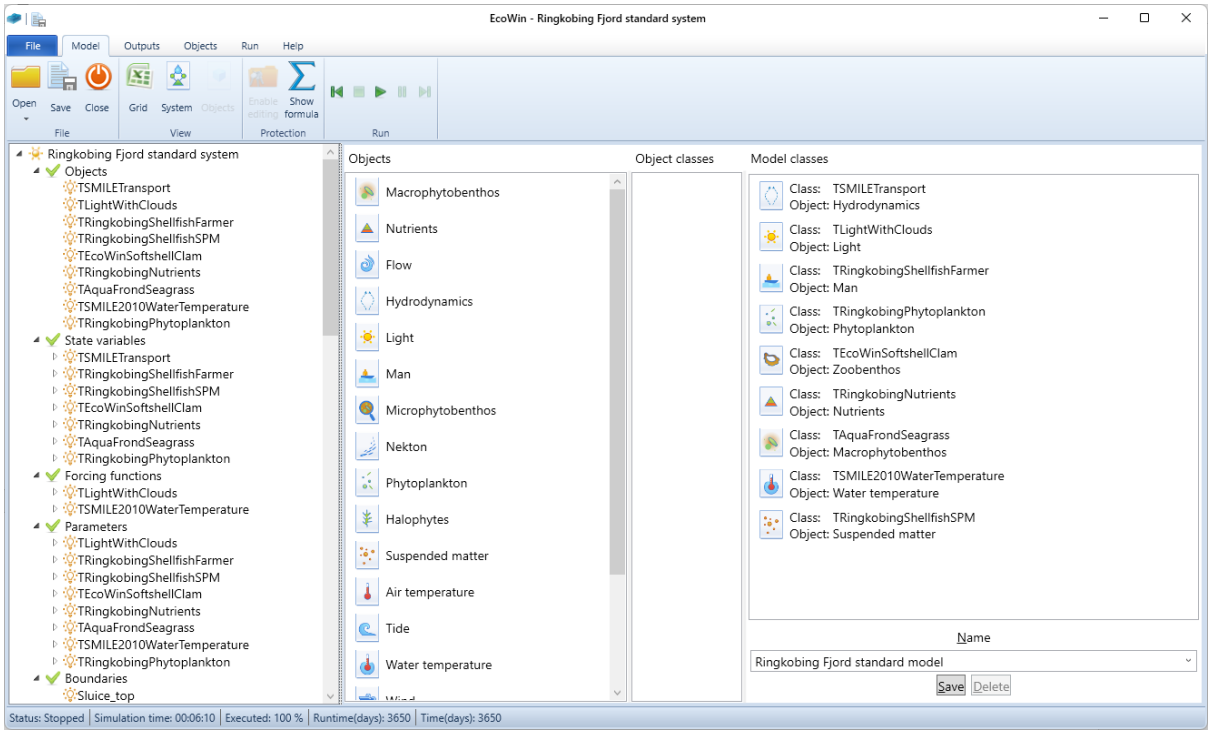


*Fig. 31. EcoWin.NET application showing the objects in the Ringkøbing Fjord model (right), the hierarchy of component state variables, forcing functions, and other components (left), an example of the available object (central panel).*

The design of the EWN application makes it straightforward to make changes to loads from land or ocean for scenario analysis, and the object-oriented formulation means that objects such as shellfish can be turned on or off to examine the role of top-down control by filter-feeders on eutrophication.

## Calibration and validation

### *Calibration*

Ecological models incorporate many processes, reflecting the complexity of coastal ecosystems (e.g. Butenschön et al., 2016); as a consequence, calibration is inherently a complex procedure. EWN is calibrated using four different approaches:

1. Calibration of external model components, and validation of these against measured data;
2. Calibration of internal model components based on measurements and/or declarative data;
3. Calibration of internal model parameters based on measurements and literature;
4. Development of bespoke objects that extend the EWN model library.

### External model components

For the Ringkøbing Fjord model, these components are part of the ecosystem modelling framework, i.e. the SWAT+, Delft3D, AquaShell, and Aquafrond models dealing with hydrology and nutrient loading, circulation, and shellfish and vegetation growth respectively.

The outputs (SWAT+ and Delft3D) and formulations (AquaShell and Aquafrond) of these models are only accepted into the EWN model after the component models have been both calibrated and validated. That process is fully described above.

### Internal model components for EWN model setup

For the Ringkøbing Fjord model, the internal components include the items listed in Table 10.

*Table 10. Variable groups calibrated for setting up the EWN standard model for Ringkøbing Fjord.*

| Variable group | Example state variables | Initial conditions | Boundary conditions |
|---|---|---|---|
| Physical parameters | Salinity, temperature | From measured data | From measured data |
| Nutrients | $NH_4$, $NO_2$, $NO_3$, $PO_4$, Si | From measured data | From measured data or other models |
| Phytoplankton | Chlorophyll | From measured data | From measured data |
| Benthic primary producers | Macrophyte density | From literature and sensitivity tests | Not applicable |
| Secondary producers | Bivalve stocking, | From measured data and sensitivity tests | Not applicable |

Delft3D provides flows across the EWN boxes for a one-year period, and the 'Delft3D' year is repeatedly cycled for a decadal simulation in EWN to ensure system stability in terms of physical and biogeochemical processes. In the case of the Ringkøbing Fjord model, the simulated year by Delft3D is 2017, chosen for its representativity in terms of climate and the availability of data to constrain the model.

To ensure no discrepancies between water movement and water quality simulated by EWN, the loadings from the land, simulated with the SWAT+ model and provided to EWN, also correspond to the year 2017. While the forcing of EWN in terms of hydrodynamic and land inputs is for a specific year, the objective of EWN is to account for typical long-term ecosystem processes occurring in the Fjord, hence the model's run over a 10-year period.

### Internal model parameters for EWN model setup

These are parameters that can be tuned in the EWN setup file for specific models. For the Ringkøbing Fjord model, these include primary production parameters such as $P_{max}$, the maximum light-limited production rate, $I_{opt}$, the optimal light energy, and $K_s$, the half-saturation constant for nutrient uptake; in addition, baseline respiration and natural mortality rates can be adjusted. For suspended particulate matter, rates such as resuspension and mineralisation of particulate organic matter (POM) can be tuned.

### Development of new objects

New processes or modifications of existing processes are implemented in code. EcoWin is written in two languages: C# and C++, and new descendant objects typically take advantage of existing, well-tested algorithms, and use object-oriented programming (OOP) to extend functionality as required.

#### *Validation*

EcoWin was validated against outputs from component models and observational data from sampling campaigns. There is only one water quality sampling site (RKB1, Fig. 5) with fortnightly measurements in Ringkøbing Fjord providing a limited spatial coverage although it is expected that the waters of the fjord are well mixed.

The validation outputs are reviewed below for key model variables.

### Volume conservation and water residence time

Fig. 32 illustrates the model stability in terms of volume conservation over a 4-year period in Box 13, located in the middle of Ringkøbing Fjord.

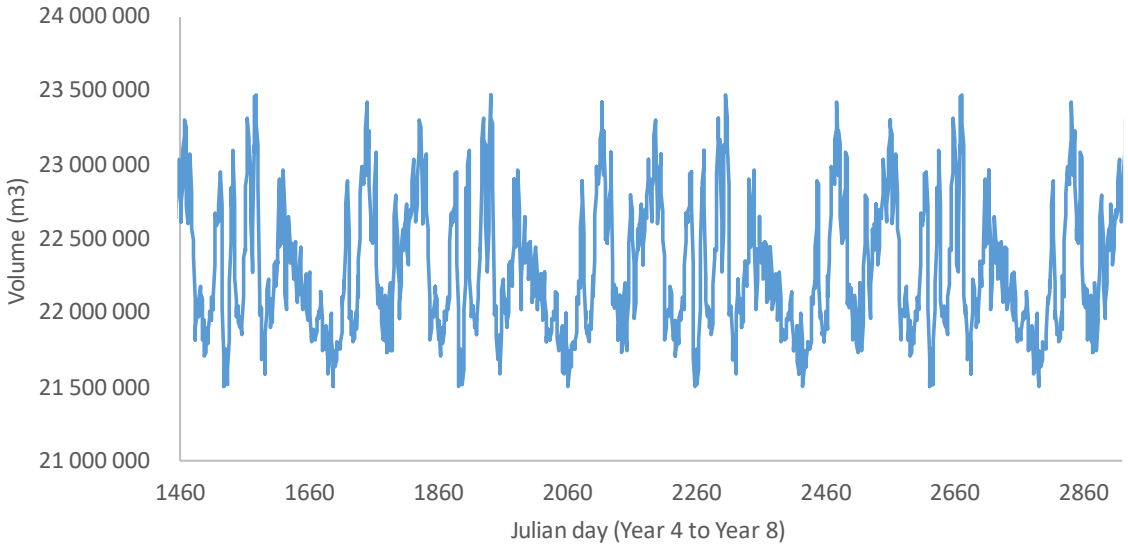


*Fig. 32. Continuity analysis for Box 13 over years 4 to 8.*

Fig. 33 shows the decay of a conservative tracer stocked in each box at 100 units at the start of the model run (year 1). As predicted by the hydrodynamic model, Ringkøbing Fjord has a water residence time close to 100 days.

EWN reproduces this behaviour: the box 1, corresponding to the location where the Skjern River discharges into the Fjord, has the lowest residence time due to large input of freshwater from the river (e-folding time of 10 days). For the rest of the fjord, residence times are generally longer with an e-folding time ranging from 80 to 95 days.

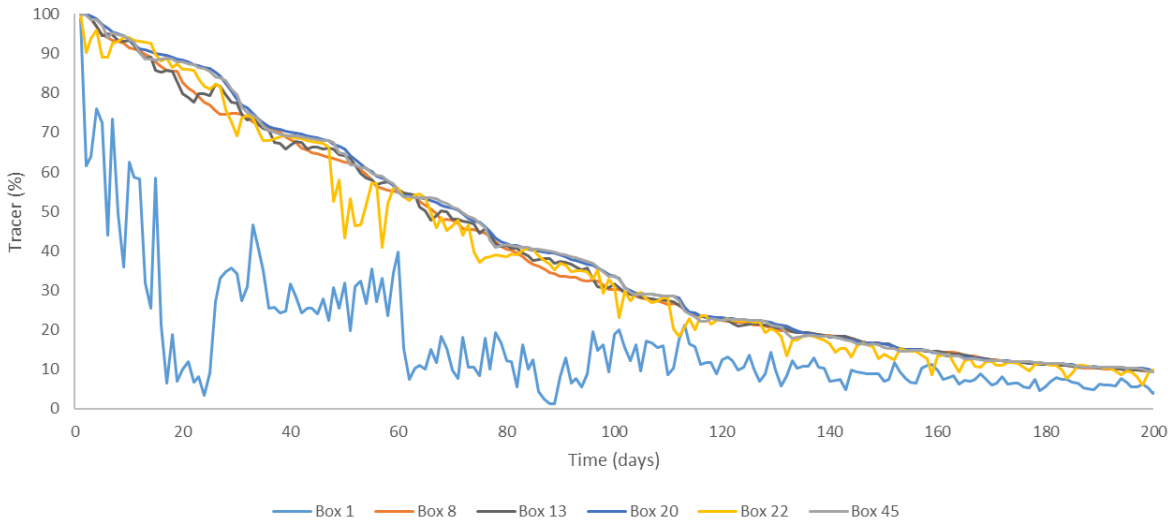


*Fig. 33. Decay of a conservative tracer along a transect from Skjern river discharge to the sluice.*

The long residence time will constrain water quality inside the fjord, where the effects of elevated nutrient loading will be felt strongest, as the residence time required for the development of an algal bloom is typically a week or so and these are all longer.

## Salinity

Comparisons were made between fortnightly observations and hourly EWN model outputs (Fig. 34). EWN was able to capture the seasonal salinity variation observed in nature. Stratification observed in boxes 13/38 was not totally reproduced by the hydrodynamic model is therefore not reproduced by EWN. This is not expected to impact the biogeochemical processes simulated at the ecosystem scale.

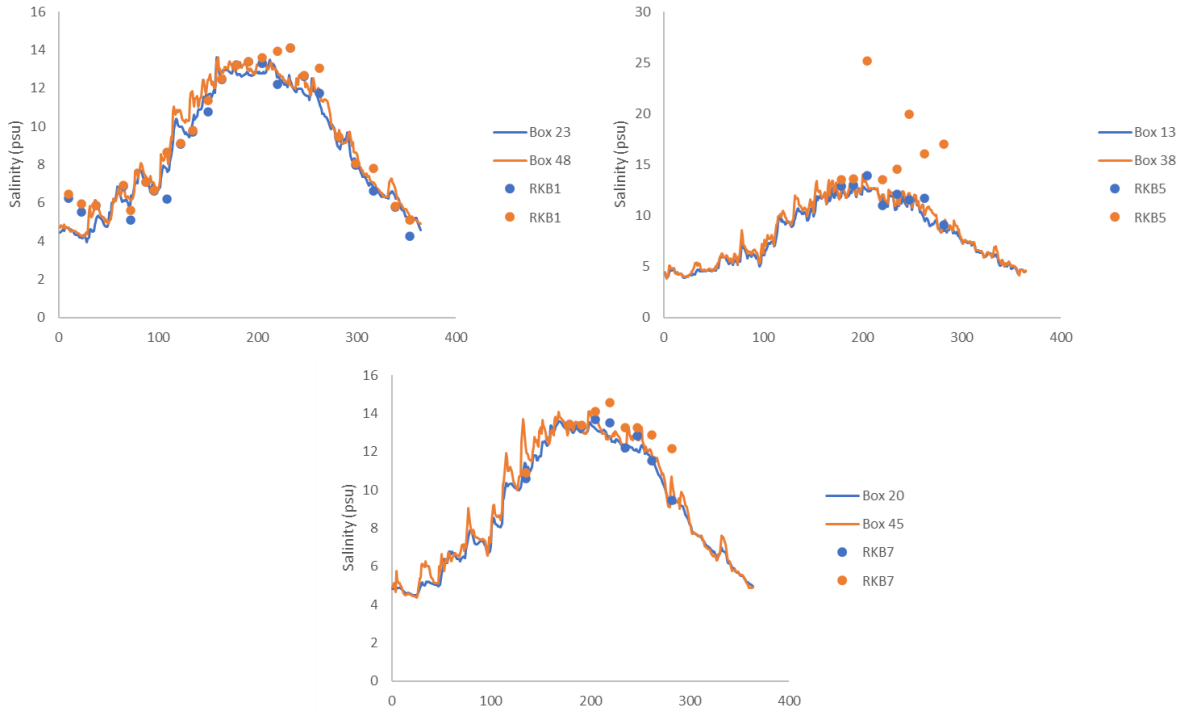


*Fig. 34. Salinity comparisons between modelled (lines) and measurement data (points). In blue we present the surface boxes, in orange the bottom boxes.*

Because the temporal and spatial resolution of EWN is not as detailed than Delft3D, the peaks and troughs tend to be less extreme, but the pattern of low salinities due to high river flows in the autumn-winter period compared to summer is well reproduced.

The capability to detect differences between the fine-scale simulation from Delft3D and the EWN model, which uses a lower horizontal and vertical resolution, is critical to ensure that the ecological model correctly simulates the physical behaviour of the system.

## Nutrients

Comparison of dissolved inorganic nitrogen (DIN) was made between monthly or fortnightly observations and daily EWN model outputs for the box corresponding to the location of the water quality station (Fig. 35). Since the objective of the model is to reproduce the typical behaviour of the Ringkøbing Fjord ecosystem, the model outputs are plotted for the 2010-2019 period.

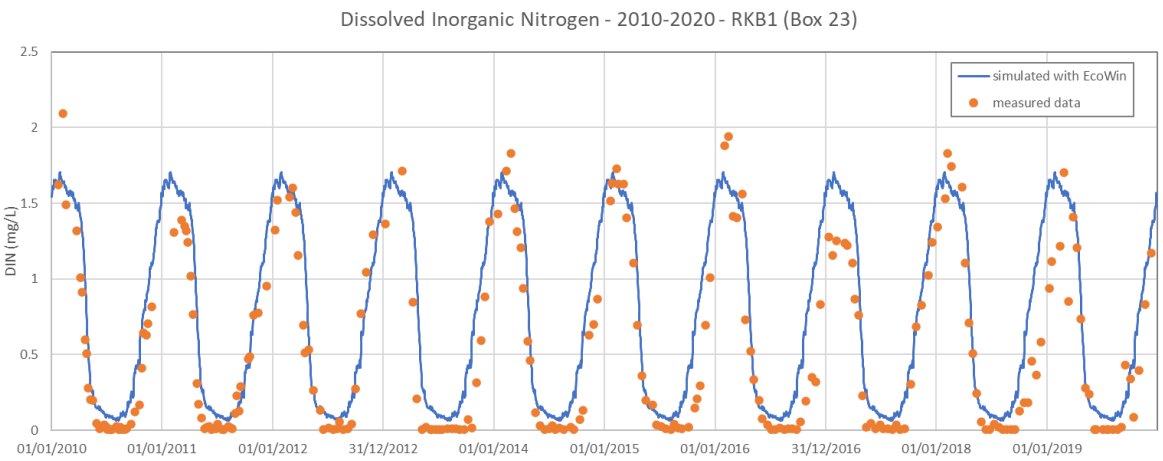


*Fig. 35. Simulated and measured dissolved inorganic nitrogen (DIN) concentrations at station RKB1 (dots) and at model box 23 (line) for the 2010-2019 period.*

There is very little interannual variability in the data, with a decrease in DIN concentrations between March and May dropping to almost 0 $mg.L^{-1}$ and increasing again between September and February, reaching between 1.5 and 2 $mg.L^{-1}$. Exceptions include lower DIN concentrations than usual in winter 2016-17 and a rise in concentrations delayed to October in 2018. The model is able to correctly reproduce the seasonal patterns of observed DIN concentrations.

### Chlorophyll and Particulate Organic Matter

Both chlorophyll-a (chla) and Particulate Organic Matter (POM) are key variables in EWN, since they constitute the food that bivalves need in order to grow. Fig. 36 and Fig. 37and show the validation curves for these two state variables.

In contrast to DIN, it is challenging to discern an annual pattern that consistently reproduces for chla. Some indications of a spring peak occurring between February and April (especially noticeable in 2013, 2016, and 2018) suggest a potential correlation with the decrease in DIN concentrations. However, the year 2019 deviates from this trend, exhibiting a significant algal bloom during the summer-autumn period—an occurrence not observed to this extend since the regime shift in the mid-90s.

The absence of clear patterns may point out the significant influence of nonlinear biogeochemical processes, such as filtration by shellfish, on chla concentrations. A higher temporal resolution of samples, particularly during the decline of DIN concentrations, could contribute to better identifying patterns during this period.

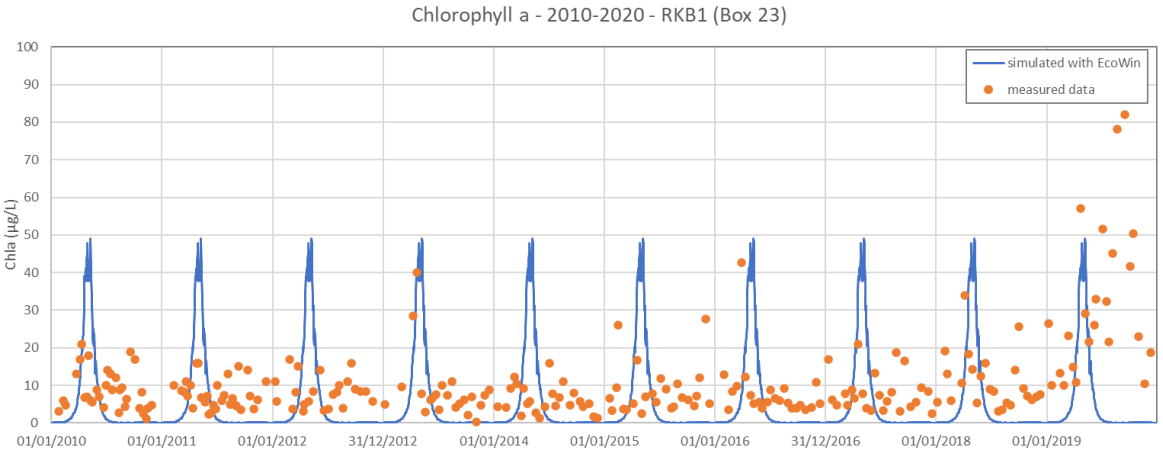

*Fig. 36. Simulated and measured chlorophyll a concentrations at station RKB1 (dots) and at model box 23 (line) for the 2010-2019 period.*

Simulating chla concentrations in a coastal ecosystem is challenging due to the dynamic and complex nature of biological processes within aquatic ecosystems. Chlorophyll is a proxy for phytoplankton biomass, and its concentration is influenced by several factors, including nutrient availability, light conditions, temperature, and grazing pressure.

All processes known to affect phytoplankton biomass in Ringkøbing Fjord, including filtration by filter-feeding clams are implemented in EWN. However, there is substantial uncertainty in key variables such as shellfish stocking density and its spatial variability, and there are no specific physiological experiments on the local population of clams. Consequently, it was not possible to improve the fit of chla concentrations without overfitting the model (i.e., forcing the model to reproduce the noise in the data). Therefore, we consider that the model reproduces the ecosystem response to the best of our knowledge and can provide useful insight in terms of management policies.

If we consider the years during which a spring peak of chla was observed, the match between observed and simulated data is acceptable, both in terms of numeric range and temporal variability. However, this is not the case for the year without an observed chla peak, where spring concentrations of chla appear to be overestimated by the model. In both situations, the model underestimates concentrations from summer to winter. As described earlier, the year 2019 is an exceptional case, and EWN is not expected to accurately reproduce concentrations for that year. Higher frequency chla data during the decrease in DIN concentrations would be useful for a better assessment of the capability of the model to reproduce chla patterns in the fjord.

Finally, the simulated value of average chla concentrations for May-September (which is used as an indicator in the WFD) was compared with observations. The simulated values of 6.5 $\mu g.L^{-1}$ matches the observed values for the 2010-2018 period that range from 5.9 to 9.8 $\mu g.L^{-1}$.

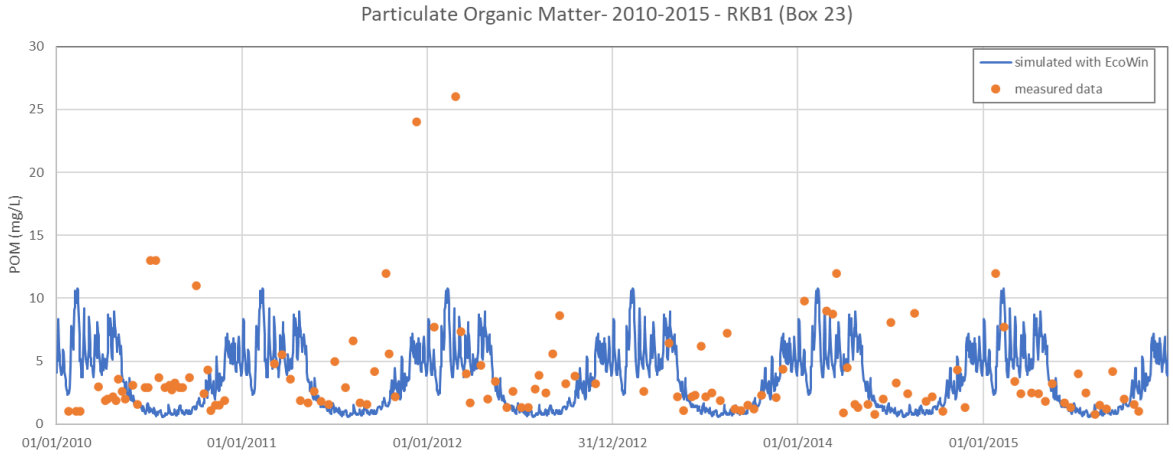


*Fig. 37. Simulated and measured particulate organic matter concentrations at station RKB1 (dots) and at model box 23 (line) for the 2010-2015 period.*

POM measurements indicate that we can distinguish the summer period, characterized by concentrations ranging between 1 and 4 $mg.L^{-1}$, from the winter period, where POM concentrations are generally above 5 $mg.L^{-1}$. The model is able to reproduce this seasonal pattern, with occasional outliers attributed resuspension due to particularly strong winds.

### Individual growth model for *Mya Arenaria*

Validation of individual growth in EWN was tested by using constant environmental drivers (temperature, salinity, and food) in both EcoWin and WinShell (the application used for running the AquaShell model), to ensure a perfect match.

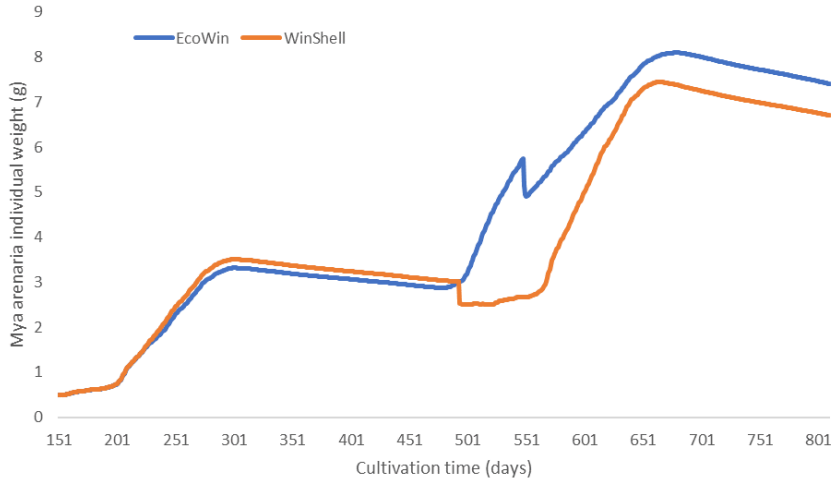


*Fig. 38. Comparison of Mya arenaria growth outputs from EcoWin and AquaShell models for an 800-day growth period.*

At a second stage, the fully loaded EWN model for Ringkøbing Fjord was used to extract time series of driver variables with a daily frequency. These were then be loaded into WinShell, allowing both models to run growth trials with realistic system data and compare growth profiles (Fig. 38).

The match is very good, with and an $r^2$ of 0.97. The small differences in growth curves are due to the way spawning is simulated in the two models.

# Results and discussion

## The standard model

- The ecosystem model developed for Ringkøbing Fjord was defined as the standard Ringkøbing Fjord model and was then used to analyse the ecosystem status under current conditions. Fig. 39 and Fig. 40 show commonly used eutrophication indicators, namely the average value of chlorophyll concentrations for the May-September period (summer chla), as used in the WFD, and average concentrations of winter dissolved inorganic nitrogen (DIN). The results indicate that summer chla is lower in the bottom boxes, as expected due to the presence of bivalves. Summer chla is relatively homogeneous across all boxes, and no spatial patterns can be identified, except for lower values in box 1 due to freshwater inputs from the Skjern River. The summer chla concentrations are below the threshold for the good ecological potential set to 8.4 µg.L$^{-1}$ in all the model boxes, with the exception of boxes 8 and 20. Winter DIN concentrations are homogeneous across all top and bottom boxes which is characteristic of a well-mixed system. Winter DIN concentrations are slightly higher in the southern part of the fjord compared to the north due to the large input of nutrients through the Skjern Å in the southeast of the fjord (box 1).

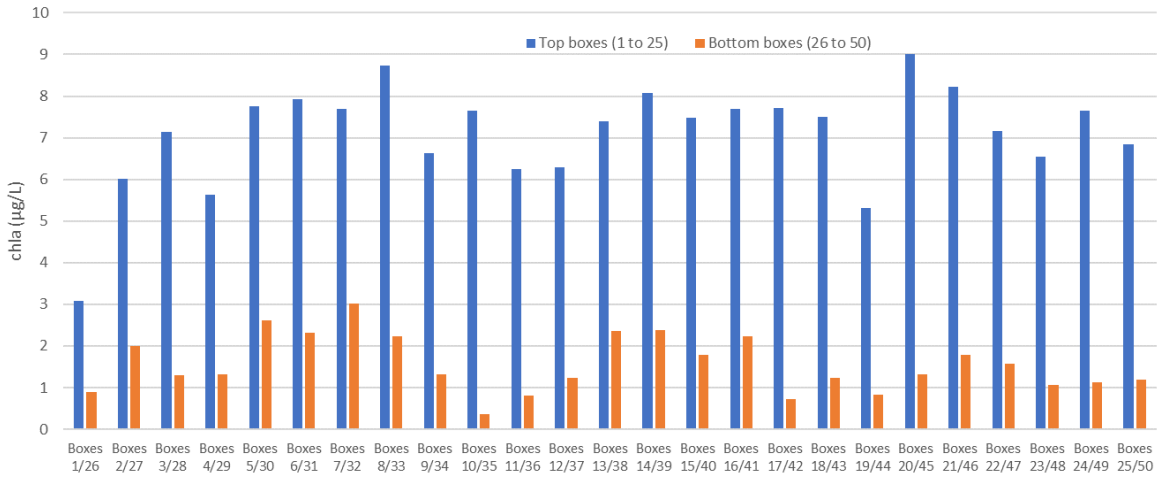


*Fig. 39. Average chlorophyll concentrations for the May-September period for top boxes (in blue) and corresponding bottom boxes (in orange).*

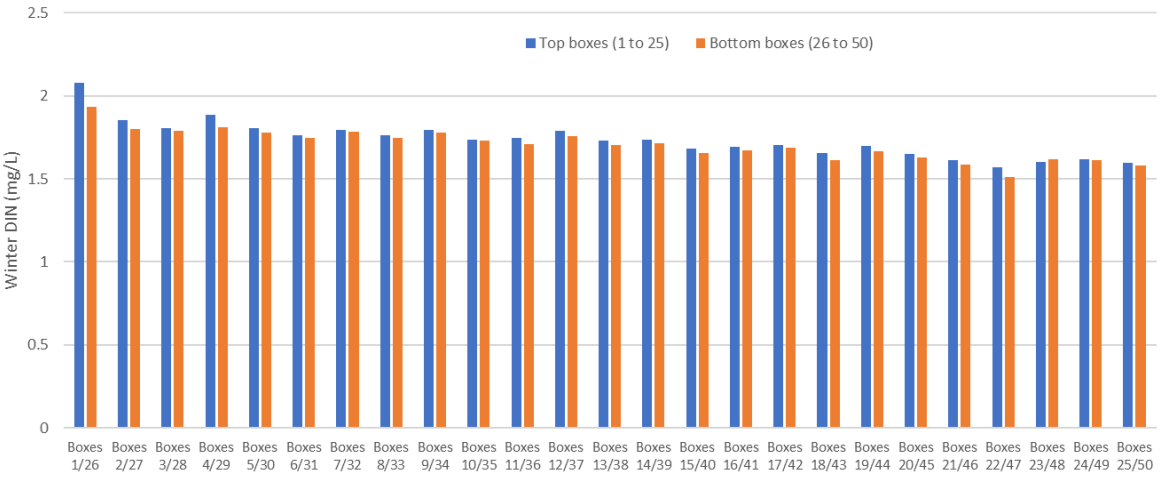


*Fig. 40. Average value of winter DIN concentrations for top boxes (in blue) and corresponding bottom boxes (in orange).*

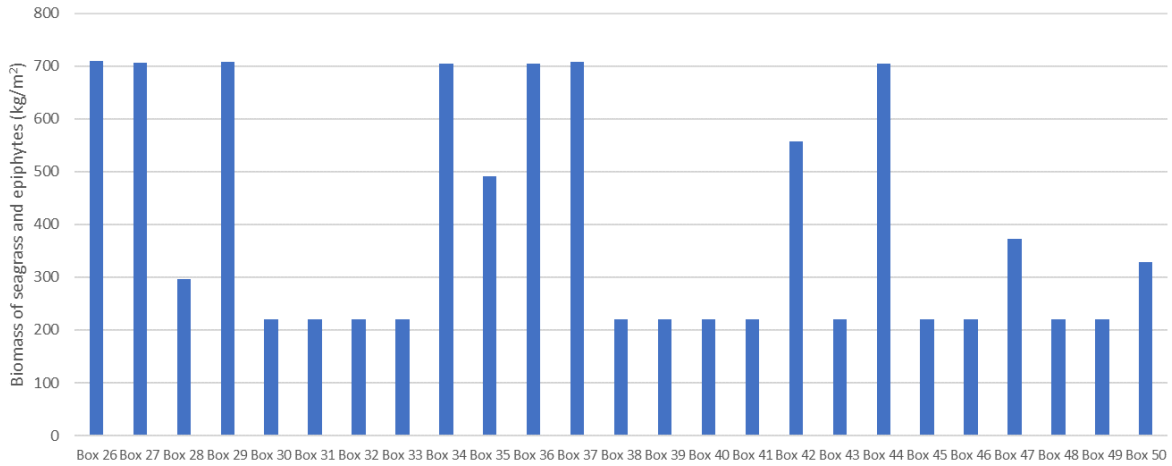


*Fig. 41. Maximum macrophyte and epiphyte biomass for each of the bottom boxes.*

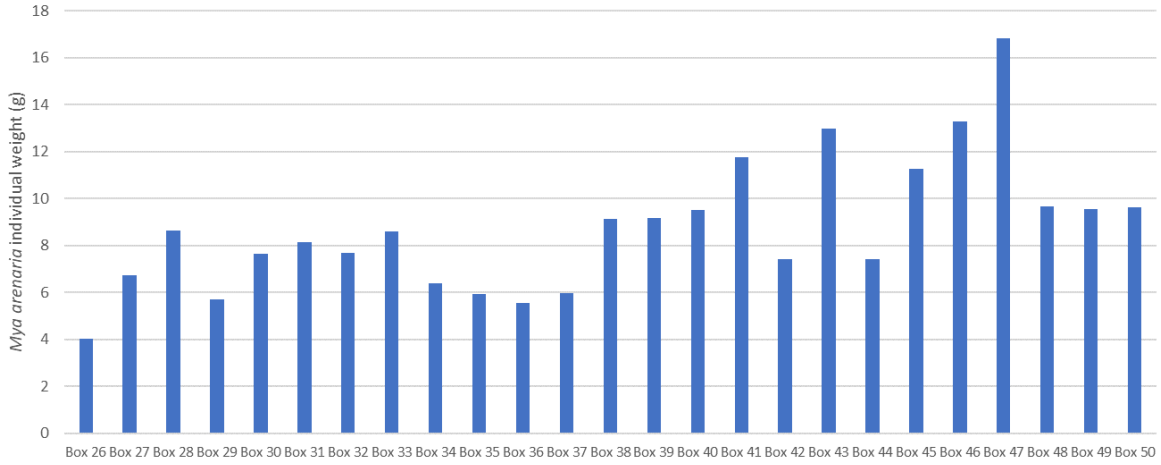


*Fig. 42. Mya arenaria individual weight for each of the bottom boxes.*

The model was also used to examine the maximum biomass of macrophytes and epiphytes, as presented in Fig. 41. Biomass values are the highest in the shallow boxes receiving land inputs (boxes 26, 27, 28, 34, 36, 37 and 44).

Finally, the model also provides information on the individual weight of *Mya arenaria* across all the boxes (Fig. 42). The values are higher for the boxes close to the sluice and can be related to higher salinity, which is favorable for *Mya arenaria* growth in this area.

## Scenarios

The catchment model was used to assess the impact of various scenarios, including wetland restoration and land use changes, on nutrient exports to the fjord. Additionally, the standard Ringkøbing Fjord model was used to simulate the effects of changes in nutrient loading from the land and the impact of top-down control by shellfish on the fjord's ecosystem.

### Catchment loadings

In addition to the current situation (baseline), the catchment model SWAT+ was used to estimate the impact of 6 scenarios on total nitrogen (TN) exports. These scenarios include:

- Scenario 1 – *No Farming*: This scenario simulates the removal of all agricultural activities in the catchment, replaced with natural grasslands. It indicates the magnitude of changes that could be expected by ceasing agricultural activities in the catchment.
- Scenario 2 – *Full Wetlands*: This scenario simulates the replacement of the entire floodplain area with wetlands. It represents the maximum nutrient retention achievable by restoring all potential wetlands in the catchment.
- Scenario 3 – *60% Wetlands*: This scenario simulates the replacement of 60% of the floodplain area (excluding urban areas) with wetlands.
- Scenario 4 – *50% Wetlands*: This scenario simulates the replacement of 50% of the floodplain area (excluding urban areas) with wetlands.
- Scenario 5 – *40% Wetlands*: This scenario simulates the replacement of 40% of the floodplain area (excluding urban areas) with wetlands.
- Scenario 6 – *No Wastewater*: This scenario simulates the absence of wastewater discharges within the Ringkøbing Fjord catchment.

In scenarios 2 to 5, the floodplain area shown in Fig. 43 is defined using a method called DEM inversion implemented in QSWAT+, the QGIS interface for SWAT+. It is calculated by negating all the DEM elevations and recalculating flow directions and accumulation. Points where the flow accumulation exceeds a threshold, are designated as ridges. A slope position for each point is then calculated. This is the ratio of the drop from each point to where its water flow meets a stream, to the total drop from its ridge point (where its inverse flow meets a ridge) to the same stream point. If this ratio is less than the slope position threshold (0.1) its landscape position is floodplain, else it is upslope. For scenarios 3 to 5, where a portion of the floodplain is subject to wetland restoration, the wetland distribution across the floodplain area is uniform, and no specific areas within the floodplain are specifically targeted.

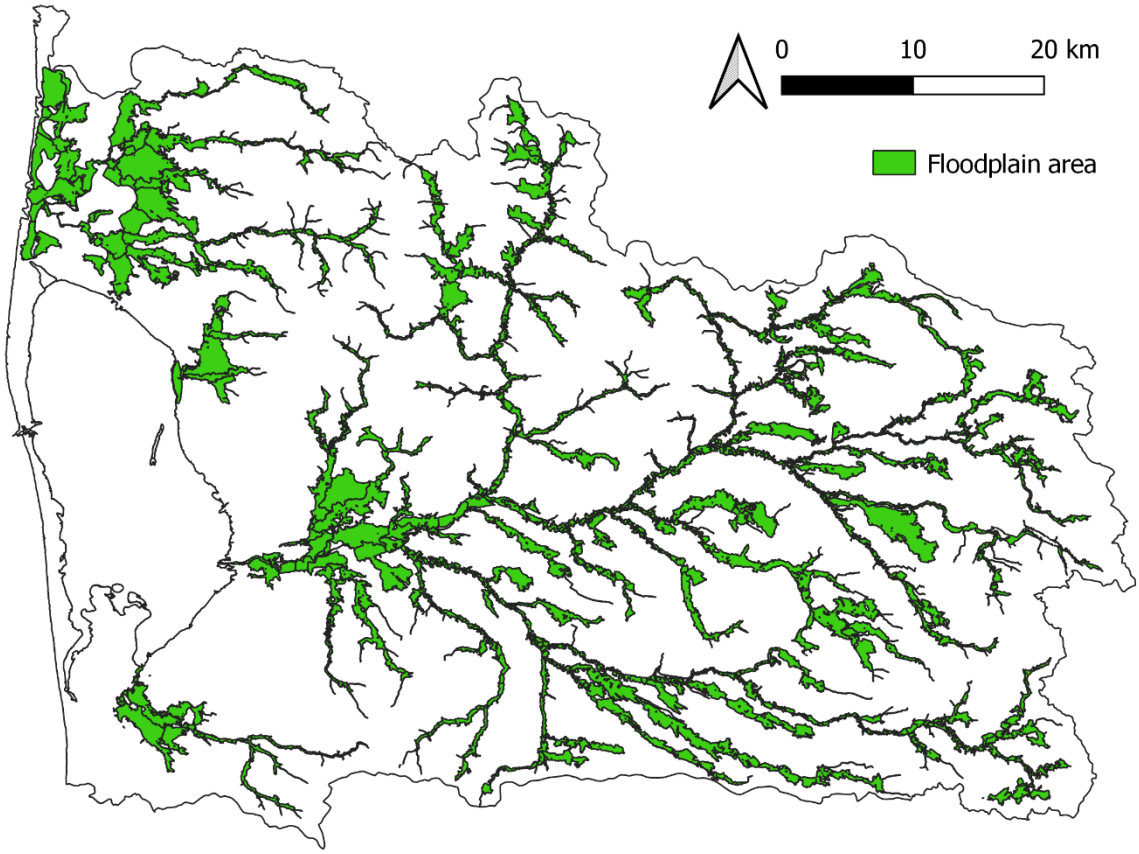


*Fig. 43. Map of the floodplain area used for the implementation of scenarios 2 to 5 (see the text for a description of the scenarios).*

Table 11 contains the main component of the TN balance simulated in the Ringkøbing Fjord catchment for the baseline and the different scenarios. The annual fluxes include input from fertilisers, leaching to groundwater, removal in groundwater, removal in wetlands, exports with surface runoff and exports to the Fjord. These fluxes correspond to annual average for the simulated period (2012-2019). In the current situation (baseline), TN exports to the fjord amount to 4 518 tons, with a significant portion (more than 12 000 tons) retained in groundwater and a smaller fraction (approximately 100 tons) removed in wetlands. These results highlight the importance of nutrient retention in groundwater for the Ringkøbing Fjord catchment, accounting for 71% of the TN leaching to the groundwater. It is worth mentioning that the exports of TN with runoff constitute a minimal portion of the overall exports to the fjord, indicating that most of the fluxes pass through the groundwater.

*Table 11. Main simulated annual fluxes (average for 2012-2019) of total nitrogen (TN) in tons for the Ringkøbing Fjord catchment for the baseline situation and the 6 simulated scenarios. Reduction compared to baseline in % and wetlands area in ha are also indicated.*

| Scenario | Fertiliser inputs | Wastewater discharges | Leaching to groundwater | Removed in groundwater | Removed in wetlands | Exports with runoff | Exports to Ringkøbing Fjord | Exports reduction compared to baseline (%) | Wetlands area (ha) |
|---|---|---|---|---|---|---|---|---|---|
| 0 – Baseline | 45 485 | 34 | 17 769 | 12 686 | 101 | 168 | 4 518 | | 4 031 |
| 1 – No farming | 0 | 34 | 77 42 | 5 243 | 51 | 77 | 2 248 | 50% | 4 031 |
| 2 – Full wetland | 37 836 | 34 | 14 354 | 10 722 | 2 470 | 115 | 1 191 | 74% | 53 937 |
| 3 – 60% wetlands | 41 005 | 34 | 15 839 | 11 833 | 1 428 | 140 | 2 425 | 46% | 32 029 |
| 4 – 50% wetlands | 41 781 | 34 | 16 185 | 11 992 | 1 105 | 154 | 2 797 | 38% | 26 966 |
| 5 – 40% wetlands | 42 557 | 34 | 16 530 | 12 164 | 947 | 149 | 3 158 | 30% | 21 903 |
| 6 – No wastewater | 45 485 | 0 | 17 769 | 12 691 | 101 | 168 | 4 507 | 0% | 4 031 |

For the *No farming* scenario, where all farming areas are converted to natural grasslands, fjord exports decrease by 50% compared to the current situation. This reduction is less than when maintaining farming activities and converting the whole floodplain area to wetlands (*Full wetland* scenario), in which case TN reduction reaches 74%. This seemingly counterintuitive result - a lower reduction in TN exports despite the stop of fertiliser application - can be explained by several factors:

(i) The conversion of cropland to grassland not only eliminates fertilizer inputs but also replaces the crops which are harvested, leading to the removal of nitrogen stored in the system. In contrast, dead biomass in grasslands returns nitrogen to the soil, keeping it within the system.
(ii) The limited fertilizer application rates in current cropland lead to efficient nutrient uptake by plants, thereby minimizing leaching from fertilizers. This is evident in the fact that, although the reduction in fertilizer inputs is substantial (45 000 tons), the simulated decrease in TN leaching to groundwater is only around 10 000 tons of TN.

The *Full Wetland* scenario, resulting in a 74% decrease in TN exports to the fjord, is considered unrealistic but serves to illustrate the expected maximum potential reduction in TN exports from the catchment. Scenarios involving the conversion of a percentage of the floodplain to wetlands present more achievable and realistic values. The rea of restored wetland exhibits a relatively linear relationship with the reduction in TN exports, enabling the estimation of the required wetland area to achieve specific objectives. For instance, to fulfil a targeted decrease of 1 647 tons, as outlined in the 3rd River Basin Management Plan (Vandområdeplanerne 2021-2027), approximately 50% of the floodplain area (around 23 000 ha) would need to be converted to wetlands. Half of this reduction (824 tons) could be achieved with roughly 22% of the floodplain (11 000 ha) converted to wetlands.

The *No wastewater* indicates that wastewater discharges are not significant for the TN exports as they represent less than 1 percent of the TN exports under baseline conditions.

The restoration of wetlands appears as a viable mitigation strategy to reduce nutrient exports from the Ringkøbing Fjord catchment. While the model does not pinpoint specific areas as especially effective for wetland implementation, priority is to be given to locations draining large agricultural areas over those draining smaller forested areas. It's crucial to note that the presented results have limitations as the model operates at the catchment scale and doesn't offer site-specific numbers. Therefore, the figures presented here serve as an indication of the potential scale of total nitrogen (TN) retention that could be attained. Site-specific studies must be performed to better assess the potential TN retention, taking into account the local characteristics of each site.

## Eutrophication in Ringkøbing Fjord

The ecosystem modelling framework (EMF) for Ringkøbing Fjord is a valuable management tool for simulating and assessing different scenarios for eutrophication status and legislative compliance, from source control of nutrient emissions to complementary approaches such as top-down control by shellfish. If diffuse sources such as agriculture are a significant part of nutrient loading, shellfish can play an important role in providing ecosystem services and offset eutrophication symptoms.

*Table 12. Indicators and rationale for analysing different loading scenarios.*

| Variable | Proxy for | Rationale |
|---|---|---|
| Chlorophyll (May-September average) | Phytoplankton biomass | Primary symptom of eutrophication, used in WFD |
| Dissolved inorganic nitrogen (winter average) | Nitrogen in the fjord | Causative factor of eutrophication |
| Epiphyte risk score (average score) | Epiphyte biomass | Symptom of eutrophication |

The three scenarios simulated include top-down control of eutrophication simulated by the removal of shellfish. The other scenarios represent bottom-up control of eutrophication with two levels of reduction in nutrient loads from the catchment and entering Ringkøbing Fjord. The first reproduces a 35% reduction, corresponding to the reduction in total nitrogen targeted by the River Basin Management Plan. The other takes into account half of this reduction (17.5%). The indicators chosen to analyse the response of the ecosystem, and the rationale for these choices, are presented in Table 12.

### *Bottom-up control of eutrophication*

Nutrient inputs to the fjord increase primary production and potentially lead to eutrophication, which would result in a degradation of water quality and ecosystem health and impact economic activities and other uses of the fjord. The EMF was applied to analyse various nutrient loading scenarios, and their effect on chla concentrations. The bottom-up control represents the effect of source-control on primary production, keeping all shellfish in the system.

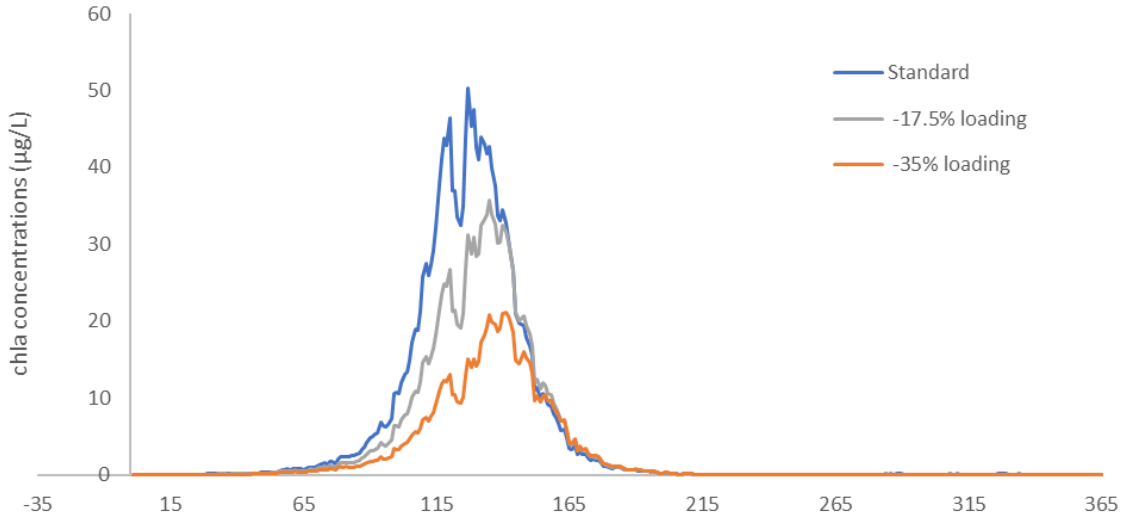


*Fig. 44. Effect of three level of loading on chlorophyll in Box 13 located in the middle of the fjord.*

The bottom-up control of chla is illustrated in Fig. 44 where the time series of chla concentrations is shown for three levels of loading in the box 13 located in the middle of the fjord. By reducing the river load by 35% (including nutrients and suspended particles), we get a reduction in summer chla values in all EWN boxes, ranging from 37 to 60% (0.2-4.2 $\mu g.L^{-1}$). This reduction ranges from 10 to 29% when the load was reduced by 17.5% (0.1-1.7 $\mu g.L^{-1}$). While the high percentage could indicate a significant decrease in summer chla, this reduction occurs on already low concentrations, so that the absolute change is not very large, averaging 1.4 $\mu g.L^{-1}$. In comparison, the limit set by the WFD for achieving good ecological potential is 8.4 $\mu g.L^{-1}$. The bottom-up control would appear to be felt stronger at peak values (Fig. 44). The bottom-up control of eutrophication by pro-rata reduction of river loads is significant across in all the fjord as shown in Table 13. Bottom-up control of macrophyte and epiphyte biomass is also significant in some model boxes. A reduction of the river load affects the amount of nutrients available for macrophyte and epiphyte growth.

*Table 13. Impact of bottom-up control on a set of indicators for a selection of bottom boxes with contrasted settings.*

| Indicator | Scenario | Box 29 | Box 45 | Box 47 |
|---|---|---|---|---|
| Summer chla (µg.L$^{-1}$) | Standard loading | 1.3 | 1.3 | 1.6 |
| | -17.5% loading | 1.0 | 1.1 | 1.2 |
| | -35% loading | 0.7 | 0.7 | 0.8 |
| Winter DIN (mg.L$^{-1}$) | Standard loading | 1.8 | 1.6 | 1.6 |
| | -17.5% loading | 1.5 | 1.3 | 1.2 |
| | -35% loading | 1.1 | 0.96 | 0.90 |
| Macrophyte + epiphyte biomass (kg.m$^{-2}$) | Standard loading | 708 | 42 | 373 |
| | -17.5% loading | 708 | 42 | 336 |
| | -35% loading | 707 | 42 | 375 |
| Epiphyte risk score | Standard loading | 3.42 | 1.10 | 2.70 |
| | -17.5% loading | 3.26 | 1.09 | 2.39 |
| | -35% loading | 3.02 | 1.06 | 2.21 |

Fig. 45 shows the epiphyte risk score for all boxes for different loading. Overall, the epiphyte risk score decreases with decreasing load, although this is not the case for the boxes with the lowest epiphyte risk score, which correspond to boxes in the middle of the fjord that are generally deeper and have less macrophyte biomass due to lower light penetration. While the decrease in epiphyte risk score is relatively homogeneous in the other boxes, a few boxes seem to be more reactive to changes in load in terms of the decrease in the epiphyte risk score, such as boxes 7 and 8, which are located in the southern part of the fjord.

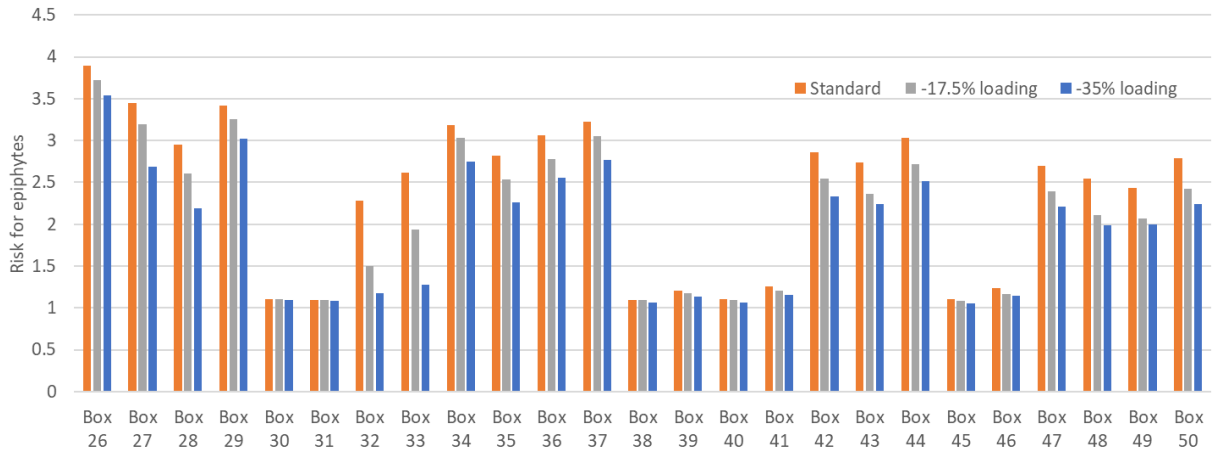


*Fig. 45. Effect of three different loading on the epiphyte risk score.*

### *Top-down control of eutrophication*

Analysis of chlorophyll concentrations with and without shellfish was carried out using the EcoWin model. Fig. 46 shows the difference in chlorophyll depending on whether or not shellfish are active in the system for a selection of upper and lower boxes and suggests that the filtration of phytoplankton and organic detritus contributes significantly to the control of eutrophication. When shellfish are 'turned off' in EcoWin, i.e. removed from the system, chlorophyll increases significantly throughout the fjord. The change in chlorophyll is always more pronounced in the lower boxes than in the upper boxes because the shellfish are only found in the lower boxes.

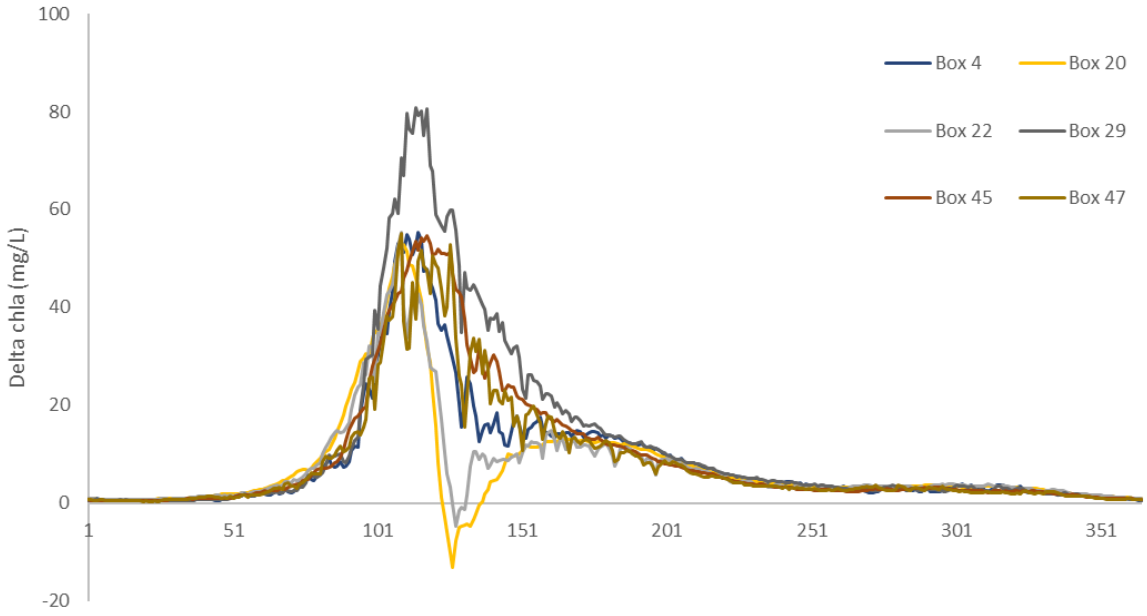


*Fig. 46. Top-down control of eutrophication by Mya arenaria at six EWN boxes in Ringkøbing Fjord.*

The results show that in the absence of Mya arenaria, summer chla values would be multiplied by 12 on average in the lower boxes and by 2 in the upper boxes.

*Table 14. Impact of top-down control on a set of indicators for a selection of bottom boxes with contrasted settings.*

| Indicator | Scenario | Box 29 | Box 45 | Box 47 |
|---|---|---|---|---|
| Summer chla (µg.L$^{-1}$) | With *Mya arenaria* | 1.3 | 1.3 | 1.6 |
| | No top-down control | 16.9 | 13.8 | 12.7 |
| | Difference (%) | +1191 | +955 | +709 |
| Winter DIN (mg.L$^{-1}$) | With *Mya arenaria* | 1.8 | 1.6 | 1.6 |
| | No top-down control | 1.8 | 1.6 | 1.5 |
| | Difference (%) | +1 | +1 | +1 |
| Macrophyte + epiphyte biomass (kg.m$^{-2}$) | With *Mya arenaria* | 708 | 42 | 373 |
| | No top-down control | 705 | 33 | 53 |
| | Difference (%) | -1 | -22 | -86 |
| Epiphyte risk score | With *Mya arenaria* | 3.42 | 1.10 | 2.70 |
| | No top-down control | 3.30 | 1.08 | 1.17 |
| | Difference (%) | -4 | -1 | -57 |

The impact of top-down control by shellfish on a set of indicators for a selection of boxes with contrasted settings is shown in Table 14. The results show that in the absence of Mya arenaria, summer chla values would be multiplied by 12 on average in the lower boxes and by 2 in the upper boxes. The presence or absence of shellfish have no impact on winter DIN. The top-down control of

chla by shellfish also affects other symptoms of eutrophication, such as the presence of epiphytes. Indeed, when the shellfish are removed, the chla increases, which reduces light penetration and therefore macrophyte biomass growth, which is divided by more than two in 16 of the 25 bottom boxes. As a result, the epiphyte risk score also decreases as their substrate is considerably reduced.

# Conclusions

A description of the ecological modelling framework (EMF) applied to Ringkøbing Fjord, including sectorial descriptions of key components, was presented in this report, together with examples of application of the modelling system to analyse options for eutrophication control in Ringkøbing Fjord

The methodologies used for calibration and validation of models representing (i) loading from land; (ii) water circulation; (iii) shellfish growth, (iv) macrophyte and epiphyte growth; and (v) ecosystem processes and functioning were reviewed and show that the various tools are fit for purpose—specifically, they may be used, together or separately, to inform policy-making options and management decisions.

The catchment model was used to simulate the impacts of land use change and wetland restoration scenarios on nitrogen loading. The results show that above a certain threshold, restoring wetlands is more effective than eliminating all agricultural activities. The model indicates that restoring 23 000 ha of wetlands (7% of the Ringkøbing Fjord catchment) could reduce the nitrogen loading by around 38% (Table 1 and Table 11). The model also indicates that urban inputs are a negligible source of nitrogen.

The integration of benthic primary (macrophytes) and secondary producers (bivalves – the softshell clam *Mya arenaria*) in this framework is a major asset since it allows policy makers to evaluate trade-offs.

The model results indicate that chlorophyll concentrations are below the threshold for good ecological potential, set to 8.4 $\mu g.L^{-1}$ in the current River Basin Management (RBMP), in 48 out of the 50 model boxes. In the examples provided in this report, a cut in land-based loading from all sources by 35% - corresponding to the reduction in nitrogen targeted by the RBMP - shows reductions of 0.2-4.2 $\mu g.L^{-1}$ in summer chlorophyll concentrations (Table 2 and Table 13). This 35% reduction also results in a reduction in the epiphyte risk score and is a potentially important measure to control the fjord eutrophication although epiphytes are not considered an indicator in the WFD Biological Quality Elements (BQE). The reduction in epiphyte risk score is greater for boxes located on the edge of the fjord, where the current risk is highest. Reducing the load by half of the 35% target indicates a reduction in summer chlorophyll concentrations of between 0.1 and 1.7 $\mu g.L^{-1}$ and a decrease in the risk for epiphytes divided by two compared with the 35% reduction.

The presence of shellfish (Mya arenaria) within the fjord is a key factor in the top-down control of eutrophication, as summer concentrations of chlorophyll can be multiplied by more than 10 in bottom boxes in the absence of Mya arenaria in the fjord and exceed the threshold for good ecological potential in the entire fjord (Table 2 and Table 14). It corresponds to an important regulatory ecosystem service supplied by bivalves. The disappearance of shellfish in the fjord would contribute to a significant increase in eutrophication in the fjord and is the main hypothesis explaining the spectacular algal bloom observed in Ringkøbing Fjord in 2019.

# References


Audet, J., Zak, D., Bidstrup, J. *et al.* Nitrogen and phosphorus retention in Danish restored wetlands. *Ambio* 49, 324–336 (2020). https://doi.org/10.1007/s13280-019-01181-2

Bayne BL, Iglesias JIP, Hawkins AJS, et al (1993) Feeding behavior of the Mussel, Mytilus edulis - Response to variations in quantity and organic content of the seston. J Mar Biol Assoc United Kingdom 73:813–829. https://doi.org/10.1017/S0025315400034743

Bieger, Katrin, Arnold, Jeffrey G., Rathjens, Hendrik, White, Michael J., Bosch, David D., Allen, Peter M., Volk, Martin, and Srinivasan, Raghavan, 2017. Introduction to SWAT+, a Completely Restructured Version of the Soil and Water Assessment Tool. Journal of the American Water Resources Association (JAWRA) 53(1): 115–130. doi.org/10.1111/1752-1688.12482

Bocci, M., Coffaro, G., Bendoricchio, G., 1997. Modelling biomass and nutrient dynamics in eelgrass (*Zostera marina* L.): applications to the Lagoon of Venice (Italy) and Øresund (Denmark)Ecological Modelling, 102(1), 67-80.

Bricker, S.B., J.G. Ferreira, T. Simas, 2003. An Integrated Methodology for Assessment of Estuarine Trophic Status. Ecological Modelling, 169(1), 39-60.

Brousseau DJ (1978) Spawning cycle, fecundity, and recruitment in a population of soft-shell clam, Mya arenaria, from Cape Ann, Massachusetts. Fish Bull 76:155–166

Brousseau DJ (1979) Analysis of growth rate in Mya arenaria using the Von Bertalanffy equation. Mar Biol 51:221–227. https://doi.org/10.1007/BF00386801

Bulthuis, D.A., 1987. Effects of temperature on photosynthesis and growth of seagrasses. Aquatic Botany, 27(1), 27-40.

Butenschön, M., Clark, J., Aldridge, J.N., Allen, J.I., Artioli, Y., Blackford, J., Bruggeman, J., Cazenave, P., Ciavatta, S., Kay, S., Lessin, G., van Leeuwen, S., van der Molen, J., de Mora, L., Polimene, L., Sailley, S., Stephens, N., Torres, R., 2016. ERSEM 15.06: a generic model for marine biogeochemistry and the ecosystem dynamics of the lower trophic levels. Geosci. Model Dev. 9, 1293-1339.

Cross ME, Lynch S, Whitaker A, et al (2012) The Reproductive Biology of the Softshell Clam, Mya arenaria , in Ireland, and the Possible Impacts of Climate Variability . J Mar Biol 2012:1–9. https://doi.org/10.1155/2012/908163

Deltares, 2010. Delft3D-FLOW, Simulation of multi-dimensional flows and transport phenomena, including sediments, Deltares, User Manual. V.3.14, Delft, the Netherlands.

Du Clos KT, Jones IT, Carrier TJ, et al (2017) Model-assisted measurements of suspension-feeding flow velocities. J Exp Biol 220:2096–2107. https://doi.org/10.1242/jeb.147934

Emerson, C. W., Minchinton, T. E., & Grant, J. (1988). Population structure, biomass, and respiration of Mya arenaria L. on temperate sandflat. *Journal of experimental marine biology and ecology*, *115*(2), 99-111.

Ferreira, J.G., S.B. Bricker, T.C. Simas, 2007. Application and sensitivity testing of an eutrophication assessment method on coastal systems in the United States and European Union. J. Environmental Management, 82, 433-445.

Ferreira JG, Bricker SB (2016) Goods and services of extensive aquaculture: shellfish culture and nutrient trading. Aquac Int 24:803–825. https://doi.org/10.1007/s10499-015-9949-9

Gerasimova A V., Maximovich N V., Filippova NA (2015) Cohort life tables for a population of the soft-shell clam, Mya arenaria L., in the White Sea. Helgol Mar Res 69:147–158. https://doi.org/10.1007/s10152-014-0423-2

Greve, M. H., Greve, M. B., Bøcher, P. K., Balstrøm, T., Breuning-Madsen, H., & Krogh, L. (2007). Generating a Danish raster-based topsoil property map combining choropleth maps and point information. Geografisk Tidsskrift-Danish Journal of Geography, 107(2), 1-12.

Jorgensen CB, Famme P, Kristenses HS, et al (1986) The bivalve pump. Mar Ecol Progr Ser 34:69–77

Ledoux T, Clements JC, Maillet M, et al (2023) Reproductive ecology of the soft-shell clam (Mya arenaria) in Eastern New Brunswick, Canada: Assessing size-at-maturity and spawning time to inform fisheries management. Fish Res 265:. https://doi.org/10.1016/j.fishres.2023.106759

Lesser, G.P., Roelvink, J.A., van Kester, J.A.T.M. and Stelling, G.S., 2004. Development and validation of a three-dimensional morphodynamic model. Coastal Engineering, 51, 883-915.

Moriasi, D.M., Pai, N., Daggupati, P., 2015. Hydrologic and Water Quality Models: Performance Measures and Evaluation Criteria. Transactions of the ASABE (American Society of Agricultural and Biological Engineers). 58. 1763-1785. 10.13031/trans.58.10715.

Nielsen, M. H., Rasmussen, B., & Gertz, F. (2005). A simple model for water level and stratification in Ringkøbing Fjord, a shallow, artificial estuary. Estuarine, Coastal and Shelf Science, 63(1–2), 235–248. doi:10.1016/j.ecss.2004.08.02413

Petersen, J. K., Bougrier, S., Smaal, A. C., Garen, P., Robert, S., Larsen, J. E. N., & Brummelhuis, E. (2004). Intercalibration of mussel Mytilus edulis clearance rate measurements. *Marine Ecology Progress Series*, *267*, 187-194.

Plus, M., Chappelle, A., Ménesguen, A., Deslous-Pauli, J.-M., Auby, I., 2003. Modelling seasonal dynamics of biomasses and nitrogen contents in a seagrass meadow (*Zostera noltii* Hornem.): application to the Thau lagoon (French Mediterranean coast). Ecological Modelling, 161 (3), 213-238.

Pouvreau S, Bourles Y, Lefebvre S, et al (2006) Application of a dynamic energy budget model to the Pacific oyster, Crassostrea gigas, reared under various environmental conditions. J Sea Res 56:156–167. https://doi.org/10.1016/j.seares.2006.03.007

Riisgård HU. 2001. Physiological regulation versus autonomous filtration in filter-feeding bivalves: Starting points for progress. Ophelia 54: 193–209

Riisgård, H. U., Kittner, C., & Seerup, D. F. (2003). Regulation of opening state and filtration rate in filter-feeding bivalves (Cardium edule, Mytilus edulis, Mya arenaria) in response to low algal concentration. *Journal of experimental marine biology and ecology*, *284*(1-2), 105-127.

Schäffer F, Zettler ML (2007) The clam sipho as indicator for growth indices in the soft-shell clam Mya arenaria. Helgol Mar Res 61:9–16. https://doi.org/10.1007/s10152-006-0049-0

Scholten H, Smaal AC (1998) Responses of Mytilus edulis L. to varying food concentrations: Testing EMMY, an ecophysiological model. J Exp Mar Bio Ecol 219:217–239. https://doi.org/10.1016/S0022-0981(97)00182-2

Wagner, P. D., Bieger, K., Arnold, J. G., & Fohrer, N. (2022). Representation of hydrological processes in a rural lowland catchment in Northern Germany using SWAT and SWAT+. *Hydrological Processes*, 36(5), e14589. https://doi.org/10.1002/hyp.14589

Wetzel R., & Neckles, 1986. A model of *Zostera marina* L. Photosynthesis and growth: Simulated effects of selected physical-chemical variables and biological interactions. Aquatic Botany, 26, 307-323.

Willmott, C. J. (1981). On the validation of models. Physical Geography, 2(2), 184–194. https://doi.org/10.1080/02723646.1981.106422

Zwarts L (1991) Seasonal variation in body weight of the bivalves Macoma balthica, Scrobicularia plana, Mya arenaria and Cerastoderman edule in the Dutch Wadden sea. Netherlands J Sea Res 28:231–245. https://doi.org/10.1016/0077-7579(91)90021-R

# Annex 1: Crop rotations integrated in the SWAT+ model.

| Crop rotation 1 Seed production/Frøavl | Main crop (afgrødefølge) | Spead/Catch crop (efterafgrøde) | N-norm | Animal manure | Mineral fertilizer | N applied | P applied in manure |
|---|---|---|---|---|---|---|---|
| | | | kg N/ha | kg total-N/ha | kg N/ha | kg N/ha | kg P/ha |
| Afgrøde 1 | spring barley | Udlæg til frø | 116 | 28 | 95 | 123 | 4.48 |
| Afgrøde 2 | rye grass. | | 170 | 40 | 140 | 180 | 6.4 |
| Afgrøde 3 | spring barley | Udlæg til frø | 98 | 23 | 81 | 104 | 3.68 |
| Afgrøde 4 | rye grass. | | 170 | 40 | 140 | 180 | 6.4 |
| Afgrøde 5 | Winter wheat | | 157 | 37 | 129 | 166 | 5.92 |
| Afgrøde 6 | spring barley | Udlæg til frø | 141 | 33 | 116 | 149 | 5.28 |
| Afgrøde 7 | rye grass. | | 170 | 40 | 140 | 180 | 6.4 |
| Afgrøde 8 | Winter wheat | | 157 | 37 | 129 | 166 | 5.92 |
| Gennemsnit | | | 157 | 35 | 121 | 147 | 21 |

| Crop rotation 3 Potato farm/kartofler | Main crop (afgrødefølge) | Spead/Catch crop (efterafgrøde) | N-norm | Animal manure | Mineral fertilizer | N applied | P applied in manure |
|---|---|---|---|---|---|---|---|
| | | | kg N/ha | kg total-N/ha | kg N/ha | kg N/ha | kg P/ha |
| Afgrøde 1 | Potato, spise | | 169 | 41 | 138 | 179 | 6.56 |
| Afgrøde 2 | spring barley | Efterafgrøde | 141 | 34 | 115 | 149 | 5.44 |
| Afgrøde 3 | spring barley | Efterafgrøde | 116 | 28 | 95 | 123 | 4.48 |
| Afgrøde 4 | Potato, spise | | 144 | 35 | 118 | 153 | 5.6 |
| Afgrøde 5 | spring barley | | 141 | 34 | 115 | 149 | 5.44 |
| Afgrøde 6 | Winter rye | | 150 | 37 | 123 | 160 | 5.92 |
| Afgrøde 7 | | | | | | 0 | 0 |
| Afgrøde 8 | | | | | | 0 | 0 |
| Gennemsnit | | | 150 | 35 | 117 | 143.25 | 21 |

| Crop rotation 2 Vegetables/Friland sgrøntsager | Main crop (afgrødefølge) | Spead/Catch crop (efterafgrøde) | N-norm | Animal manure | Mineral fertilizer | N applied | P applied in manure |
|---|---|---|---|---|---|---|---|
| | | | kg N/ha | kg total-N/ha | kg N/ha | kg N/ha | kg P/ha |
| Afgrøde 1 | spring barley | Efterafgrøde | 123 | 74 | 67 | 141 | 11.84 |
| Afgrøde 2 | Salat | | 123 | 74 | 67 | 141 | 11.84 |
| Afgrøde 3 | Carrots | | 152 | 92 | 83 | 175 | 14.72 |
| Afgrøde 4 | Peas | | 0 | 0 | 0 | 0 | 0 |
| Afgrøde 5 | spring barley | Efterafgrøde | 123 | 74 | 67 | 141 | 11.84 |
| Afgrøde 6 | Carrots | | 145 | 88 | 79 | 167 | 14.08 |
| Afgrøde 7 | spring barley | Efterafgrøde | 138 | 83 | 75 | 158 | 13.28 |
| Afgrøde 8 | Salat | | 123 | 74 | 67 | 141 | 11.84 |
| Gennemsnit | | | 123 | 70 | 63 | 115.5 | 42 |

| Crop rotation 4 Cattlefarm with more than 20% wholecrop for fodder | Main crop (afgrødefølge) | Spead/Catch crop (efterafgrøde) | N-norm | Animal manure | Mineral fertilizer | N applied | P applied in manure |
|---|---|---|---|---|---|---|---|
| | | | kg N/ha | kg total-N/ha | kg N/ha | kg N/ha | kg P/ha |
| Afgrøde 1 | spring barley | Kl.græs udlæg e korn | 141 | 125 | 47 | 172 | 20 |
| Afgrøde 2 | Grass w legume | | 270 | 240 | 90 | 330 | 38.4 |
| Afgrøde 3 | Grass w legume | | 270 | 240 | 90 | 330 | 38.4 |
| Afgrøde 4 | Maize | Efterafgrøde | 53 | 47 | 18 | 65 | 7.52 |
| Afgrøde 5 | Maize | Efterafgrøde | 143 | 127 | 48 | 175 | 20.32 |
| Afgrøde 6 | Maize | Efterafgrøde | 143 | 127 | 48 | 175 | 20.32 |
| Afgrøde 7 | spring barley | | 116 | 103 | 39 | 142 | 16.48 |
| Afgrøde 8 | Winter wheat | | 175 | 156 | 58 | 214 | 24.96 |
| Gennemsnit | | | 175 | 146 | 55 | 164.5 | 87.6 |

| Crop rotation 5 Organic Cattlefarm with more than 20% wholecrop for fodder | Main crop (afgrødefølge) | Spead/Catch crop (efterafgrøde) | N-norm | Animal manure | Mineral fertilizer | N applied | P applied in manure |
|---|---|---|---|---|---|---|---|
| | | | kg N/ha | kg total-N/ha | kg N/ha | kg N/ha | kg P/ha |
| Afgrøde 1 | spring barley | Kl.græs udlæg e korn | 26 | 20 | 0 | 20 | 3.2 |
| Afgrøde 2 | Grass w legume | | 270 | 209 | 0 | 209 | 33.44 |
| Afgrøde 3 | Grass w legume | | 270 | 209 | 0 | 209 | 33.44 |
| Afgrøde 4 | Winter wheat | | 60 | 46 | 0 | 46 | 7.36 |
| Afgrøde 5 | Maize | Efterafgrøde | 168 | 130 | 0 | 130 | 20.8 |
| Afgrøde 6 | spring barley | Kl.græs udlæg e korn | 141 | 109 | 0 | 109 | 17.44 |
| Afgrøde 7 | Grass w legume | | 270 | 209 | 0 | 209 | 33.44 |
| Afgrøde 8 | Grass w legume | | 270 | 209 | 0 | 209 | 33.44 |
| Gennemsnit | | | 270 | 142 | 0 | 106.5 | 85.2 |

| Crop rotation 7 Plant farm | Main crop (afgrødefølge) | Spead/Catch crop (efterafgrøde) | N-norm | Animal manure | Mineral fertilizer | N applied | P applied in manure |
|---|---|---|---|---|---|---|---|
| | | | kg N/ha | kg total-N/ha | kg N/ha | kg N/ha | kg P/ha |
| Afgrøde 1 | spring barley | | 116 | 76 | 59 | 135 | 12.16 |
| Afgrøde 2 | winter barley | | 172 | 113 | 87 | 200 | 18.08 |
| Afgrøde 3 | winter rape | | 190 | 125 | 96 | 221 | 20 |
| Afgrøde 4 | Winter wheat | Efterafgrøde | 157 | 103 | 80 | 183 | 16.48 |
| Afgrøde 5 | spring barley | Efterafgrøde | 116 | 76 | 59 | 135 | 12.16 |
| Afgrøde 6 | spring barley | Efterafgrøde | 116 | 76 | 59 | 135 | 12.16 |
| Afgrøde 7 | | | | | | | |
| Afgrøde 8 | | | | | | | |
| Gennemsnit | | | 116 | 95 | 73 | 144.25 | 57 |

| Crop rotation 6 Cattlefarm with less than 20% wholecrop for fodder | Main crop (afgrødefølge) | Spead/Catch crop (efterafgrøde) | N-norm | Animal manure | Mineral fertilizer | N applied | P applied in manure |
|---|---|---|---|---|---|---|---|
| | | | kg N/ha | kg total-N/ha | kg N/ha | kg N/ha | kg P/ha |
| Afgrøde 1 | spring barley | Kl.græs udlæg o. 50% e korn | 141 | 136 | 39 | 175 | 21.76 |
| Afgrøde 2 | Clover grass | Efterafgrøde | 284 | 273 | 79 | 352 | 43.68 |
| Afgrøde 3 | Maize | Efterafgrøde | 28 | 27 | 8 | 35 | 4.32 |
| Afgrøde 4 | spring barley | | 116 | 112 | 32 | 144 | 17.92 |
| Afgrøde 5 | Winter wheat | Efterafgrøde | 175 | 168 | 49 | 217 | 26.88 |
| Afgrøde 6 | spring barley | | 116 | 112 | 32 | 144 | 17.92 |
| Afgrøde 7 | Winter wheat | | 175 | 168 | 49 | 217 | 26.88 |
| Afgrøde 8 | Potato (starch) | | 206 | 198 | 57 | 255 | 31.68 |
| Gennemsnit | | | 206 | 149 | 43 | 154.75 | 89.4 |

| Crop rotation 8 Plant farm | Main crop (afgrødefølge) | Spead/Catch crop (efterafgrøde) | N-norm | Animal manure | Mineral fertilizer | N applied | P applied in manure |
|---|---|---|---|---|---|---|---|
| | | | kg N/ha | kg total-N/ha | kg N/ha | kg N/ha | kg P/ha |
| Afgrøde 1 | spring barley | | 116 | 80 | 56 | 136 | 12.8 |
| Afgrøde 2 | Winter wheat | Efterafgrøde | 175 | 121 | 84 | 205 | 19.36 |
| Afgrøde 3 | spring oats | | 90 | 62 | 43 | 105 | 9.92 |
| Afgrøde 4 | Winter wheat | Efterafgrøde | 175 | 121 | 84 | 205 | 19.36 |
| Afgrøde 5 | spring barley | | 116 | 80 | 56 | 136 | 12.8 |
| Afgrøde 6 | Winter rye | Efterafgrøde | 150 | 104 | 72 | 176 | 16.64 |
| Afgrøde 7 | | | | | | | |
| Afgrøde 8 | | | | | | | |
| Gennemsnit | | | 150 | 95 | 66 | 137.25 | 57 |

| Crop rotation 9 | Main crop (afgrødefølge) | Spead/Catch crop (efterafgrøde) | N-norm | Animal manure | Mineral fertilizer | N applied | P applied in manure |
|---|---|---|---|---|---|---|---|
| Organic plant farm | | | kg N/ha | kg total-N/ha | kg N/ha | kg N/ha | kg P/ha |
| Afgrøde 1 | spring barley | Efterafgrøde | 141 | 139 | 0 | 139 | 22.24 |
| Afgrøde 2 | Horse bean | | 0 | 0 | 0 | 0 | 0 |
| Afgrøde 3 | Winter wheat | Efterafgrøde | 175 | 172 | 0 | 172 | 27.52 |
| Afgrøde 4 | spring oats | | 90 | 89 | 0 | 89 | 14.24 |
| Afgrøde 5 | Winter rye | | 150 | 148 | 0 | 148 | 23.68 |
| Afgrøde 6 | spring oats | | 115 | 113 | 0 | 113 | 18.08 |
| Afgrøde 7 | | | | | | | |
| Afgrøde 8 | | | | | | | |
| Gennemsnit | | | 115 | 132 | 0 | 99 | 79.2 |

| Crop rotation 11 | Main crop (afgrødefølge) | Spead/Catch crop (efterafgrøde) | N-norm | Animal manure | Mineral fertilizer | N applied | P applied in manure |
|---|---|---|---|---|---|---|---|
| Pig farm with more than 80 kg N pr ha fertilizer | | | kg N/ha | kg total-N/ha | kg N/ha | kg N/ha | kg P/ha |
| Afgrøde 1 | spring barley | Efterafgrøde | 116 | 96 | 39 | 135 | 15.36 |
| Afgrøde 2 | Potato (starch) | | 181 | 150 | 61 | 211 | 24 |
| Afgrøde 3 | spring barley | | 141 | 117 | 47 | 164 | 18.72 |
| Afgrøde 4 | Winter wheat | Efterafgrøde | 175 | 145 | 59 | 204 | 23.2 |
| Afgrøde 5 | spring barley | | 116 | 96 | 39 | 135 | 15.36 |
| Afgrøde 6 | Winter wheat | | 175 | 145 | 59 | 204 | 23.2 |
| Afgrøde 7 | Winter rye | Efterafgrøde | 150 | 125 | 50 | 175 | 20 |
| Afgrøde 8 | | | | | | | |
| Gennemsnit | | | 150 | 125 | 51 | 151 | 75 |

| Crop rotation 10 | Main crop (afgrødefølge) | Spead/Catch crop (efterafgrøde) | N-norm | Animal manure | Mineral fertilizer | N applied | P applied in manure |
|---|---|---|---|---|---|---|---|
| Organic plant farm | | | kg N/ha | kg total-N/ha | kg N/ha | kg N/ha | kg P/ha |
| Afgrøde 1 | spring barley | | 116 | 89 | 0 | 89 | 14.24 |
| Afgrøde 2 | Clover grass | Efterafgrøde | 284 | 219 | 0 | 219 | 35.04 |
| Afgrøde 3 | spring oats | | 0 | 0 | 0 | 0 | 0 |
| Afgrøde 4 | Winter rye | | 150 | 116 | 0 | 116 | 18.56 |
| Afgrøde 5 | spring barley | | 141 | 109 | 0 | 109 | 17.44 |
| Afgrøde 6 | Winter wheat | Efterafgrøde | 165 | 127 | 0 | 127 | 20.32 |
| Afgrøde 7 | | | | | | | |
| Afgrøde 8 | | | | | | | |
| Gennemsnit | | | 165 | 110 | 0 | 82.5 | 66 |

| Crop rotation 12 | Main crop (afgrødefølge) | Spead/Catch crop (efterafgrøde) | N-norm | Animal manure | Mineral fertilizer | N applied | P applied in manure |
|---|---|---|---|---|---|---|---|
| Pig farm with more than 80 kg N pr ha fertilizer | | | kg N/ha | kg total-N/ha | kg N/ha | kg N/ha | kg P/ha |
| Afgrøde 1 | spring barley | | 116 | 97 | 38 | 135 | 15.52 |
| Afgrøde 2 | winter barley | | 172 | 144 | 56 | 200 | 23.04 |
| Afgrøde 3 | winter rape | | 190 | 160 | 62 | 222 | 25.6 |
| Afgrøde 4 | Winter wheat | Efterafgrøde | 157 | 132 | 52 | 184 | 21.12 |
| Afgrøde 5 | spring barley | | 116 | 97 | 38 | 135 | 15.52 |
| Afgrøde 6 | Winter wheat | Efterafgrøde | 175 | 147 | 57 | 204 | 23.52 |
| Afgrøde 7 | spring barley | Efterafgrøde | 116 | 97 | 38 | 135 | 15.52 |
| Afgrøde 8 | | | | | | | |
| Gennemsnit | | | 116 | 125 | 49 | 149 | 75 |

| Crop rotation 13 | Main crop (afgrødefølge) | Spead/Catch crop (efterafgrøde) | N-norm | Animal manure | Mineral fertilizer | N applied | P applied in manure |
|---|---|---|---|---|---|---|---|
| Organic Pig farm with more than 80 kg N pr ha fertilizer | | | kg N/ha | kg total-N/ha | kg N/ha | kg N/ha | kg P/ha |
| Afgrøde 1 | spring barley | | 116 | 119 | 0 | 119 | 19.04 |
| Afgrøde 2 | Clover grass | Efterafgrøde | 284 | 290 | 0 | 290 | 46.4 |
| Afgrøde 3 | Winter rye | | 10 | 10 | 0 | 10 | 1.6 |
| Afgrøde 4 | spring barley | Udlæg til frø | 141 | 144 | 0 | 144 | 23.04 |
| Afgrøde 5 | rye grass. | | 170 | 174 | 0 | 174 | 27.84 |
| Afgrøde 6 | spring oats | | 97 | 99 | 0 | 99 | 15.84 |
| Afgrøde 7 | spring barley | Efterafgrøde | 141 | 144 | 0 | 144 | 23.04 |
| Afgrøde 8 | | | | | | | |
| Gennemsnit | | | 141 | 140 | 0 | 112 | 84 |

| Crop rotation 15 | Main crop (afgrødefølge) | Spead/Catch crop (efterafgrøde) | N-norm | Animal manure | Mineral fertilizer | N applied | P applied in manure |
|---|---|---|---|---|---|---|---|
| Pig farm with less than 80 kg N pr ha fertilizer | | | kg N/ha | kg total-N/ha | kg N/ha | kg N/ha | kg P/ha |
| Afgrøde 1 | spring barley | | 116 | 31 | 92 | 123 | 4.96 |
| Afgrøde 2 | winter barley | | 172 | 45 | 136 | 181 | 7.2 |
| Afgrøde 3 | winter rape | | 190 | 50 | 150 | 200 | 8 |
| Afgrøde 4 | Winter wheat | Efterafgrøde | 157 | 41 | 124 | 165 | 6.56 |
| Afgrøde 5 | spring barley | Mellemafgrøde | 116 | 31 | 92 | 123 | 4.96 |
| Afgrøde 6 | Winter wheat | Efterafgrøde | 175 | 46 | 138 | 184 | 7.36 |
| Afgrøde 7 | spring barley | Mellemafgrøde | 116 | 31 | 92 | 123 | 4.96 |
| Afgrøde 8 | Winter wheat | Efterafgrøde | 175 | 46 | 138 | | |
| Gennemsnit | | | 175 | 40 | 120 | 152 | 24 |

| Crop rotation 14 | Main crop (afgrødefølge) | Spead/Catch crop (efterafgrøde) | N-norm | Animal manure | Mineral fertilizer | N applied | P applied in manure |
|---|---|---|---|---|---|---|---|
| Organic Pig farm with more than 80 kg N pr ha fertilizer | | | kg N/ha | kg total-N/ha | kg N/ha | kg N/ha | kg P/ha |
| Afgrøde 1 | spring barley | Efterafgrøde | 116 | 145 | 0 | 145 | 23.2 |
| Afgrøde 2 | Horse bean | | 0 | 0 | 0 | 0 | 0 |
| Afgrøde 3 | Winter wheat | | 157 | 196 | 0 | 196 | 31.36 |
| Afgrøde 4 | Maize | | 168 | 210 | 0 | 210 | 33.6 |
| Afgrøde 5 | spring barley | Efterafgrøde | 141 | 176 | 0 | 176 | 28.16 |
| Afgrøde 6 | spring oats | | 90 | 113 | 0 | 113 | 18.08 |
| Afgrøde 7 | | | | | | 0 | 0 |
| Afgrøde 8 | | | | | | | |
| Gennemsnit | | | 90 | 140 | 0 | 112 | 84 |

| Crop rotation 16 | Main crop (afgrødefølge) | Spead/Catch crop (efterafgrøde) | N-norm | Animal manure | Mineral fertilizer | N applied | P applied in manure |
|---|---|---|---|---|---|---|---|
| Cattle > 170 kg N | | | kg N/ha | kg total-N/ha | kg N/ha | kg N/ha | kg P/ha |
| Afgrøde 1 | spring barley | Kl.græs udlæg e korn | 124 | 113 | 39.3 | 152.2 | 18.1 |
| Afgrøde 2 | Grass w legume | | 270 | 246 | 85.7 | 331.4 | 39.3 |
| Afgrøde 3 | Grass w legume | | 270 | 246 | 85.7 | 331.4 | 39.3 |
| Afgrøde 4 | Grass w/o clover | | 383 | 349 | 121.5 | 470.2 | 55.8 |
| Afgrøde 5 | Maize | Efterafgrøde | 150 | 137 | 47.6 | 184.1 | 21.8 |
| Afgrøde 6 | Maize | Efterafgrøde | 151 | 137 | 47.9 | 185.4 | 22.0 |
| Afgrøde 7 | Maize | Efterafgrøde | 151 | 137 | 47.9 | 185.4 | 22.0 |
| Afgrøde 8 | | | | | | | |
| Gennemsnit | | | 151 | 195 | 67.9 | 214.1 | 117.0 |

| crop rotation 17 | Main crop (afgrødefølge) | Spead/Catch crop (efterafgrøde) | N-norm | Animal manure | Mineral fertilizer | N applied | P applied in manure |
|---|---|---|---|---|---|---|---|
| organic Cattlefarm with less than 20% wholecrop for fodder | | | kg N/ha | kg total-N/ha | kg N/ha | kg N/ha | kg P/ha |
| Afgrøde 1 | spring barley | | 124 | 102 | 0 | 101.5 | 16.2 |
| Afgrøde 2 | Grass w legume | | 270 | 221 | 0 | 221.1 | 35.4 |
| Afgrøde 3 | Grass w legume | | 270 | 221 | 0 | 221.1 | 35.4 |
| Afgrøde 4 | Spring rye green | | 0 | 0 | 0 | 0.0 | 0.0 |
| Afgrøde 5 | Grass w legume | | 270 | 221 | 0 | 221.1 | 35.4 |
| Afgrøde 6 | Grass w legume | | 270 | 221 | 0 | 221.1 | 35.4 |
| Afgrøde 7 | spring barley | | 26 | 21 | 0 | 21.3 | 3.4 |
| Afgrøde 8 | Winter rye | Efterafgrøde | 138 | 113 | 0 | | |
| Gennemsnit | | | 138 | 140 | 0 | 112.0 | 84.0 |

| crop rotation 19 | Main crop (afgrødefølge) | Spead/Catch crop (efterafgrøde) | N-norm | Animal manure | Mineral fertilizer | N applied | P applied in manure |
|---|---|---|---|---|---|---|---|
| Cattle < 80 kg N | | | kg N/ha | kg total-N/ha | kg N/ha | kg N/ha | kg P/ha |
| Afgrøde 1 | Grass w legume | | 135.0 | 48.3 | 98.8 | 147.1 | 7.7 |
| Afgrøde 2 | Grass w clover | | 0.0 | 0.0 | 0.0 | 0.0 | 0.0 |
| Afgrøde 3 | spring barley | | 52.5 | 18.8 | 38.4 | 57.2 | 3.0 |
| Afgrøde 4 | Grass w/o clover | | 191.5 | 68.6 | 140.1 | 208.6 | 11.0 |
| Afgrøde 5 | Grass w clover | | 40.0 | 14.3 | 29.3 | 43.6 | 2.3 |
| Afgrøde 6 | | | | | | | |
| Afgrøde 7 | | | | | | | |
| Afgrøde 8 | | | | | | | |
| Gennemsnit | | | 40.0 | 30.0 | 61.3 | 85.3 | 18.0 |

| crop rotation 18 | Main crop (afgrødefølge) | Spead/Catch crop (efterafgrøde) | N-norm | Animal manure | Mineral fertilizer | N applied | P applied in manure |
|---|---|---|---|---|---|---|---|
| Anden planteavl | | | kg N/ha | kg total-N/ha | kg N/ha | kg N/ha | kg P/ha |
| Afgrøde 1 | Potato (starch) | | 169 | 105 | 90 | 195.2 | 16.8 |
| Afgrøde 2 | spring barley | Efterafgrøde | 141 | 87 | 75 | 162.9 | 14.0 |
| Afgrøde 3 | spring barley | Efterafgrøde | 116 | 72 | 62 | 134.0 | 11.5 |
| Afgrøde 4 | Grass w legume | | 245 | 152 | 131 | 283.0 | 24.3 |
| Afgrøde 5 | Potato (starch) | | 54 | 33 | 29 | 62.4 | 5.4 |
| Afgrøde 6 | spring barley | | 141 | 87 | 75 | 162.9 | 14.0 |
| Afgrøde 7 | Winter rye | | 150 | 93 | 80 | 173.3 | 14.9 |
| Afgrøde 8 | | | | | | | |
| Gennemsnit | | | 150 | 90 | 78 | 145.1 | 54.0 |

| crop rotation 20 | Main crop (afgrødefølge) | Spead/Catch crop (efterafgrøde) | N-norm | Animal manure | Mineral fertilizer | N applied | P applied in manure |
|---|---|---|---|---|---|---|---|
| organic Cattle < 80 kg N | | | kg N/ha | kg total-N/ha | kg N/ha | kg N/ha | kg P/ha |
| Afgrøde 1 | Grass w legume | | 135.0 | 33.9 | 0.0 | 33.9 | 5.4 |
| Afgrøde 2 | Grass w legume | | 135.0 | 33.9 | 0.0 | 33.9 | 5.4 |
| Afgrøde 3 | spring barley | | 0.0 | 0.0 | 0.0 | 0.0 | 0.0 |
| Afgrøde 4 | Grass w legume | | 135.0 | 33.9 | 0.0 | 33.9 | 5.4 |
| Afgrøde 5 | Grass w/o clover | | 191.5 | 48.2 | 0.0 | 48.2 | 7.7 |
| Afgrøde 6 | | | | | | | |
| Afgrøde 7 | | | | | | | |
| Afgrøde 8 | | | | | | | |
| Gennemsnit | | | 191.5 | 30.0 | 0.0 | 22.5 | 18.0 |